

**A Comprehensive Evaluation of Operational and Safety Performance of Directional
Rumble Strips on Freeway Off-Ramps**

by

Chennan Xue

A dissertation submitted to the Graduate Faculty of
Auburn University
in partial fulfillment of the
requirements for the Degree of
Doctor of Philosophy

Auburn, Alabama
December 12, 2020

Keywords: Directional Rumble Strips; Wrong-Way Driving; Driver Behavior; Off-Ramps

Copyright 2020 by Chennan Xue

Approved by

Huaguo Zhou, Chair, Professor of Civil and Environmental Engineering
Rod E. Turochy, Professor of Civil and Environmental Engineering
Jeffrey J. LaMondia, Associate Professor of Civil and Environmental Engineering
Timothy P. McDonald, Professor of Biosystems Engineering

Abstract

A freeway off-ramp is a short section of roadway that allows vehicles to exit the freeway. Wrong-way driving (WWD) and failure in speed management were found to be the major issues on these off-ramps. Countermeasures have been implemented at off-ramp terminals to prevent wrong-way (WW) entries and control vehicle speeds, including signs and pavement markings. Intelligent transportation system (ITS) technologies were also implemented at limited sites due to the higher cost and lack of quick emergency responses in rural areas. Studies found that these signs or pavement markings might not be effective. Moreover, the costly ITS technologies, with inherent false alarm rate, request a quick emergency response. To overcome the issues of WWD and speed control on freeway off-ramps, this study presents the field evaluation results of a low-cost countermeasure – directional rumble strips (DRS), which are expected to deter WWD and slow down right-way (RW) vehicles. Initially, five DRS patterns (named A to E) with various configurations were developed and tested. Three patterns (D3, C, and E.1) of DRS were recommended for field implementation based on the closed-course test results. Pattern D3 was installed at the off-ramp terminal near the stop bar or yield line. Pattern C was implemented at the segment between the terminal and ramp curve. Pattern E.1 was placed on the tangent part before the ramp curve. Southbound off-ramps at Exits 208 and 284 on I-65 in Alabama were selected for implementation as they were ranked as high-risk locations by a network screening tool developed by Auburn University. A total of 1, 296 hours of video data was recorded to monitor WW incidents using portable cameras. Another 1, 344 hours of traffic speed data were collected using magnetic sensors. Field driving tests were conducted to collect sound and vibration data at various speed categories for both RW and WW directions. Before-and-after studies evaluated the effectiveness of the DRS patterns in reducing WW incidents and traffic speeds on off-ramps. Sound and

vibration analysis quantified the differences between RW and WW drivers' perceptions. Results showed that the number of WWD incidents and average driving distances were significantly reduced after implementing all the DRS. The results confirmed that WW drivers can perceive elevated sound and vibrations when passing the DRS. The DRS can also reduce the mean, 85th percentile, and standard deviations of RW traffic speeds. Transportation agencies can utilize these findings as well as the general guidelines developed from this study to implement DRS for the purpose of deterring WWD and controlling traffic speeds on the freeway off-ramps.

Acknowledgments

This dissertation was funded by Alabama Department of Transportation and University Transportation Center Region 5. Many people provided their expert assistance and cordial cooperation in successful completion of this study.

I would like to acknowledge the advice, guidance, continued support, and encouragement received from my advisor, Dr. Huaguo Zhou. Without his, this dissertation would have not been possible. I wish to express my gratitude to Dr. Turochy, Dr. LaMondia, Dr. McDonald, and Dr. Zhang for their servings as advisory committee members. My sincere appreciations go to all professors who taught me during my time at Auburn University, and to Dr. Lin for his help and encouragement.

Finally, I would like to thank my wife Dan Xu, our parents, and our families for their priceless love and support.

Table of Contents

Abstract.....	ii
Acknowledgments.....	iv
Chapter 1. Introduction.....	1
1.1 Background	1
1.2 Research Objectives	3
1.3 Dissertation Organization.....	4
Chapter 2. Literature Review.....	5
2.1 WWD Countermeasures.....	5
2.2 Vehicle Speed Control on Off-Ramps.....	12
2.3 Transverse Rumble Strips	14
2.4 Directional Rumble Strips.....	16
2.5 Evaluation of Sound and Vibrations	19
2.6 Gaps in Previous Research and Proposed Work	22
Chapter 3. Methodology	23
3.1 Closed-Course Verification Tests	23
3.1.1 Site Description.....	23
3.1.2 Data Collection	24
3.1.3 DRS Patterns for Verification Tests	25
3.1.4 Verification Test Schemes	28
3.2 Field Implementation Tests.....	29
3.2.1 Site Description.....	29
3.2.2 Data Collection	34

3.2.3	DRS Implementation and Installation.....	39
3.2.4	Field Implementation Schemes.....	49
3.2.5	Evaluation of Sound and Vibrations.....	50
3.3	Summary	52
Chapter 4.	Analysis and Results from Closed-Course Tests.....	54
4.1	Comparisons of Sound and Vibration at the Different Speeds	54
4.2	Speed Analysis on Freeway Ramps	59
4.3	Analysis of Sound and Vibrations.....	63
4.4	Recommendations from Verification Tests Results	69
Chapter 5.	Field Implementation Results	73
5.1	Impacts of DRS on Number of WWD Incidents and WWD Distances	73
5.2	Analysis of Sound and Vibrations caused by DRS	83
5.3	Impacts of DRS on Vehicle Speeds	97
5.4	Other Findings.....	118
Chapter 6.	Guidelines for Implementing DRS	121
6.1	DRS Implementation Guidelines.....	121
6.2	Cost and Benefit	124
Chapter 7.	Conclusions.....	126
Chapter 8.	Limitations and Future Study.....	130
References.....		131
Appendix A: Summary of Wrong-Way Incidents		
Appendix B: Speed Characteristics		
Appendix C: Sound and Vibration Profiles		

Appendix D: MATLAB Code

List of Tables

Table 2.1 Countermeasures for deterring WWD (Pour-Rouholamin et al. 2015)	7
Table 2.2 TRS configurations of several states (Zhou et al. 2018).....	16
Table 3.1 Verification Test Schemes	28
Table 3.2 DRS field implementation schemes.....	50
Table 4.1 <i>P</i> -values of Difference of Sound and Vibrations between RW and WW Directions at Different Speeds.....	55
Table 4.2 Speed Characteristics at Three Spots of Ramps	62
Table 5.1 Comparisons of WW Incidents before and after Installing DRS at Exit 284.....	76
Table 5.2 Statistical Analysis of Number of WWD Incidents.....	78
Table 5.3 Statistical Analysis of Average WWD Distances.....	79
Table 5.4 Records of WW Incidents (W1-W8) at Exit 208.....	81
Table 5.5 Records of WW Incidents (W1-W8) at Exit 284.....	82
Table 5.6 Exterior Sound Levels Caused by DRS	91
Table 5.7 Variables of Raw Speed Data (Partial).....	98
Table 5.8 Pattern E.1 Helped Drivers Follow the Advisory Ramp Speed.....	103
Table 5.9 Z-tests Results of Changes in Average Speeds.....	103
Table 5.10 Characteristics of Upper 15th Percentile Speeds from Sensors #99 and #100 at Exit 208.....	106
Table 5.11 <i>F</i> -test Results of Changes in Speed Variances	108
Table 5.12 Comparisons of Daytime and Nighttime Average Speeds after Implementing Pattern E.1	115

Table 5.13 Comparisons of Daytime and Nighttime Speed Standard Deviations after Implementing Pattern E.1	115
Table 5.14 Comparisons of Daytime and Nighttime Average Speeds after Implementing Pattern C.....	116
Table 5.15 Comparisons of Daytime and Nighttime Speed Standard Deviations after Implementing Pattern C	116
Table 5.16 Comparisons of Daytime and Nighttime Average Speeds after Implementing Pattern D3	117
Table 5.17 Comparisons of Daytime and Nighttime Speed Standard Deviations after Implementing Pattern D3	117
Table 5.18 Change in Left-Turn Confusions	118
Table 6.1 Summary of Benefits of DRS Implementation.....	122

List of Figures

Figure 2.1 ALDOT standard drawing of TRS (ALDOT 2020)	15
Figure 2.2 Conceptual designs of DRS (Zhou et al. 2018).....	18
Figure 2.3 Typical frequency ranges and effects of vibration on the body (Mansfield 2004)	21
Figure 3.1 Location for DRS Verification Tests (Imagery © 2019 Google, Map data © 2019 Google.)	24
Figure 3.2 DRS Patterns for Verification Tests	27
Figure 3.3 Southbound Off-Ramp at Exit 208 on I-65, AL (Imagery © 2019 Google, Map data © 2019 Google.).....	31
Figure 3.4 Southbound off-ramp at Exit 208 on I-65, AL (Imagery © 2019 Google, Map data © 2019 Google.).....	33
Figure 3.5 Data Collection Equipment: (a) Video Camera; (b) Magnetic Sensor; (c) Sound Level Meter; (d) Accelerometer.....	34
Figure 3.6 Camera Deployment at (a) Exit 208 and (b) Exit 284 on I-65, AL (Imagery © 2019 Google, Map data © 2019 Google.).....	35
Figure 3.7 NC-350 Deployments at Exit 208 on I-65, AL (Imagery © 2019 Google, Map data © 2019 Google.).....	37
Figure 3.8 NC-350 Deployments at Exit 284 on I-65, AL (Imagery © 2019 Google, Map data © 2019 Google.).....	38
Figure 3.9 NC-350 Field Installation	39
Figure 3.10 DRS Pattern D3 Implementation Design	41
Figure 3.11 DRS Pattern C Implementation Design.....	42

Figure 3.12 DRS Pattern E.1 Implementation Design	43
Figure 3.13 DRS Implementation at Exit 208 on I-65, AL (Imagery © 2019 Google, Map data © 2019 Google.).....	44
Figure 3.14 DRS Implementation at Exit 284 on I-65, AL (Imagery © 2019 Google, Map data © 2019 Google.).....	45
Figure 3.15 Field Photos of DRS Patterns	46
Figure 3.16 Procedure of DRS Installation.....	48
Figure 4.1 Sound Levels Generated by DRS	57
Figure 4.2 Vibration Levels Generated by DRS.....	58
Figure 4.3 Spots where Speeds were Measured on Ramps	60
Figure 4.4 Speed Distributions at (a) Ramp Terminals, (b) Middle Points of Ramps, and (c) Tangent of Ramp Curves	61
Figure 4.5 Analysis of Sound and Vibrations Generated by Pattern C	66
Figure 4.6 Analysis of Sound and Vibrations Generated by Pattern D3	68
Figure 4.7 Analysis of Sound and Vibrations Generated by Pattern E.1.....	69
Figure 4.8 Proposed Implementation of Pattern D3	70
Figure 4.9 Proposed Implementation of Pattern C.....	71
Figure 4.10 Proposed Implementation of Pattern E.1.....	72
Figure 5.1 WWD (a) Frequencies and (b) Distances before and after DRS Installations	75
Figure 5.2 Sample RW Sound Data along the Off-Ramp.....	84
Figure 5.3 RW and WW Sound of (a) Pattern E.1, (b) Pattern C, and (c) Pattern D3	88
Figure 5.4 Data Collection of Exterior Sound Caused by DRS.....	89
Figure 5.5 Sample RW Vibration Data along the Off-Ramp.....	92

Figure 5.6 RW and WW Spectrums of Pattern E.1	93
Figure 5.7 RW and WW Spectrums of Pattern C: (a) 5-ft, (b) 2-ft, and (c) 1-ft Spacing	96
Figure 5.8 RW and WW Spectrums of Pattern D3.....	97
Figure 5.9 Sample traffic volume and speed data: (a) week volume; (b) Thursday volume in (a); (c) speed histogram of (b)	99
Figure 5.10 Average Speeds on Southbound Off-Ramps at Exits (a) 208 and (b) 284.....	102
Figure 5.11 85th Percentile Speeds on Southbound Off-Ramps at Exits (a) 208 and (b) 284	105
Figure 5.12 Speed Standard Deviations on Southbound Off-Ramps at Exits (a) 208 and (b) 284.....	107
Figure 5.13 Driver Adoption of Pattern E.1 at Exits (a) 208 and (b) 284	111
Figure 5.14 Driver Adoption of Pattern C at Exits (a) 208 and (b) 284	112
Figure 5.15 Driver Adoption of Pattern D3 at Exits (a) 208 and (b) 284.....	113
Figure 5.16 Example of Left-Turn Confusion Captured at Exit 208.....	119
Figure 5.17 Motorcycle Using the Center Gaps to Pass DRS Pattern C	120
Figure 6.1 Recommended DRS Deployments with Relevant Signs and Pavement Markings	121
Figure 6.2 Pattern D3 with Red Retroreflective Paint	124

List of Abbreviations

BAC	Blood Alcohol Content
DNE	Do Not Enter
DOT	Department of Transportation
DRS	Directional Rumble Strips
FFT	Fast Fourier Transform
FHWA	Federal Highway Administration
ITS	Intelligent Transportation System
MUTCD	Manual on Uniform Traffic Control Devices
RMS	Root Mean Square
RRPM	Raised Reflective Pavement Markers
RW	Right-Way
SD	Standard Deviation
TRS	Transverse Rumble Strips
WW	Wrong-Way
WWD	Wrong-Way Driving

Chapter 1. Introduction

1.1 Background

A freeway off-ramp is an exit lane for traffic from the freeway to a crossroad. According to the National Transportation Safety Board (NTSB), the primary origin of wrong-way (WW) movement occurs when a driver enters an off-ramp (NTSB 2012). Drivers who make WW entries onto freeways via off-ramps pose a serious risk to the safety of other motorists and themselves (Baratian-Ghorghi et al. 2014). Wrong-way driving (WWD) crashes may occur because of such entries. They are infrequent but are more likely to produce serious injuries and fatalities compared with other types of crashes (Pour-Rouholamin and Zhou 2016). A recent study of the Fatality Analysis Reporting System (FARS) showed that WWD caused between 300 and 400 annual traffic fatalities from 2004 to 2011 in the United States (Zhou et al. 2012). The number of fatalities has been consistent, even though total traffic fatalities dropped by 4% over the eight-year period from 2004 through 2011. Traffic control devices such as signs, pavement markings, signals, and intelligent transportation systems (ITS) have been used to combat WWD at freeway off-ramps for decades. Conventional countermeasures are limited by providing visual information to potential WW drivers only, while applications of ITS such as thermal cameras have higher costs for installation and maintenance regardless of their false alarm rates (Xue et al. 2019; Zhou and Xue 2019).

Accordingly, for the right-way (RW) traffic on off-ramps, speeds play an important role in their safety. Motor vehicle crashes occur more frequently on horizontal curves and are more severe than crashes that occur on straight roadway sections (Retting et al. 2000). Speed is a significant factor in crashes on curves and in the severity of these crashes (Zegeer et al. 1991; Elvik et al.

2004; Asrts and Van Schagen 2006; Xue and Xu 2019). A study analyzed data from the FARS and National Automotive Sampling System (NASS) and reported that more than twice as many occupants were involved in crashes per kilometer of a curved road than were on straight sections (Troxel et al. 1994). Furthermore, crashes on curves resulted in nearly three times as many fatalities per kilometer as those on straight sections. As freeway off-ramps usually consist of horizontal and vertical curves, a study of crashes on freeway off-ramps suggested that both crash rate and severity are related to the difference between speeds approaching the off-ramp and the posted advisory off-ramp speed (Garber et al. 1992). Therefore, it is important to discourage excessive speeds. Frequently used traffic control devices such as advisory ramp speed sign, chevron sign, and advance curve warning sign were found ineffective on controlling vehicle speeds at freeway off-ramps (Retting et al. 2000).

To deal with issues of WWD entries for WW drivers and speeding for RW drivers on freeway off-ramps, transverse rumble strips (TRS) have shown potential for solving both issues at the same time. TRS is a warning system that provides motorists with audible, visual, and tactile signals when approaching a decision point. A recent study determined whether applying transverse rumble strips was an effective warning device for drivers approaching high-speed intersections (Yang et al. 2016). The results showed that TRS produced a recognizable amount of interior noise and a moderate amount of vibration when vehicles crossed over the TRS. TRS also reduced average vehicle speeds at least by 3 to 5 mph at the signalized intersection. However, TRS was not originally designed to deter WWD. Therefore, with one step forward, a research project, “Directional Rumble Strips for Reducing Wrong-Way-Driving Freeway Entries,” tested five directional rumble strips (DRS) designs (named A to E) with various configurations (e.g., A1, A2...) inspired by the designs of TRS (Zhou et al., 2018). The results showed that all the tested

patterns can generate an adequate sound increase in the WW direction to alert drivers to slow down (7.2 to 16.6 dBA increases). Statistical analyses were conducted to examine if there was a significant difference in the sound and vibration between RW and WW directions. Pattern C generated different sound and vibration signals between RW and WW directions when driving from 10 to 25 mph. Pattern E was found to generate different vibration at 45 mph. Recommendations were developed to implement three DRS design patterns in the field which were Pattern D3 (one configuration of Pattern D), Pattern C, and Pattern E.1 (a variant of Pattern E).

1.2 Research Objectives

This dissertation first verified and modified the recommended three DRS patterns (i.e., C, D3, E.1) based on closed-course test results, then evaluated the effectiveness of them based on field implementation results. The verification tests were conducted on a ramp at the Auburn University Erosion and Sediment Control Testing Facility (AU-ESCTF) at the National Center for Asphalt Technology (NCAT). DRS were installed by researchers using tape rumble strips. Sound and vibration data were collected by a sound meter and an accelerometer. Results were compared with previous test results and recommendations for implementing DRS were made. During the field implementation part, southbound off-ramps at Exits 208 and 284 on I-65 in Alabama were selected for implementation based on prediction model results (Zhou and Atiquzzaman, 2019) and the number of WWD incidents observed. DRS was implemented by a contractor using thermoplastic. WWD incidents were monitored using video cameras. Vehicle speed data was collected by magnetic sensors. Sound and vibration data were also collected by a sound meter and an accelerometer. Field driving tests were conducted to collect data of sound and vibrations at various speed categories for both RW and WW directions by driving a full-size passenger car. Before and after studies were conducted to evaluate DRS patterns regarding WW incidents, as well

as drivers' speed, behavior, and adoption of the DRS. Speed analysis was performed to evaluate the impacts on vehicle speeds by DRS patterns. Time-series and spectrum analysis were employed to analyze the sound and vibrations caused by DRS. Based on the findings, guidelines for implementing the DRS in the field was developed to deter WWD entries at freeway off-ramps.

The specific objectives of this dissertation are to:

1. evaluate the performance of DRS for deterring WWD on freeway off-ramps.
2. assess the impacts of DRS on RW drivers on freeway off-ramps.
3. develop guidelines for implementing DRS on freeway off-ramps.

1.3 Dissertation Organization

This dissertation contains eight chapters. Chapter 1 discusses the background, research objectives, and organization of the dissertation. A comprehensive review of previous research on WWD crashes, WWD countermeasures and speed control strategies on freeway off-ramps, and analysis of sound and vibrations is provided in Chapter 2. The methodology is documented in Chapter 3, which includes detailed discussions on experiment designs, data collection efforts, and data analysis methods. Chapters 4 and 5 discuss the results of DRS for deterring WWD. Chapter 6 presents guidelines for implementing DRS on freeway off-ramps. Chapter 7 concludes the findings from this study. Chapter 8 points out the limitations of this study and the needs of future studies.

Chapter 2. Literature Review

The literature review is divided into six main sections for this dissertation proposal. Due to the two issues found on freeway off-ramps. To have an overview of strategies for deterring WWD, the first part summarizes the practices of WWD detection and warning technologies adopted by the DOTs. The second section reviewed the effectiveness of traffic control devices used on off-ramps for controlling vehicle speeds. The third and fourth sections discuss the potential countermeasure - TRS - and how DRS were developed. This will lead to the next section documenting how past research evaluates the effectiveness of rumble strips. The final section concludes the past efforts and lists the research questions that need to be answered.

2.1 WWD Countermeasures

Freeway off-ramps are prone to wrong-way driving (WWD) (NTSB 2012). According to the American Traffic Safety Services Association (Zhou et al. 2014), WWD happens when a driver, inadvertently or deliberately, drives in the opposite direction of traffic flow along a physically divided highway or its access ramps. With regard to WWD entry points, attention should be given to the characteristics of intersections of off-ramps and crossroads, including signs, pavement markings, signals, and geometric design features (Baisyet and Stevens 2015; Baratian-Ghorghi et al. 2015; Xing, 2013).

In 2013, the first National Wrong-Way Driving Summit provided a platform for practitioners and researchers to develop the best practices to reduce WWD incidents and crashes by evaluating current countermeasures (Pour-Rouholamin et al. 2015; Zhou and Pour-Rouholamin 2014a; Zhou and Pour-Rouholamin 2014b). Attendees included members from the National Transportation Safety Board (NTSB), Federal Highway Administration (FHWA), American Traffic Safety

Services Association (ATSSA), state departments of transportation (DOTs), state police, state highway patrols, tollway authorities, universities, and consulting firms. Based on the survey, discussions, and presentations at the summit, the countermeasures outlined in **Table 2.1** are candidates that were implemented or worthy of implementation for mitigating WWD incidents and crashes.

Table 2.1 Countermeasures for deterring WWD (Pour-Rouholamin et al. 2015)

<p>Signage</p>	<ul style="list-style-type: none"> ▪ Implementing Standard Wrong-Way Sign Package ▪ Improved Static Signs ▪ Lowering Sign Height ▪ Using Oversized Signs ▪ Mounting Multiple Signs on the Same Post ▪ Applying Red Retroreflective Strip to the Vertical Posts ▪ “Freeway Entrance” Sign for All Entrance Ramps
<p>Pavement Marking</p>	<ul style="list-style-type: none"> ▪ Stop Line ▪ Wrong-Way Arrow ▪ Turn/Through Lane Only Arrow ▪ Red Raised Pavement Markers ▪ Short Dashed Lane Delineation Through Turns
<p>Geometric Improvement</p>	<ul style="list-style-type: none"> ▪ Entrance/Exit Ramp Separation ▪ Raised Curb Median ▪ Longitudinal Channelizers ▪ Change in Ramp Geometrics: Obtuse Angle; Sharp Corner Radii
<p>Intelligent Transportation Systems (ITS) Technologies</p>	<ul style="list-style-type: none"> ▪ LED Illuminated Signs ▪ Dynamic Signs: Warn Other Drivers ▪ Use Existing GPS Navigation Technologies to Provide Wrong-way Movement Alerts ▪ Provide Messages or Alerts that are Intuitive to the Driver

In the past decades, strategies were adopted by state transportation agencies for deterring WW entries at freeway off-ramps, which included the modification or additional deployment of signs, pavement markings, signals, and ITS applications.

Arizona

Arizona DOT (ADOT) started developing strategies to deter WWD in 2010. Different technologies were employed to determine the viability of existing detector systems to identify WWD vehicles, including microwave, Doppler radar, video imaging, thermal sensors, and magnetic sensors (Simpson 2013).

In January 2018, the Arizona DOT implemented the first-in-nation WW driver pilot system along I-17 in Phoenix (Cain, Riley, and McKelvey 2018). The 15-mile system of 3.7 million total costs included thermal cameras, internally illuminated signs with flashing borders, message boards, and the decision-support software. Though the system provided accurate detection, around 10 false detections per camera were caused by camera shaking due to the wind in one month.

California

California DOT (Caltrans) first used cameras to detect WW drivers in early 1967. A Kodak Instamatic camera triggered by two tubes stretched across the roadway was installed. An image of the roadway and the WW vehicle was captured if the camera was triggered when a WW vehicle crossed the tubes in the reversed direction. The images were used for identifying off-ramps with large numbers of WW entries (Rinde 1978).

In the early 1970s, Caltrans first lowered the mounting height of WW signs. A study showed that the average WW entries dropped from 55 entries per month to 4 after WW signs were lowered (Leduc 2008).

In 1989, a Caltrans study recommended adding a second set of WW signs to give WW drivers extra chances to self-correct prior to entering the freeway mainline in the wrong direction (Copelan 1989).

In 2004, Caltrans deployed in-pavement warning lights on off-ramps, which were susceptible to WW incidents (Cooner, Cothron, and Ranft 2004). They utilized an inductive loop detector for activating a series of warning lights. The lights were activated when a vehicle entered the off-ramp in the WW direction; however, no evaluation regarding their success was conducted.

Florida

In 2006, a low-power microwave radar detector was implemented at approximately 1000 ft prior to a bridge. Once a WW movement was detected, flashing beacons visibly enhanced the DNE and WW signs above the roadway (Williams 2007).

In 2010, the Florida DOT (FDOT) tested video-detection techniques on expressway off-ramps (Rose 2011). The study simulated test runs for this study and a 27-day field trial. A number of false alarms were reported due to movements of vehicles on the shoulder, dark shadows, and the reflection of headlights from the wet pavement. According to a recent study on testing and evaluating video systems in Florida, the systems performed with detection accuracies of above 94%. They were able to send an email notification to the traffic management center if a WWD was detected (Lin, Chen, and Ozkul 2018).

In 2014, FDOT installed WW detection devices on 10 off-ramps in Miami-Dade County and 5 off-ramps in Broward County (FDOT 2014). LED-enhanced signs illuminated, and law enforcement and authorities were notified of WW entries when the devices were activated.

Illinois

The Illinois Department of Transportation (IDOT) studied the magnitude of WWD in the state and developed countermeasures to mitigate such crashes (Zhou, et al. 2012). At the 12 highest ranked wrong-way entry locations, researchers recommended combinations of countermeasures ranging from signing adjustments to pavement markings, geometric design, and traffic signal arrow modifications. Some WW countermeasures for implementation included:

- Oversized DNE and WW signs
- Red reflective sheeting on sign supports
- WRONG WAY signs with flashing LEDs around the border
- Pavement marking and geometric design enhancements

Texas

The Texas Department of Transportation (TxDOT) has been studying WWD detection and warning systems over the last 20 years. In 2002, a study analyzed the causes and consequences of WW entries on Texas freeway (Cooner, Cothron, and Ranft 2004). The recommended guidelines and practices for WW countermeasures included:

- Installing reflectorized WW arrows on freeway off-ramps.
- Adding raised pavement markers to the standard freeway pavement markings.
- Installing WW arrows and make frequent maintenance.
- Lowering WW signs.
- Installing inductive loops or the other detectors on freeway off-ramps for future projects.

In 2007, the Harris County Toll Road Authority in Texas installed a WW detection system on 13.2 miles of toll roads (TransCore 2008). The system consisted of radar sensors for detecting WW vehicles and audible alarm software for dispatching the closest law enforcement. Additionally,

a message on the changeable message sign advised motorists of the oncoming driver (ITS International 2010). Accordingly, no fatalities were reported, and 23 WW drivers had been stopped or turned around since the implementation (Willey 2011).

In 2011, TxDOT conducted research to determine if spike strips could be used to stop WWD vehicles (TxDOT 2011). The testing results did not suggest the usage of spike strips for the following reasons:

- Tire spike strips are designed for speeds lower than 5 mph.
- Spike strips did not deflate tires quickly enough to stop vehicles from entering the wrong direction.
- This device is a hazard for motorcycles and small cars in the right direction.

In 2012, TxDOT installed WW signs and radar devices at 16 locations to deter WWD in the San Antonio area (Fariello 2012). The results suggested that WW signs with flashing LEDs around the board are visible at a longer distance without LEDs. A 30-month follow-up study showed that the WWD rates were reduced by 30 percent on average (Gianotti 2015).

In 2014, TxDOT evaluated the effectiveness of WWD countermeasures including LEDs around WW signs activated by WW drivers (Finley et al. 2014). Results suggested the use of red retroreflective sheeting on the sign supports to increase the conspicuity of WW and DNE signs. Additionally, oversized signs or signs with flashing red LEDs around the border may be considered.

Virginia

A two-year survey conducted at Virginia showed that over 70 percent of WW entries occurred in the darkness by impaired drivers (Vaswani 1973). The proposed strategies to mitigate this issue were to channelize the left-turn lane of the off-ramp, make the on-ramp conspicuous and the off-ramp inconspicuous, re-locate the signs to improve visibility, add geometry signing to the

intersection, add illumination to the entry points at the intersection terminal, and bring stop lines closer to the crossroad.

Wisconsin

In 2012, Wisconsin DOT installed 9 wireless alert notification systems. Notifications are sent instantly to Traffic Operation Center and the Sheriff's Office when a motion sensor is triggered (Rich 2015). No research has been published on the effectiveness of this system.

To conclude, conventional countermeasures such as signage or pavement markings have the limitation in providing sufficient information to WW drivers in time. For instance, WW signs can only visually alert WW drivers in the assumption of being seen by them. Regardless of the false alarms, new ITS techniques cost relatively more for construction, equipment, and maintenance. Therefore, there is an urgent need to deploy low-cost but effective countermeasures that can alert WW drivers, especially those older or impaired drivers by elevated in-vehicle sounds and vibrations.

2.2 Vehicle Speed Control on Off-Ramps

Freeway off-ramps often are designed with horizontal curves, which can become crash-prone when traffic speeds are excessive for ramp geometry (Retting et al. 2000). The speed at which a vehicle enters a curve is related more to the speed of its approach than to the sharpness of the curve (Puvanachandran 1995).

Research indicated that smaller speed differences between vehicles within one lane would cause a less frequent occurrence of small headways, and a reduction in congestion and conflicts (Van den Hoogen and Smulders 1994; Lin et al. 2004). Large variations in the vehicle speeds could lead to unsafe situations (Hegyi et al. 2005; Aarts and Van Schagen 2006). An old but often-cited study of 10,000 cases in the United States found that drivers with a speed higher or lower than 6

mph above the modus speed have an increased rate of crash involvement (Solomon 1964). A few years later, another study only analyzed crashes between two or more vehicles that moved in the same direction (Cirillo 1968). The relationship between speed differences and crash rates was confirmed. The increase in the standard deviation of vehicle speeds can increase the likelihood of having a crash based on a study by Oh et al. (2001). Two Australian studies (Kloeden et al. 1997; Kloeden et al. 2001) found an increased risk for vehicles moving faster than the others. A log-linear model predicted the crash likelihood indicated that crash risks were related to the coefficients of variations of speeds (Lee et al. 2002; Lee et al. 2003). A study investigated 1,590 injury crashes in the UK also found that traffic speed variance is related to the crash frequency (Taylor et al. 2000). More recent research revealed that making average vehicle speeds closer to the speed limit can reduce the overall crash potential by 5-17% (Lee et al. 2006; Allaby et al. 2007).

According to 2009 MUTCD, the primary method used to control vehicles' speeds when they enter off-ramp curves from tangent approaches is to post advisory curve warning or off-ramp speed signs (FHWA 2009). However, a large body of studies indicated that these signs are not effective. Nighttime vehicle speeds were reported to be increased by using post-mounted delineators and chevrons (Zador 1987). A study examined the effectiveness of five sign treatments for controlling vehicle speeds on horizontal curves (Lyles 1980). Signs examined ranged from the standard curve warning arrow to a regulatory speed zone sign in conjunction with a curve warning sign. No sign or sign group was found effective for reducing vehicle speeds. A study investigated the attentional factors associated with curve warnings (Charlton 2004). Results indicated that advance warning signs failed to reduce speeds. There is also evidence showing that warning signs are poorly understood by drivers (Stokes et al. 1996). Because drivers often exceed the posted

advisory speed, research has questioned the validity of criteria for determining advisory speeds (Chowdhury et al. 1998).

Therefore, at such as curved off-ramps where sudden changes from straight alignments to sharp curves occur, conventional countermeasures may not be enough.

2.3 Transverse Rumble Strips

In order to address issues of WWD incidents for WW drivers and speed-related safety concerns for RW drivers on the freeway off-ramps, transverse rumble strips (TRS) showed the potential based on the previous research. TRS is a warning system that provides motorists with audible, visual, and tactile signals when approaching a decision point. They are effective in reducing speeds and alerting drivers through both visual and tactile stimuli (Campbell 2010). A study tested the effectiveness of TRS on reducing vehicle speeds (Agent and Creasey 1986). The results showed that TRS increased the curve delineation and was able to decrease vehicle speeds. A 1962 study investigated the effectiveness of TRS installed at four different locations in Contra Costa County, California. The results concluded that vehicle speeds and deceleration rates before a sharp curve were reduced (Kermit and Hein 1962). A more recent study based on the before-and-after studies of 11 sites in Texas revealed significant reductions in mean and 85th percentile speed on approaches with the TRS (Fitzpatrick 2003). Generally, the speed reductions were less than 4 mph, with most drivers slowing by 1 to 2 mph. Several studies in China approved that TRS can reduce vehicles' speeds before they approach horizontal curves, vertical curves, and toll stations on freeways (Gao et al. 2004; Hou et al. 2010; Yang et al. 2010).

In the United States, TRS are mainly installed on approaches to intersections, toll plazas, horizontal curves, and work zones (FHWA 2014). According to a Minnesota DOT synthesis (Corkle et al. 2001), over 80 percent of counties in Minnesota responded to a survey on the use of

TRS. These counties typically use two sets of rumble strips prior to an intersection or change in traffic control. TxDOT stated that TRS should only be used at incident-prone and special geometric locations (Texas DOT 2006). Besides, Maryland DOT also suggests that TRS may be useful to address the need for a reduced speed zone with a posted speed reduction of 20 mph or greater, or an entrance to a town, business district, or locations where significant pedestrian activity is anticipated. Also, the TRS may be used in work zones in advance of detours, flaggers, lane transitions, lane closures, temporary traffic signals, and locations with major reductions in speed limits (SHA 2011).

The 2009 MUTCD contains no provisions regarding the design and placement of TRS but points out that the color should be not similar to the pavement (FHWA 2009). Guidelines of designs and implementation vary among states. According to Alabama DOT (ALDOT) standard drawings (ALDOT 2020) (**Figure 2.1**), it suggests 5 sets of 5 strips on each approach of an intersection. The distances between the first set and the intersections depend on the speed limit on the roadway. The first three sets are spaced 50 ft. apart while the rest two are spaced 100 ft. For thermoplastic TRS, the spacing between each strip is equally 9 in. The width of each strip is 6 in. The project “Directional Rumble Strips for Reducing Wrong-Way-Driving Freeway Entries” (Zhou et al. 2018) summarized current TRS design practices in the other states (**Table 2.2**).

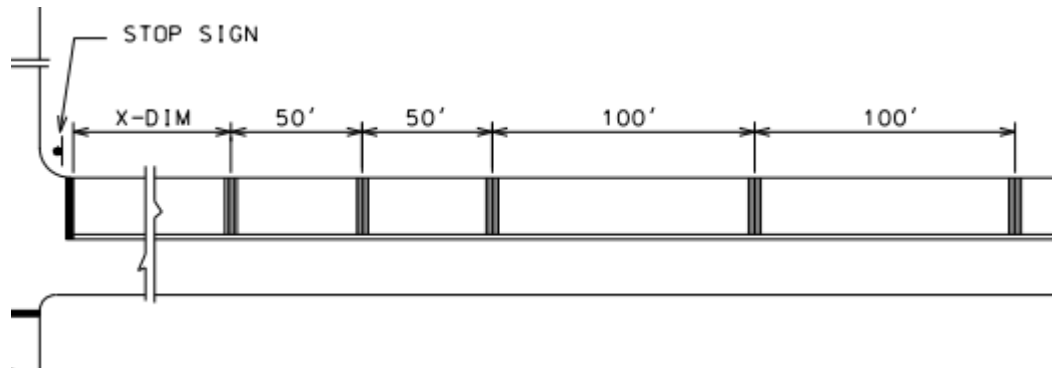


Figure 2.1 ALDOT standard drawing of TRS (ALDOT 2020)

Table 2.2 TRS configurations of several states (Zhou et al. 2018)

State	Type	Strips in each set	Length (ft)	Width (in.)	Spacing (in.)	Thickness (in.)	Offset (in.)
Minnesota	Grooved	6	3.3*2	5.9±0.2	5.9	0.4±0.1	7.9 from centerline 19.7 from shoulder
Michigan	Grooved	25	-	4	8	0.5	12
Maryland	Raised	10	-	5+5 10+5	54 or 72	-	-
Montana	Grooved	16	12	4	8	5/8	12
Oregon	Grooved	11	10	5(1/2)	12.5	1/2	12*(Lane width-10ft)/2
Arizona	Grooved	6	Lane width/cos (15 degree)	4	12	3/8	0
Texas	Raised	5	4*2	-	24	-	6-12
New Hampshire	Grooved	11 (minimum)	-	-	-	-	3/8

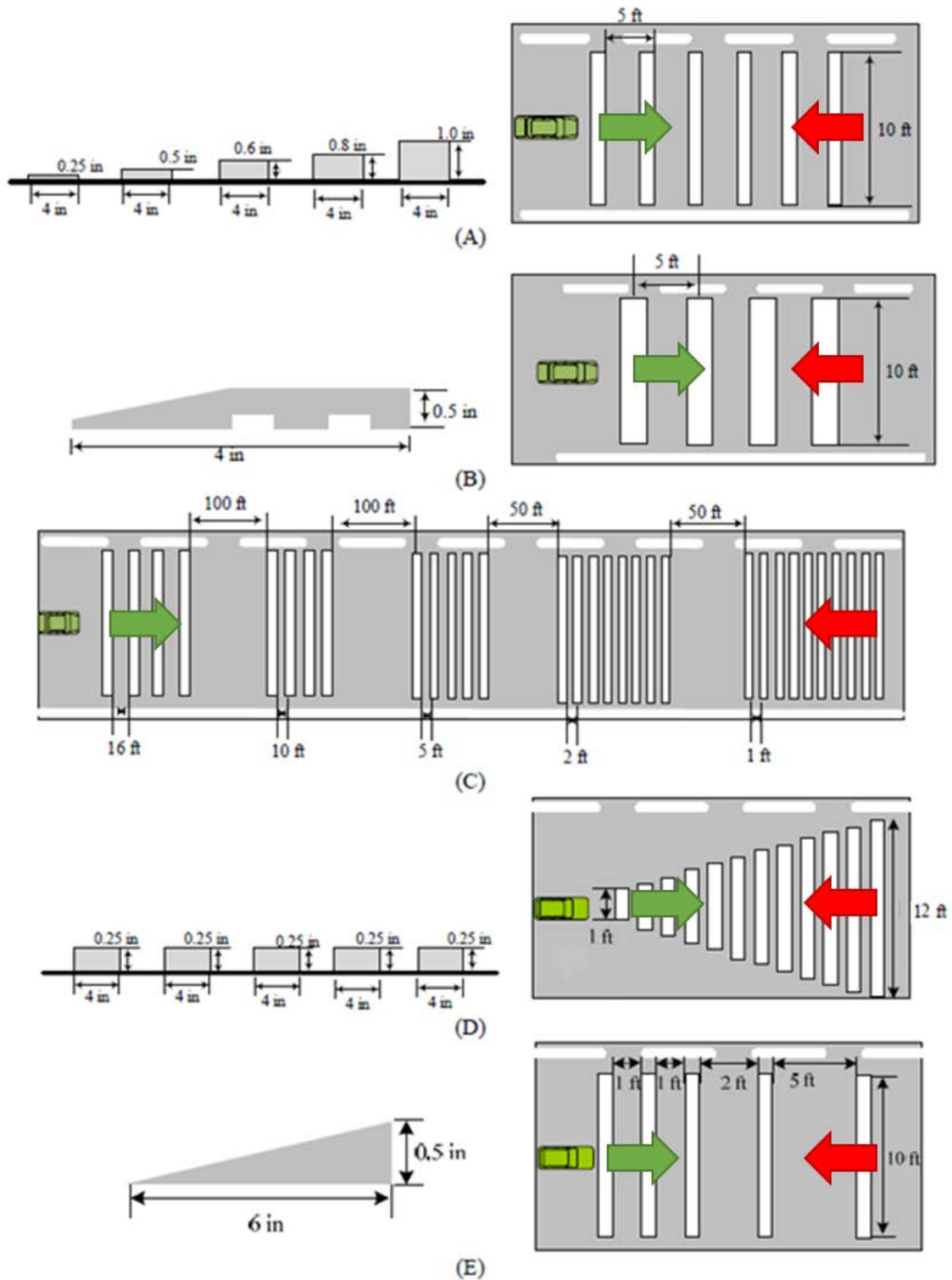
2.4 Directional Rumble Strips

As TRS was not originally designed for deterring WWD incidents, directional rumble strips (DRS), which can be regarded as a variation of TRS, were developed to fill the gap. In 2015, DRS was first designed to generate elevated sound and vibrations to warn WW drivers and normal sound and vibration to slow down traffic for the RW direction when they are approaching off-ramp terminals (Zhou et al. 2018). Other than that, DRS can also provide a visual cue for the off-ramp curves and terminals.

In this pilot research, five conceptual designs of DRS, which are illustrated in **Figure 2.2**, were selected based on a national survey. Pattern A utilizes the removable rumble strips. The

thickness of the strip gradually increases from 0.25 to 1.0 in. by combining different thicknesses of tapes. In Pattern B, the raised wedge strips may offer audible and tactile signals of DRS. The 20-degree angle enables a gradual climb. The 90-degree edge makes it possible to create a more alarming feel for drivers traveling in the wrong direction. Pattern C attempts to create different audible and physical warnings by a varied number of strips and spacings among them. For Pattern D, the top view of the strips is like a triangle that can provide a visual cue. The length of the strips decreases from 12 to 1 ft. In the wrong direction, the drivers encounter decreasing strip length, and the arrow gives a visual warning to the WW drivers. In Pattern E, the strips have the cross-section of triangles which are designed to offer audible and tactile signals. Each pattern has different configurations regarding the thickness of strips and spacing between strips.

Based on the initial test results, Pattern C, Pattern D Configuration 3 (D3), and Pattern E were recommended for further verification and evaluation based on their attention-getting effects (sound and vibrations) and visual attentiveness. All three patterns can generate adequate sound increases in the WW direction to alert drivers (7.2 to 16.6 dBA increases over the ambient condition). Pattern D3 and Pattern E produced recognizable vibration changes based on the field tests. The statistical tests found that Pattern C generated significantly different sound and vibration signals between the RW and WW directions at speeds between 10 and 25 mph. Pattern E showed a difference in vibration at the vehicle speed of 45 mph.



Note: Green Arrow = Right Direction; Red Arrow = Wrong Direction.

Figure 2.2 Conceptual designs of DRS (Zhou et al. 2018)

2.5 Evaluation of Sound and Vibrations

The attention-getting effects of rumble strips were commonly measured by sound and vibration levels in contrast with ambient conditions. NCHRP 641 recommends the following three noise level increases in ambient in-vehicle noise levels for effective rumble strips (Torbic et al. 2009):

- Minimum design value: 3 dBA
- Desirable design value: 6 dBA
- Maximum design value: 15 dBA

Researchers considered increases of 4 dB or greater to be sufficient to alert drivers coming into contact with rumble strips (Watts 1977, Elefteriadou et al. 2000, Miles and Finley 2007). A study by Outcalt regarded a sound level of a 6-dB change as a “clearly noticeable change” and 10 dB changes as twice as loud according to human perception of changes (Outcalt 2001). Tests conducted by Walton and Meyer revealed an average increase in sound from TRS (10 dB for cars and 4 dB for trucks [Walton and Meyer 2002]). Schrock et al. tested 10 different configurations of four to six strips (24- and 36-in. spacing plastic TRS and CIP strips spaced at 18-in. intervals) and found that in-vehicle sound levels ranged from 79.4 to 85.0 dB for a truck and from 75.7 to 85.7 dB for a passenger car (Schrock et al. 2010). Lank and Steinauer reported that the A-weighted volume in the area of the TRS is, on average, 10 dBA above the basic sound level without TRS (Lank and Steinauer 2011). Horowitz and Nothbohm also measured the sound level generated by permanent cut-in-pavement (CIP) rumble strips and adhesive rumble strips (Horowitz and Nothbohm 2005). The average sound level at 40 mph was found to be 75.2 and 70.9 dBA for standard CIP strips and adhesive rumble strips, respectively.

Humans are sensitive to mechanical vibrations ranging in frequency from well below 1 Hz up to at least 100 kHz. The range of sensitivity to vibration is much broader than the range of human hearing (Guignard 1971). The results from Guignard's study (1971) showed that the sensitivity is higher for lower frequencies compared to higher. A study was conducted to identify the threshold of vertical vibrations (Morioka and Griffin 2008). The results indicated that sensitivity was greatest for vertical vibration at the seat at frequencies between 8 and 80 Hz, while sensitivity was greatest for vertical vibration at the hand at frequencies greater than 100 Hz. Because of the complexity of the sensory mechanisms, there have been few satisfactory laboratory studies regarding the threshold of the sensation of vibration (Guignard 1975). The threshold was found to be remarkably low as 0.001 g (0.032 ft/s²). In terms of discomfort, the lowest tolerance level for vibration occurs at about 5 Hz (Grether 1971). And, a sudden increase in vertical acceleration caused by vibrations can lead to an overall discomfort for drivers (Griffin 1986; Griffin 2007; Mansfield 2012). The effects of vibration depend on the frequency of the vibration, the magnitude of the vibration, the waveform and direction, and the application site (Mansfield 2004). Broadly, the response to vibration can be categorized into three areas (**Figure 2.3**):

- Motion sickness: Very low-frequency motion of the whole body, which may cause minor discomfort.
- Whole-body vibration: Vibration usually between about 1 and 50 Hz, typically experienced in vehicles.
- Hand-arm vibration: High-frequency vibration potentially into the kHz range, typically experienced through the use of power tools.

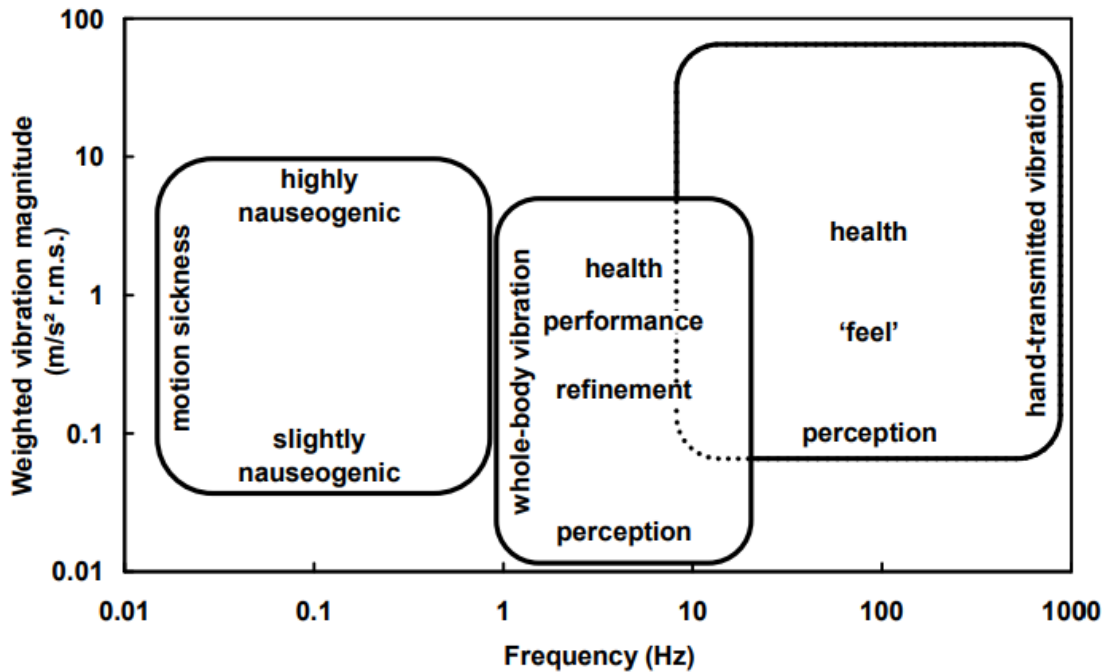


Figure 2.3 Typical frequency ranges and effects of vibration on the body (Mansfield 2004)

For the vibration analysis, the spectrum analysis is commonly used (Goldman 1999). Fast Fourier transforms are mathematical calculations that transform, or convert, a time-domain waveform (amplitude versus time) into a series of discrete sine waves in the frequency domain (Cochran et al. 1967). It initially was applied for diagnosing mechanical issues caused by vibrations. For instance, Farokhzad (2013) conducted a study using FFT to analyze the machine vibration to detect faults in the mechanical components. In 2005, a study analyzed the frequencies of vibrations when vehicles passing the temporary work zone rumble strips using FFT. All of the sounds were dominated by frequencies below 200 Hz. Kim et al. (2013) studied the relationship of vibration levels and shapes of rumble strips located on the highway tollgate in Korea using FFT. A study investigated the noise emission effects of TRS on urban road traffic by using FFT (Sabato and Niezrecki 2016). FFT was also adopted in a rumble strip study to determine the bicycle-friendly rumble strip configurations (Torbic 2001).

2.6 Gaps in Previous Research and Proposed Work

According to the literature review, conventional countermeasures such as signage or pavement markings have the limitation in providing sufficient information to WW drivers in time. For example, WW signs can only visually alert WW drivers in the assumption of being seen by them. Regardless of the false alarms, applying ITS costs more because of construction, equipment, and maintenance. Furthermore, existing countermeasures have little or no effect on controlling vehicle speeds on freeway off-ramps. Therefore, there is an urgent need to deploy low-cost but effective countermeasures that can alert WW drivers by elevated in-vehicle sounds and vibrations; meanwhile, discourage excessive speeds and lower speed differences for RW drivers. The literature showed that DRS, as modifications from TRS, have the potential to deter WWD incidents and speeding issues on freeway off-ramps. They have not been implemented or studied by other transportation agencies in the past. Providing guidelines for the DRS implementation to DOTs, traffic agencies, and policymakers is also in demand.

Chapter 3. Methodology

3.1 Closed-Course Verification Tests

The purpose of verification tests was to verify the previous test results and modify conceptual designs for field implementation. The procedure of testing and analyzing is parallel to the previous study conducted by Yang et al. (2018). The results showed the consistency with previous study and recommendations of field implementation plans were proposed based on the findings.

3.1.1 Site Description

DRS verification tests were conducted at the pavement test track of the National Center for Asphalt Technology (NCAT) at Auburn University. Different patterns of DRS were deployed on a ramp at the Auburn University Erosion and Sediment Control Testing Facility (AU-ESCTF) in NCAT. **Figure 3.1** shows the testing location, which has two 12-ft lanes and closed facilities during the study period. The testing road is over 1,000 ft long, which provides enough space to install different DRS patterns and accommodates the need for the frequent acceleration and deceleration of the testing vehicle.



Figure 3.1 Location for DRS Verification Tests (Imagery © 2019 Google, Map data © 2019 Google.)

3.1.2 Data Collection

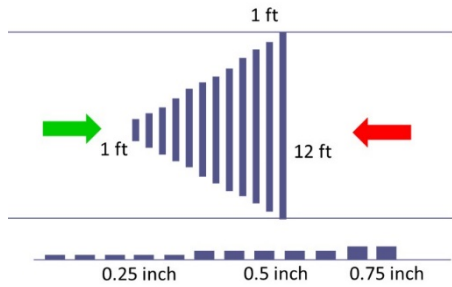
Sound and vibrations inside the vehicle were measured using a full-size passenger cars (2016 Nissan Altima). The acoustical signature was recorded by an Extech HD600 Sound Level Meter, which records 10 decibel readings every second. The vibration data was recorded using a Measurement Specialists 35201A accelerometer, which collects 100 samples per second. This device allows researchers to measure acceleration rates along the longitudinal, lateral, and gravitational axes. The sound level meter was located at an average driver's ear height, and the tri-axial accelerometer was placed on the driver's seat. Both the sound level meter and accelerometer were controlled by a laptop computer via the equipment software and serial port. After conditioning the sound and vibration signals, all information was logged directly into an Excel file. During the tests, the air-conditioner, stereo, and any other sound-producing sources were turned off, and the windows were closed to eliminate as much noise as possible.

3.1.3 DRS Patterns for Verification Tests

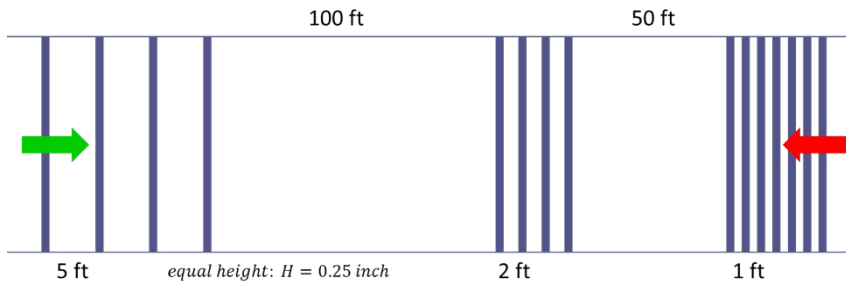
Five DRS design patterns with different configurations (thickness of rumble strips) were tested before (Yang et al. 2018). Three patterns (i.e., C, D3, and E) were recommended for further verification. Pattern D3 was modified based on the advance warning markings for speed humps (see Figure 3B-31 in the MUTCD), which has a triangle appearance from the top view as the length of the strip gradually increases from 1 to 12 ft. The thickness of the strip with a length from 1 to 5 ft is 0.25 in. The 6 to 10-ft strips have the same thickness of 0.5 in. The longest two strips (11 and 12 ft long) are both 0.75 in. thick. In **Figure 3.2-a**, the green arrow indicates the RW driving direction. When an RW driver drove through, the first five strips had an equal thickness of 0.25 in. The thickness of the following five strips was increased to 0.5 in., while the last two were 0.75 in. thick. Pattern C is similar to the TRS but has different spacing. Three sets of strips with different spacings of 1, 2, and 5 ft, respectively, were placed apart with 100 and 50-ft spacing, as shown in **Figure 3.2-b**. All the strips had the same thickness of 0.25 in. The strips in Pattern E (**Figure 3.2-c**) have a triangular cross section. The width of the strip was also 6 in., and the maximum thickness was about 0.5 in. A new Pattern E.1 (**Figure 3.2-d**) was developed to double the number of strips on the inside of the travel lane to increase vibration for WW drivers. All the strips had the same thickness of 0.25 in.

The preformed polymer tape strips provided by the vendor are nonreflective, self-adhesive, and come in 50-ft rolls. The strips were first cut to the appropriate length using a utility knife. The adhesive, which was pre-applied to the strip by the manufacturer, was exposed by removing the protective backing. These strips were used for testing all the patterns except Pattern E, which needed to be custom manufactured because of the triangular cross section. The mold was made of wood covered with non-stick aluminum foil. Thermoplastic was used to make the strips. The DRS

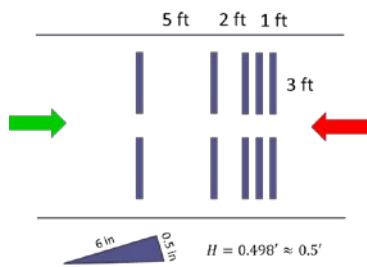
was installed following the standard procedure when the pavement was dry, and its temperature just before installation was warmer than 50° F. The pavement was swept with a push broom to remove loose debris. Once the pavement was clean, it was marked using masking tape to indicate the proper placement for the strips.



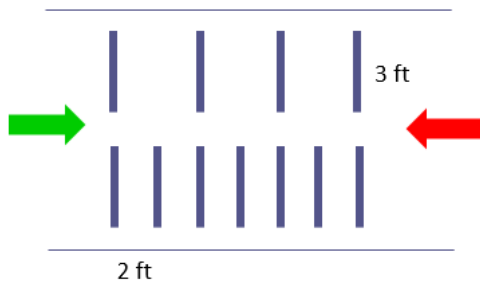
(a) Pattern D3



(b) Pattern C



(c) Pattern E



(d) Pattern E.1



Note: Green Arrow = Right-Way Direction; Red Arrow = Wrong-Way Direction

Figure 3.2 DRS Patterns for Verification Tests

3.1.4 Verification Test Schemes

Sound and vibration data were collected for both RW and WW directions for different DRS patterns. The experiment vehicle traveled in both directions at speeds of 10, 15, 20, 25, 35, and 45 mph. These present typical approach speeds at different segments of off-ramps. The sound and vibration measurements were taken for the ambient condition and DRS patterns. The ambient condition was defined as the test vehicle traveling at a specified speed along the roadway section before the installation of DRS. Data collection was then duplicated on the same road segment with the installation of the DRS patterns. At least 6 runs were conducted for each DRS pattern for each direction and speed category.

The verification test was performed on November 19, 2016, and November 1, 2017. On November 19, 2016, the test verified the previous results of Pattern C, Pattern D3, and Pattern E including sound and vibration levels, and their differences between RW and WW directions. The modified Pattern E.1 was tested on November 1, 2017.

Table 3.1 Verification Test Schemes

Date	DRS Pattern	Test Speed (mph)	Total Runs
November 19, 2016	Pattern C	10, 15, 20, 25, 35, 45	60
	Pattern D3	10, 15, 20, 25, 35, 45	60
	Pattern E	10, 15, 20, 25, 35, 45	60
	Ambient Condition	10, 15, 20, 25, 35, 45	36
November 1, 2017	Pattern E.1	10, 15, 20, 25, 35, 45	60
	Ambient Condition	10, 15, 20, 25, 35, 45	36

3.2 Field Implementation Tests

The field implementation tests were conducted for the purpose of collecting data on WWD incidents, vehicle speeds, sound and vibrations caused by DRS after implementing them on two freeway off-ramps in Alabama.

3.2.1 Site Description

To select the locations for implementing DRS, a prediction model was first applied to identify high-risk locations for WWD (Atiquzzaman and Zhou 2018). The model can estimate the probability of WWD entries at an off-ramp terminal of a partial cloverleaf and a diamond interchange based on geometric design features, usage of traffic control devices, area types, and traffic volumes. Two southbound off-ramps at Exits 208 and 284 on I-65 in Alabama were ranked as the top-two-highest probabilities for WWD entries within the state. Exit 208 had the WW entry probability of 61% (the chance of having one WWD crash within five years), while Exit 284 had 79%. WWD incident data were collected to verify the prediction results. A total of 10 and 17 WWD incidents were observed at Exits 208 and 284, respectively, during a typical weekend. Therefore, these two sites were selected to implement the DRS.

Exit 208 on I-65 is a partial cloverleaf interchange located near Clanton, Alabama. According to the 2017 Alabama Traffic Data, the annual average daily traffic (AADT) on the southbound off-ramp was 1,550 vehicles per day, which included 20% heavy vehicles. The lane width of the southbound off-ramp is about 16 ft. The southbound on and off-ramps are separated by a wide median. The off-ramp terminal is a stop-controlled unsignalized intersection.

Figure 3.3 shows an aerial photo of Exit 208 on I-65. Along the southbound off-ramp, several traffic control devices were installed to prevent drivers from entering the WW. Two DNE

(Do Not Enter) signs were installed on both sides of the ramp terminal which are visible to potential WW drivers from the crossroad. Stop signs were mounted on the back of the DNE signs facing the RW drivers. A combination of signs of DNE, Stop, and One Way signs were placed at the center of the channelization island. About 85 ft away from the ramp terminal, a pair of WW arrows with raised reflective pavement markers (RRPMs) were installed with red lenses facing WW drivers. Two WW signs were placed on both sides of the ramp around 45 ft farther. Two single WW arrows and two lane-use arrows were installed on the ramp curve. Enhanced by RRPMs, they were 430, 500, 780, and 850 ft away from the ramp terminal, respectively. An advisory ramp speed sign of 25 mph was located near the freeway gore area, which was 890 ft away from the ramp terminal. A new channelization island was installed at the ramp terminal by ALDOT regional engineers in summer 2018.

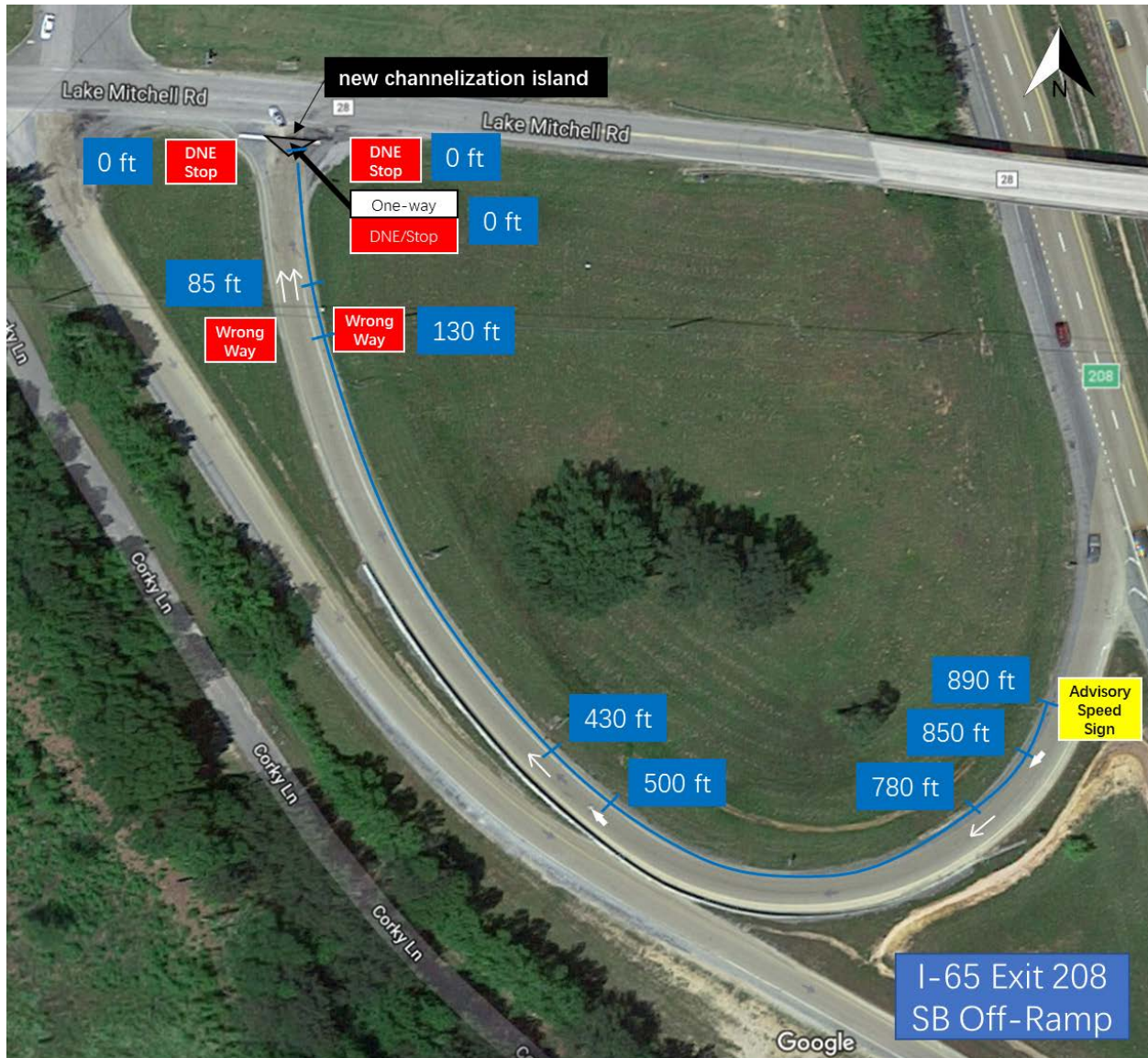


Figure 3.3 Southbound Off-Ramp at Exit 208 on I-65, AL (Imagery © 2019 Google, Map data © 2019 Google.)

Exit 284 on I-65 is a partial cloverleaf interchange located 25 miles north of Birmingham, AL. According to the 2017 Alabama Traffic Data, the AADT on the southbound off-ramp was 1,260 vehicles per day, which consisted of 26% heavy vehicles. The lane width of the off-ramp is about 12 ft. The southbound on- and off-ramps are divided by a concrete barrier. At the southbound off-ramp terminal, right-turn traffic is yield-controlled at the unsignalized intersection, while left-turn traffic requires a complete stop.

Figure 3.4 shows an aerial photo of Exit 284. Compared with Exit 208, fewer traffic control devices were installed on the southbound off-ramp at this site. A DNE sign was placed on the roadside of the ramp terminal to prevent drivers from entering the ramp. A yield sign was mounted on the back of the DNE sign for the right-turn vehicles. A combination of DNE, Stop, and One-Way signs was placed at the center of the channelization pavement marking. Thirty feet away from the ramp terminal, a KEEP RIGHT sign (see R4-7 in MUTCD) with an object marker (see OM1-1 in MUTCD) was installed on the concrete barrier. Dual WW arrows enhanced by RRPMS were placed 100 ft away from the ramp terminal. It should be noted that the dual WW arrows were faded and RRPMS were damaged. Two WW signs on the right side of the off-ramp were installed sequentially, which are 100 and 215 ft away from the ramp terminal. An advisory ramp speed sign of 30 mph is located near the freeway gore area, which is 690 ft away from the ramp terminal.



Figure 3.4 Southbound off-ramp at Exit 208 on I-65, AL (Imagery © 2019 Google, Map data © 2019 Google.)

3.2.2 Data Collection

The collected data included video data that captured WW incidents, speed data on the off-ramp, and in-vehicle sound and vibration data caused by the DRS and exterior sound (noise level) generated by the DRS. Portable traffic cameras (COUNTcam2) were used to monitor WW incidents and driver behavior. The speed data were collected by magnetic sensors called an NC-350 BlueStar Portable Traffic Analyzer (NC-350). Unlike other speed-measurement equipment, such as radar guns and tube counters, the NC-350 can provide individual vehicle data, including speed, direction, length, gap, etc. The NC-350's battery can last up to 21 days. Additionally, the sealed design of NC-350 made it robust against moisture and pressure. Protective covers were used to cover and secure the sensors. In-vehicle sound and vibrations were measured using a full-size passenger car (2016 Nissan Altima). The acoustical signature was recorded by an EXTECH HD600 Sound Level Meter, which collected 10 decibel readings every second. The vibration data was recorded using a Measurement Specialists 35201A accelerometer, which recorded 100 samples per second. This device measured acceleration rates along the longitudinal, lateral, and gravitational axes. The data collection devices are shown in **Figure 3.5**.



Figure 3.5 Data Collection Equipment: (a) Video Camera; (b) Magnetic Sensor; (c) Sound Level Meter; (d) Accelerometer

Video cameras were set at a traffic sign support on the opposite side of the crossroad at the off-ramp terminals. They were secured to extension poles, which were locked to the sign support on the roadside. The poles can be extended so that cameras had an approximate height of 10 ft. The cameras further had a wide, color viewing angle of 170 degrees to accommodate the entire off-ramp. The cameras can record videos with a resolution of 720P up to 72 hours after being fully charged. The sealed design made these cameras weather-proof. **Figure 3.6** shows the view ranges of video cameras. All the RW and WW movements can be recorded.

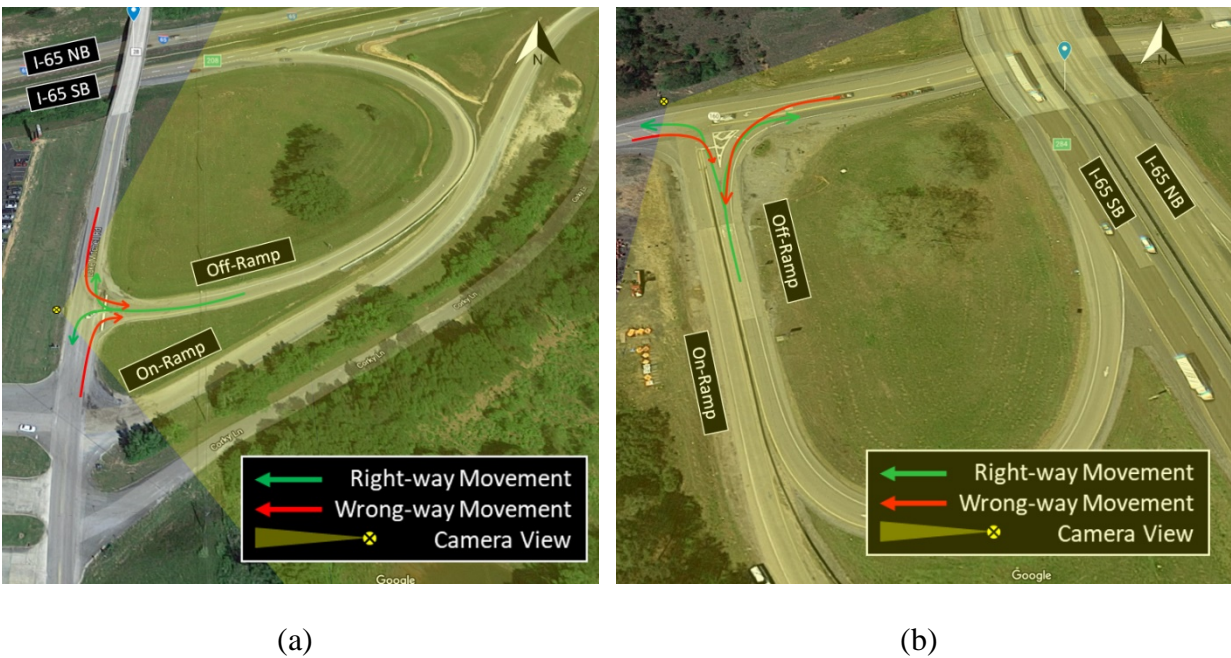


Figure 3.6 Camera Deployment at (a) Exit 208 and (b) Exit 284 on I-65, AL (Imagery © 2019 Google, Map data © 2019 Google.)

A total of nine magnetic speed sensors (NC-350), which were labeled following their device serial numbers from #96 to #104, were used to collect speeds on off-ramps. At Exit 208 (**Figure 3.7**), sensors #96 and #97 were installed in front of two stop bars to record RW speeds near stop bars and WW entering speeds. Sensor #98 was positioned behind the dual WW arrows to record RW speeds, while vehicles approached the off-ramp terminal, and WW speeds near WW

signs. Sensor #99 was placed near the end of the concrete barrier, about 180 ft away from #98. Sensor #100 was installed 30 ft before the advisory ramp speed sign to record RW speeds before entering the ramp curve segment and WW speeds before entering the freeway mainline.

At Exit 284 (**Figure 3.8**), sensor #101 was placed ahead of the yield line to collect RW speeds under the yield control and WW entering speeds. Based on the WWD monitoring, very few WW incidents were found to enter the off-ramp crossing the stop bar at Exit 284. Therefore, no speed sensor was placed there due to limited number of sensors. Sensor #102 was installed immediately behind the dual WW arrows to collect RW approaching speeds near the off-ramp terminal and WW speeds around the first WW sign. Sensor #103 was placed 180 ft away from #102 to measure speeds of RW/WW vehicles exiting/entering the ramp curve. As with Exit 208, sensor #104 was also installed 30 ft before the advisory ramp speed sign to measure the RW and WW speeds close to freeway mainline.

Protective covers were applied to secure and protect the sensors. To install covers, 3/16" holes were predrilled; 1/4" × 3-1/4" hex washer head self-tapping masonry screws were then installed with extra 1/4" washers. A total of eight screws were used to completely cover and secure each sensor. The installation and finished conditions are shown in **Figure 3.9**.



Figure 3.7 NC-350 Deployments at Exit 208 on I-65, AL (Imagery © 2019 Google, Map data © 2019 Google.)



Figure 3.8 NC-350 Deployments at Exit 284 on I-65, AL (Imagery © 2019 Google, Map data © 2019 Google.)



(a) Installing the Protective Cover



(b) An NC-350 with the Protective Cover

Figure 3.9 NC-350 Field Installation

During the field tests, a full-size passenger car (2018 Nissan Maxima) was used. The sound-level meter was mounted close to the driver's right ear, and an accelerometer was fixed on the driver's seat between the driver's legs. Both the sound level meter and accelerometer were controlled by a laptop computer via the equipment software and serial ports. After conditioning the sound and vibration signals, all information was logged. During the tests, sound-producing sources such as air-conditioner and stereo were turned off, and the windows were closed to eliminate as much noise as possible.

3.2.3 DRS Implementation and Installation

According to the recommendations from the previous tests (Zhou et al. 2018), Pattern D3 was proposed to be installed near the stop bars of off-ramps. Pattern C was recommended to be placed in the middle of the straight long segment of an off-ramp. It was suggested that Pattern E.1 should be installed at the tangent before sharp horizontal ramp curves.

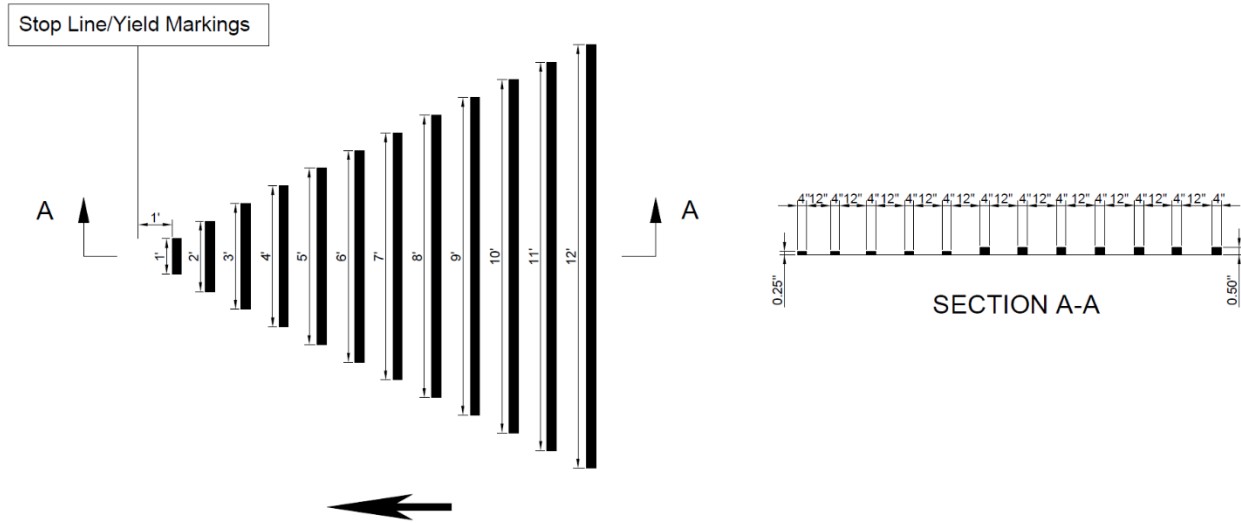
DRS Patterns and Field Deployments

Figure 3.10 shows Pattern D3 modified based on the advance warning markings for speed humps (see Figure 3B-31 in the MUTCD), which has a triangle appearance, as the length of the strip gradually increases from 1 to 12 ft. Strip with lengths from 1 to 5 ft were 0.25 in. in thickness. The remaining strips had the same thickness of 0.5 in. No strips have thickness over 0.5 in. according to the recommendation from ALDOT. Pattern D3 was designed to be positioned 1 ft after stop bars or yield lines in the field. Based on the ALDOT panel members' suggestions, the direction of Pattern D3 was reversed. Like an arrow, the triangle shape can now provide a visual cue for helping both RW and WW drivers understand the correct direction of the traffic flow.

Pattern C was similar to the TRS but had various spacings. Three sets of strips with spacings of 1, 2, and 5 ft, respectively, were placed apart with 100 and 50 ft spacing, as shown in **Figure 3.11**. All the strips had the same thickness of 0.25 in. Due to different lane widths, strips have unequal lengths at the two sites, which were 7 ft at Exit 208 and 4.5 ft at Exit 284. A 2-ft center gap was left in the middle of the lane to allow motorcycles and emergency vehicles to bypass the strips. They can utilize the gaps to pass the DRS without experiencing additional sound and vibrations. To avoid the overlapping effects of sound and vibrations from WW arrows, Pattern C was placed 3 ft behind the dual WW arrows at both sites.

Pattern E.1 (**Figure 3.12**) was designed to have double strips on the inside of the RW travel lane for increasing sound and vibrations for WW drivers. Spacing between the strips on the RW driver side was 4 ft and 2 ft on the WW driver's side. Yellow strips were applied on the RW driver's side at Exit 208, and white strips were used for both sides at Exit 284. A 2-ft center gap was also left in the middle of the lane to serve motorcycles and emergency vehicles. Pattern E.1

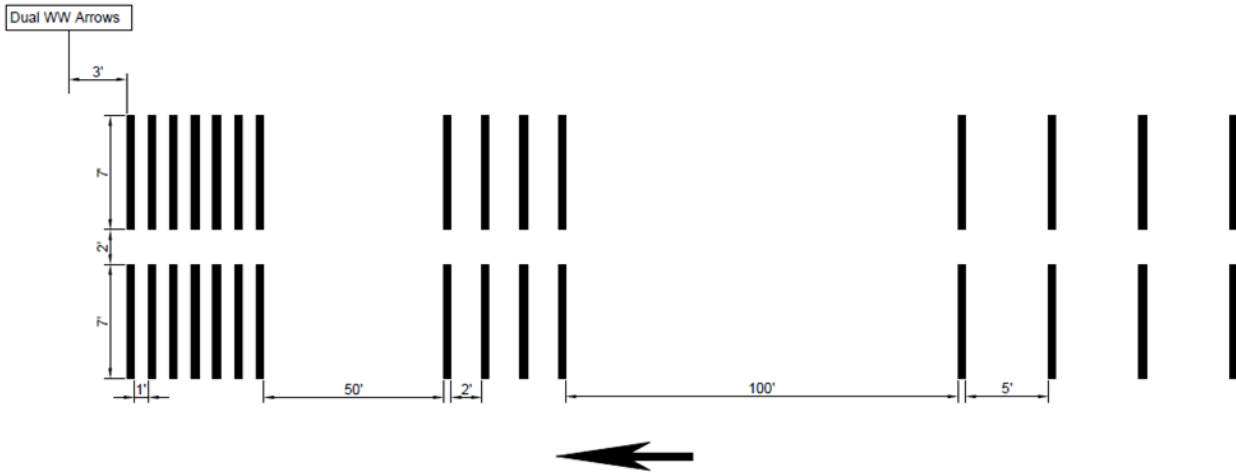
was installed 30 ft ahead of the advisory ramp speed sign. At that point, RW drivers were able to clearly see the advisory speed sign and horizontal curve ahead based on the field review.



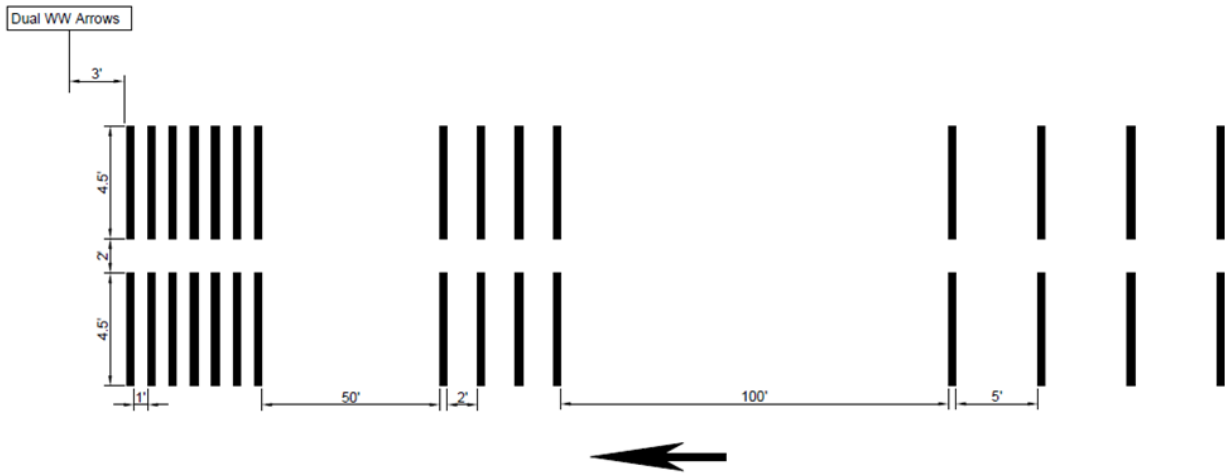
Note:

- 1) Not to scale;
- 2) ← = Traffic Flow.

Figure 3.10 DRS Pattern D3 Implementation Design



(a) Pattern C at Exit 208

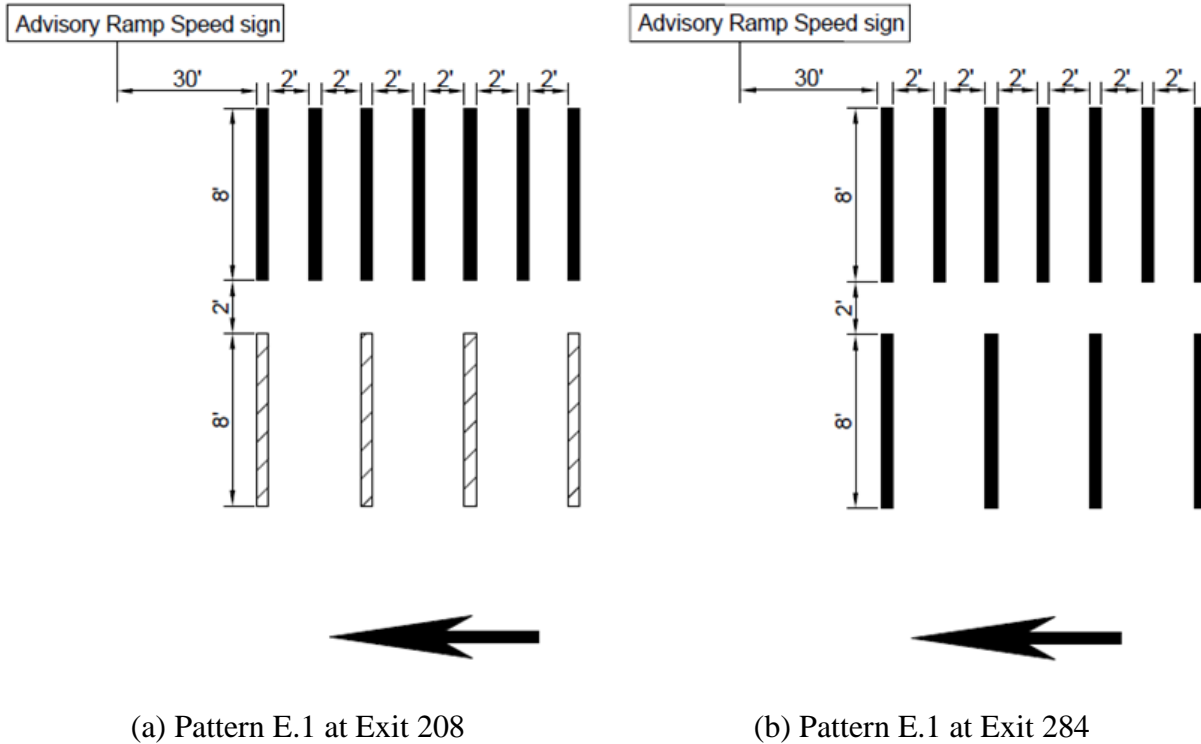


(b) Pattern C at Exit 284

Note:

- 1) Strips have equal thickness of 0.25" and width of 4";
- 2) Strips have different lengths at two sites (Exit 208: 7'; Exit 284: 4.5');
- 3) Not to scale;
- 4) ← = Traffic Flow.

Figure 3.11 DRS Pattern C Implementation Design



Note:



- 1) Strips have the equal thickness of 0.25" and width of 4";
- 2)  = Yellow strips;
- 3) Not to scale;
- 4)  = Traffic Flow.

Figure 3.12 DRS Pattern E.1 Implementation Design

Figure 3.13 and **Figure 3.14** illustrate the implementation configurations of the DRS in the field. In addition to alerting WW drivers directly via sound and vibrations caused by DRS patterns, they can also alert WW drivers to pay more attention to the other WW-related traffic control devices. Pattern D3 can work together with DNE and/or One Way signs to counter initial WW entries. Pattern C can alert WW drivers of WW signs. Pattern E.1 can serve as the last

countermeasure to deter WWD onto the freeway mainline. **Figure 3.15** shows field photos of DRS patterns.



Figure 3.13 DRS Implementation at Exit 208 on I-65, AL (Imagery © 2019 Google, Map data © 2019 Google.)



Figure 3.14 DRS Implementation at Exit 284 on I-65, AL (Imagery © 2019 Google, Map data © 2019 Google.)



(a) Pattern D3 at stop bars



(b) Pattern D3 at the yield line



(c) Pattern C (1-ft group)



(d) Pattern C (2-ft group)



(e) Pattern C (5-ft group)



(f) Pattern E.1 (yellow strips)



(g) Pattern E.1

Figure 3.15 Field Photos of DRS Patterns

DRS Installation

Installation of the DRS was conducted by a contractor (Ozark Striping, Inc) in Alabama. The material of the strips was thermoplastic. Therefore, installing the DRS required a dry pavement surface. Additionally, the surface temperature needed to be above 10°C (50°F).

Figure 3.16 summarizes the procedure for installing the DRS. First, the temporary traffic control was provided by ALDOT division maintenance crews. From the point 500 ft away from the advisory ramp speed sign, cones were placed on the right lane of freeway mainlines. The cones were used to prevent traffic from approaching and entering the off-ramp. Flashing LED message and arrow boards mounted on the trucks alerted vehicles of the closed off-ramp and making lane changes. A truck with a truck-mounted attenuator and dynamic message board was located ahead of the installation area to protect workers. Workers then started measuring distance based on parameters from the above section. Edges of strips were marked by road chalk before the surface being cleaned by the blower. Masking tape was applied to the ends of each strip. Afterward, a worker operated a hand-pushed thermoplastic screed road marking machine to install the DRS. Upon finishing the installation, glass beads were sprinkled on the strips to improve their retroreflectivity. Masking tape, as well as the excessive thermoplastics on them, were removed. Lastly, installations were inspected by using a tape measure.



(a) Traffic control (ramp closed)



(b) Protection (truck-mounted attenuator and dynamic message board)



(c) Measure distance



(d) Mark and sketch



(e) Clean the surface



(f) Tape the ends of the strips



(g) Install the DRS



(h) Improve reflection and remove tapes



(i) Inspection after installation

Figure 3.16 Procedure of DRS Installation

3.2.4 Field Implementation Schemes

Table 3.2 summarizes the study periods and schedule of the DRS implementations. The week from November 2 to 8, 2018, was defined as the before week (W0), when the speed data was first collected. The after periods consisted of 8 weeks. During W0, no DRS was installed. To eliminate the potential overlapping effects of different DRS patterns, Pattern E.1 was first implemented on the first day of W1. At the beginning of W2, Pattern C was installed. On the first day of W3, Pattern D3 was placed in the field. Additional video data was collected to monitor WW incidents during random weekends (named W4-8). Speed data was recorded for W0 to W3. In addition, 72-hour (weekend) video data was recorded during the weekend of each study period. These two locations will continue to be randomly monitored for WWD incidents.

The installation of the DRS typically took 3 hours for one site, including transportation from one site to another. Thus, speed data collected during the DRS installations was removed. Traffic volumes counted by NC-350 are also listed in **Table 3.2**. The volumes were consistent throughout the weeks. Compared with the 2017 Alabama Traffic Data, it was found that volumes at Exit 208 were relatively lower than the reference data. Seasonal variations of traffic volumes (which are typically higher in the summer and lower in the winter) could result in the reduction of traffic volumes. To evaluate the operational and safety impacts of the DRS, other modifications such as geometric changes at these off-ramps should be avoided. According to the ALDOT district administrators, a resurfacing project at Exit 284 started from Week5 (W5). All the pavement markings including DRS except the stop bar on the surface have not been reinstalled.

Table 3.2 DRS field implementation schemes

Schedule		DRS Pattern Installed			Traffic Volume*	
Phase	Time	E.1	C	D3	Exit 208	Exit 284
Before	W0				1,347	1,127
After	W1	×			1,291	1,180
	W2	×	×		1,299	1,195
	W3	×	×	×	1,379	1,208
	W4	×	×	×	-	-
	W5-8	×**	×**	×**	-	-

Note:

- W0 = Week0 (11/02/2018-11/08/2018); W1 = Week1 (12/12/2018-12/18/2018); W2 = Week2 (12/18/2018-12/24/2018); W3 = Week3 (01/06/2019-01/12/2019); W4 = Week4 (03/08/2019-03/11/2019); W5 = Week5 (08/09/2019-08/12/2019); W6 = Week6 (08/30/2019-09/02/2019); W7 = Week7 (09/07/2019-09/10/2019); W8 = Week8 (12/13/2019-12/15/2019).
- *Data from NC-350; **DRS removed at Exit 284.
- Reference AADT: Exit 208 = 1,550; Exit 284 = 1,260 (Source: 2017 Alabama Traffic Data).

3.2.5 Evaluation of Sound and Vibrations

The time-series technique was used to visualize the sound data. It was applied to obtain an understanding of sound data taken over time, including the peaks when vehicles pass the DRS. The mean was employed to show the average sound level. *T*-tests at the significance level of 0.05 were also used to discern significant differences between the average RW and WW sound levels.

For evaluating vibrations, root mean square (RMS) amplitudes of vibrations were employed to present the equivalent constant values. Due to the different presentations of the sound and vibration data, it was close to zero by averaging the vibrations on the DRS. Thus, it was more meaningful to compare their variances between RW and WW directions. Thus, *F*-tests at the significance level of 0.05 were then used to check whether there was a significant difference in variance between RW and WW vibrations.

In contrast with sound data, vibration required a spectrum analysis because different vibration patterns may be expressed similarly in the time series. Equation 3.1 presents the Fourier Series, which shows the procedure of dividing a nonstandard vibration signal into a list of standard vibration signals (i.e., sine and cosine signals). The vibration signals caused by the DRS can be presented as $f(x)$, which equals to the sum of various standard signals with different phases kx (i.e., $1/2\pi, \pi, 3/2\pi, \dots$) and the halved offset (a_0):

$$f(x) = \frac{a_0}{2} + \sum_{k=1}^n [a_k \cos(kx) + b_k \sin(kx)] \quad (3.1)$$

where $f(x)$ is the original signal, a_0 is the offset phase, a_k and b_k are the amplitudes of associated standard signals, kx is the multiple of $1/2 \pi$ (e.g., $1/2\pi, \pi, 3/2\pi, \dots$).

The fast Fourier transform (FFT) algorithm can be employed to compute a Discrete Fourier transform (DFT). The DFT can be used to characterize the magnitude and phase of a signal. Consider a finite sequence of N signal data points that are sampled at intervals of Δt , $x(j) = x(j\Delta t)$, where $j = 0, 1, 2, \dots, N-1$, and Δt is the sampling interval. The DFT of $x(j)$, denoted as $X(n)$, has the form

$$X(n) = \sum_{j=0}^{N-1} x(j) e^{-\frac{i2\pi nj}{N}} \quad (3.2)$$

For $n = 0, \dots, N-1$, where $i = (-1)^{1/2}$. The inverse DFT is defined by

$$x(j) = \frac{1}{N} \sum_{n=0}^{N-1} X(n) e^{\frac{i2\pi nj}{N}} \quad (3.3)$$

Equations 3.2 and 3.3 make up the Fourier transform pair. The value n in $X(n)$ is related to the frequency by

$$f(n) = \frac{n}{N\Delta t} \quad (3.4)$$

where N is the number of elements of the sequence considered and $N\Delta t$ the total length of the sample. Using Equation 3.2 implies that the analysis is undertaken in the frequency domain, and the sampling interval in the frequency domain is given by

$$\Delta f = \frac{1}{N\Delta t} \quad (3.5)$$

Δf defines the frequency resolution, and Δt the time resolution. It is seen from Equation 3.5 that the product of Δf and Δt is a constant for a given value of N . It indicates that increasing the frequency resolution reduces the time resolution and vice versa.

Because Equations 3.2 and 3.3 are of the same form, a single FFT algorithm can be used to perform both transformations, and the time series $x(j)$ and its DFT $X(n)$ can be transformed without losing information. The reason for using the FFT is its capability of time saving, owing to the efficiency of the FFT algorithm. The number of mathematical computations required is proportional to $N \log_2 N$ instead of N^2 for the direct implementation of the DFT if N is a highly composite number such as a power of 2.

Hence, FFT was employed to measure vibration amplitudes as a function of frequency. FFT converted the original vibration data from the time domain to the representation in the frequency domain. Nonstandard vibrations can be treated as a combination of various vibrations with different frequencies and amplitudes. The X-axis in the FFT plot stands for frequencies ranging from low to high, while the Y-axis shows the amplitude associated with each frequency.

3.3 Summary

This chapter introduces the data used, data collection methods, DRS patterns, sites for testing and implementation, and methods employed to analyze the data.

Three DRS patterns were developed for field implementation. They were first tested in the closed-course facility and were later installed at different locations on two freeway off-ramps in Alabama. Four types of data were collected. Video data was used for monitoring WWD incidents in the field. Speed data which was collected by magnetic sensors was to evaluate the speed changes caused by DRS. Sound and vibration levels were measured by using a sound level meter and an accelerometer. The data was processed to assess the difference in sound and vibration levels between RW and WW directions. Different methods were used to analyze the data, including descriptive statistics and statistical analysis. Time-series and spectrum analysis were specifically employed to evaluate sound and vibrations.

Chapter 4. Analysis and Results from Closed-Course Tests

This chapter summarizes the results from the closed-course tests. The purpose of these tests was to 1) verify the results from previous studies, 2) further investigate the characteristics of DRS, and 3) propose recommendations for field implementation.

4.1 Comparisons of Sound and Vibration at the Different Speeds

The analysis results of the verification tests were found consistent with previous test results (Yang et al. 2018). Both testing results indicated that all three recommended patterns can generate adequate sound and vibration in the WW direction to alert drivers with a minimum increase of 7.2 dBA in sound and 0.2 *g* increase in vibration over the ambient condition. *T*-tests were conducted to verify if there was a significant difference at a confidence level of 95% in sound and vibrations generated by DRS between RW and WW directions. **Table 4.1** summarizes the results of the *t*-tests with a confidence level of 95%. According to *p*-values, Pattern C showed a significant difference in sound and vibration levels between RW and WW at speeds (10, 15, 20 and 25 mph) with *p*-values less than 0.05. Pattern D Configuration 3 showed no significant difference between RW and WW directions for both sound and vibration at the same speed with *p*-values over 0.05. Pattern E was only significantly different in the vibration at a speed of 45 mph (*p*-value < 0.01) but not significantly different in the sound levels. However, the modified Pattern E.1 did show significantly different vibrations at speeds of 35 mph or lower and different sound levels at speeds of 10 and 15 mph.

Table 4.1 P-values of Difference of Sound and Vibrations between RW and WW Directions at Different Speeds

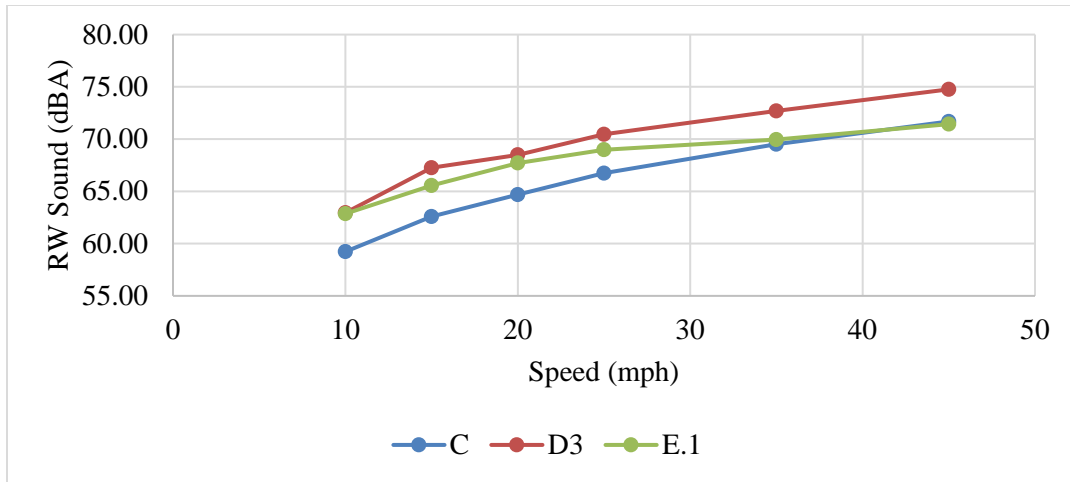
	Pattern	10 mph	15 mph	20 mph	25 mph	35 mph	45 mph
	Sound (dBA)	Pattern D3	0.60	0.51	0.63	0.27	0.18
Pattern C		0.01	< 0.01	0.04	< 0.01	0.09	0.55
Pattern E		0.27	0.11	0.39	0.52	0.43	0.41
Pattern E.1		0.03	0.04	0.09	0.36	0.42	0.48
Pattern		10 mph	15 mph	20 mph	25 mph	35 mph	45 mph
Vibration (g)	Pattern D3	0.08	0.13	0.08	0.10	0.19	0.07
	Pattern C	< 0.01	< 0.01	< 0.01	< 0.01	0.65	0.65
	Pattern E	0.17	0.28	0.10	0.59	0.18	< 0.01
	Pattern E.1	< 0.01	< 0.01	0.02	0.04	0.01	0.06
	Pattern	10 mph	15 mph	20 mph	25 mph	35 mph	45 mph

Besides the statistical analysis, relationships between levels of sound and vibrations and vehicle speeds were investigated. Results indicated that vehicle speeds have strong correlations with the sound and vibrations generated by DRS. In **Figure 4.1**, the average sound levels at each speed category were compared. Sound levels increase with the increase of vehicle speeds at both RW and WW directions. The difference (WW minus RW) between RW and WW directions showed that Pattern E.1 has the largest difference in sound at 45 mph. Pattern C presented no significant difference in sound levels generated from RW and WW directions. Pattern D3 created louder sound in the RW direction than WW at lower speeds (less than 25 mph); it was then reversed at higher speeds.

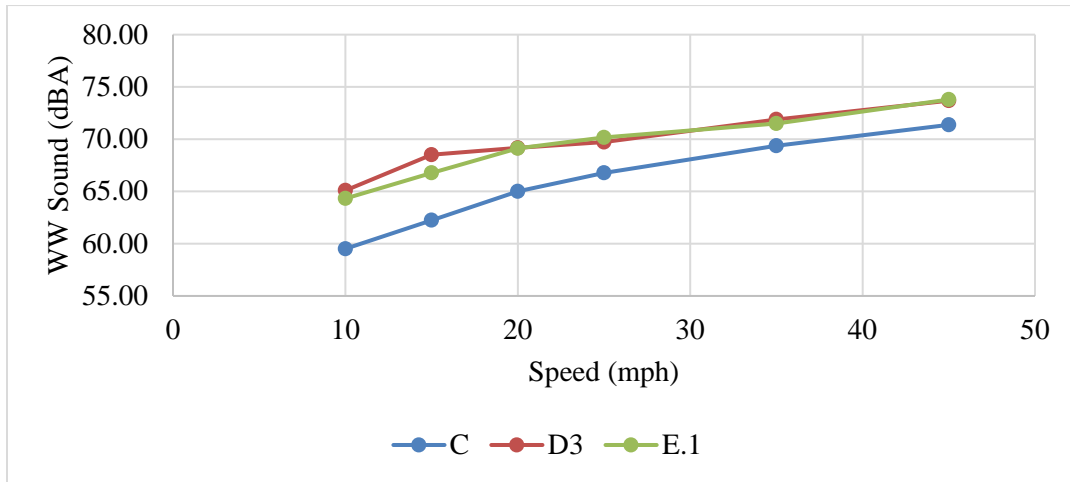
Moreover, RMS values of vibrations at each speed category were compared. **Figure 4.2** showed the vibration levels generated by DRS at different speeds. For Patterns C and E.1, higher speeds can result in vibrations with larger RMS values. However, decreased RMS values were observed for Pattern D3 as vehicle speeds increase. By observing the differences (WW minus RW)

between RW and WW directions, Pattern E.1 presented the largest number in RMS value of vibrations at 45 mph. Similar to the sound levels, Pattern C showed almost no difference. The difference in RW and WW vibrations suggested that Pattern D3 can create larger amount of vibrations in RW direction at lower speeds (less than 25 mph); WW direction will produce larger amount of vibrations at higher speeds.

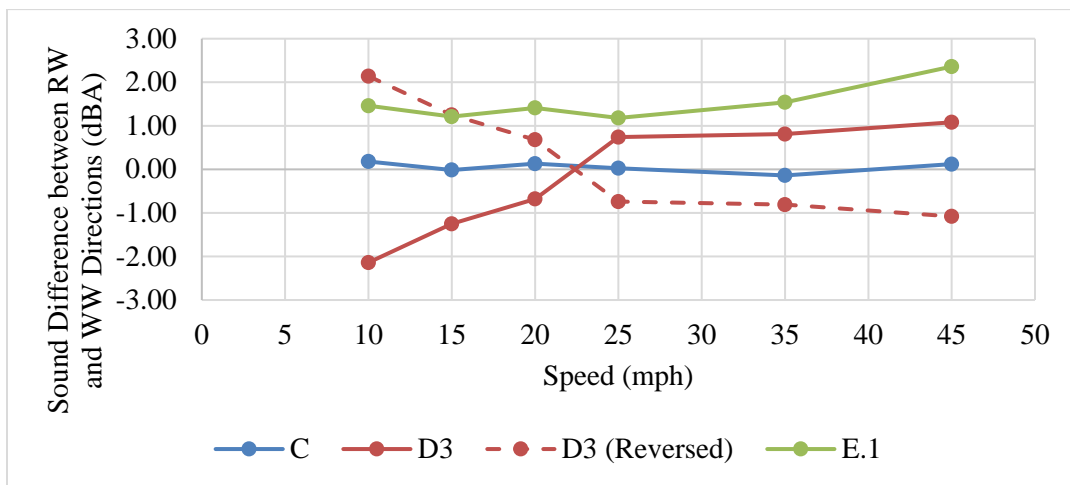
Based on the above results, the sound and vibrations generated by DRS are related to vehicle speeds. Pattern E.1, on average, can produce more amount of sound and vibrations in WW direction than RW direction. This pattern also generates the largest amount of sound and vibrations at 45 mph in WW direction than RW direction. Drivers could perceive much louder sound and severe vibrations at lower speeds when passing Pattern D3. An increased travelling speed will increase the levels of sound and vibrations with Pattern C. To further identify where to deploy these patterns on the off-ramps, speed studies are required. RW and WW vehicle speeds will be used as inputs to estimate the levels of sound and vibrations that drivers would perceive while crossing the DRS patterns.



(a)

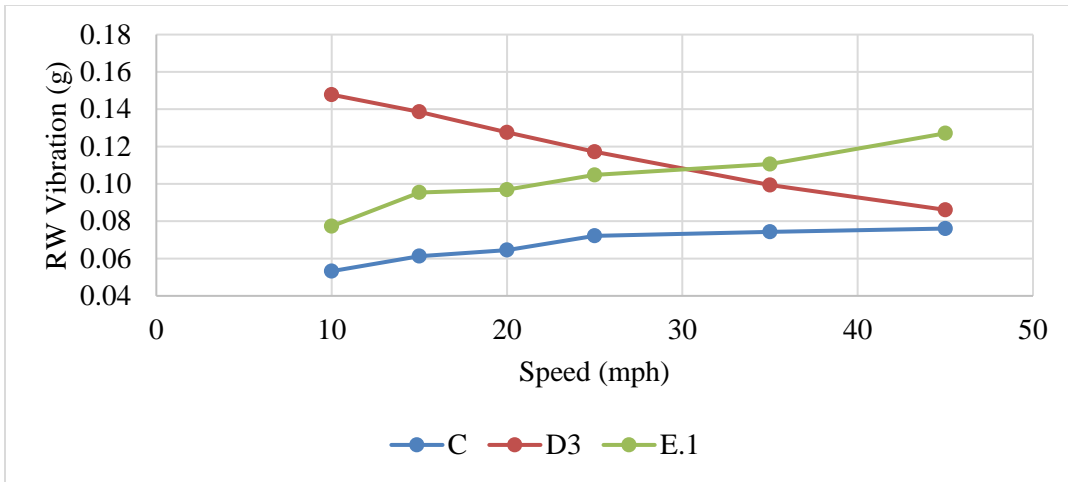


(b)

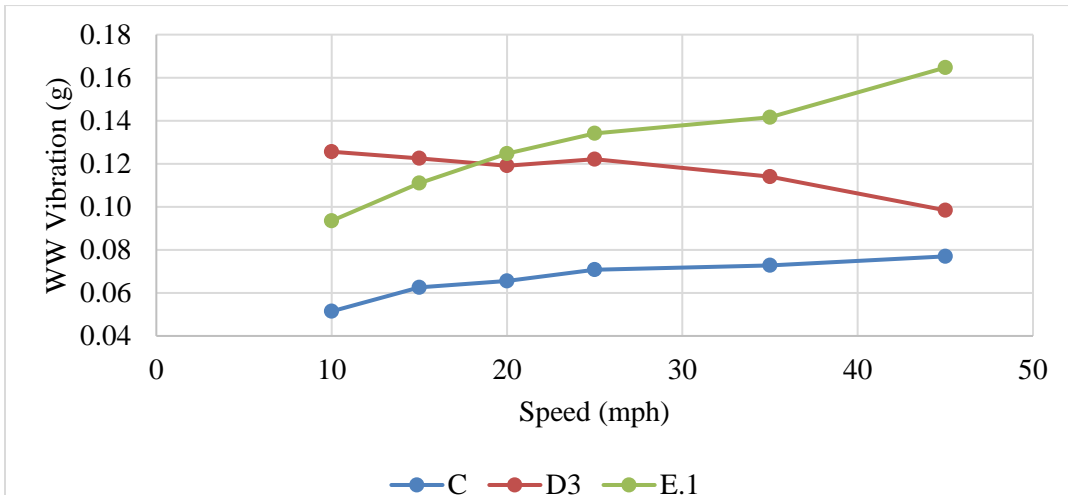


(c)

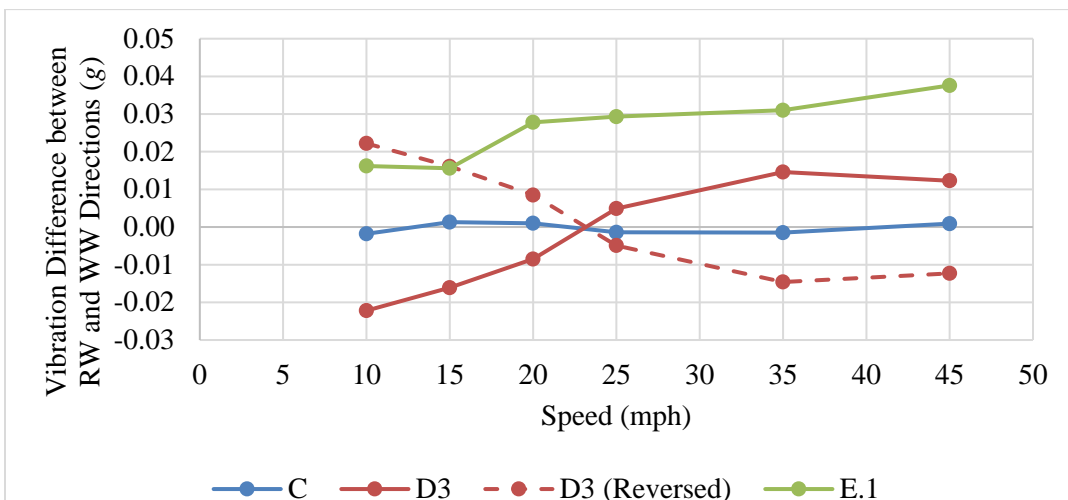
Figure 4.1 Sound Levels Generated by DRS



(a)



(b)



(c)

Figure 4.2 Vibration Levels Generated by DRS

4.2 Speed Analysis on Freeway Ramps

Considering drivers are likely driving at different speeds at the same spot on the off-ramp when driving in WW and RW directions, a speed study was conducted at the interchange of Exit 60 on I-85 to collect average speed at specific spots along on- and off-ramps. A radar gun (Traffic Advisor Model PR1000-TA) was used to record the RW and WW driving speeds on ramps. Three spots on both the on and off-ramps were selected. A hundred records were measured for each spot. As shown in **Figure 4.3**, the first spot is at the terminal of on- and off-ramp terminals. The RW speed (V_{1rw}) was measured close to the stop bar of the off-ramp terminal. The WWD speed (V_{1ww}) on off-ramps was assumed to be the same as the speed at the corresponding spot of the on-ramps. The second spot is the middle point of on and off-ramps. The RW speed (V_{2rw}) on off-ramps was collected. The WWD speed (V_{2ww}) was assumed to be the same as the RW speed measured at the middle point of the on-ramp. The third spot that is close to the freeway mainline was selected. The RW driving speed (V_{3rw}) was collected at the tangent of the incoming curve, while the speeds obtained at the tangent after the curve of an on-ramp were assumed the same as the WWD speeds.

Figure 4.4 and **Table 4.2** present a summary of the speed study results. Results showed that the mean speed is 16.1 mph at the on-ramp while only 9.8 mph at the same spot as the off-ramp at the ramp terminal. The second spot was the middle point of the straight segment (180 ft from the ramp terminal) of the ramps. The mean speed at this spot of the on-ramp is 33.6 mph when compared to 25.6 mph on the off-ramp. Close to the freeway, the mean speeds of 17.7 and 15.8 mph are similar on both on- and off-ramp curves with a radius of 106 ft.

The speed study results can help develop recommendations of proper locations for installing DRS based on approximate driving speeds by RW and WW drivers. For instance, the reversed Pattern D3 can be installed at the off-ramp terminal as it can produce more amount of

sound and vibrations in the WW direction at lower speeds. Pattern C can be implemented at the middle part of the off-ramp because the three groups of strips can differentiate the directions. Pattern E.1 is recommended for be placed at the ramp tangent close to freeway mainline. This pattern can generate more amount sound and vibrations in WW direction than RW direction for almost all speed categories, which gives it the most potential to deter WW drivers close to the freeway mainline.

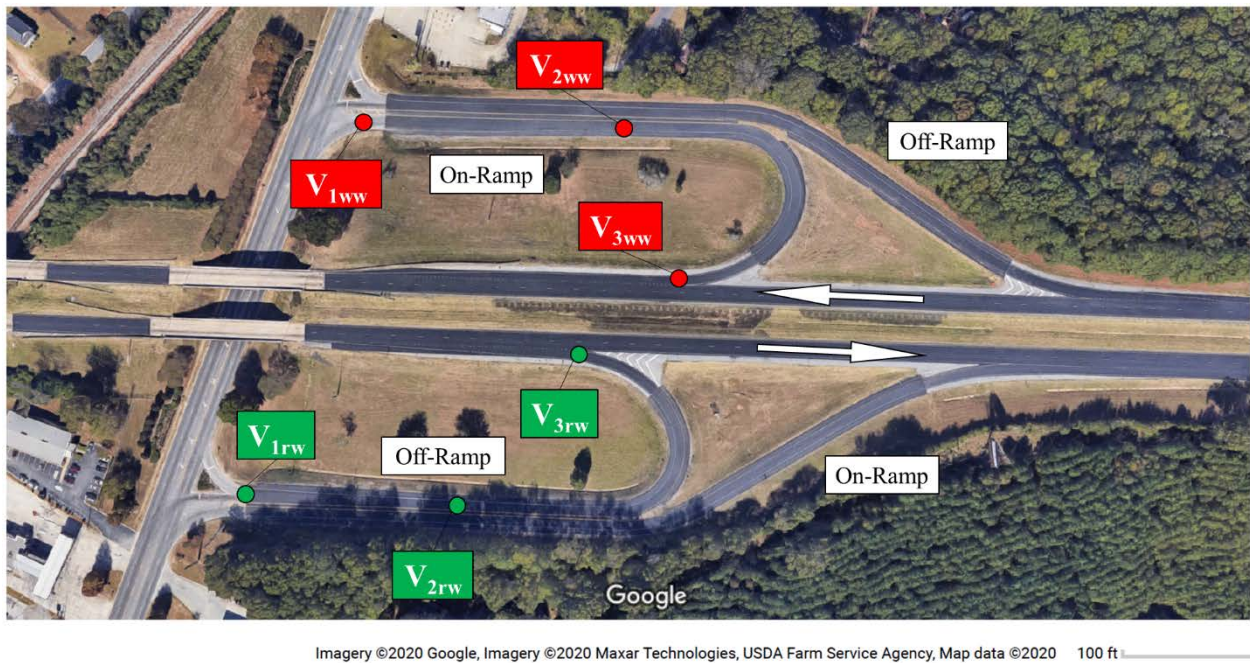
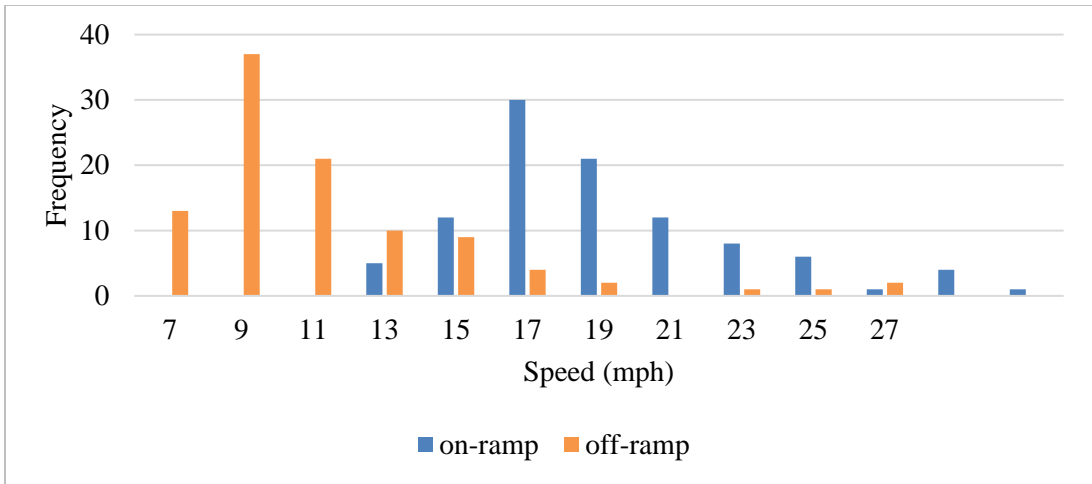
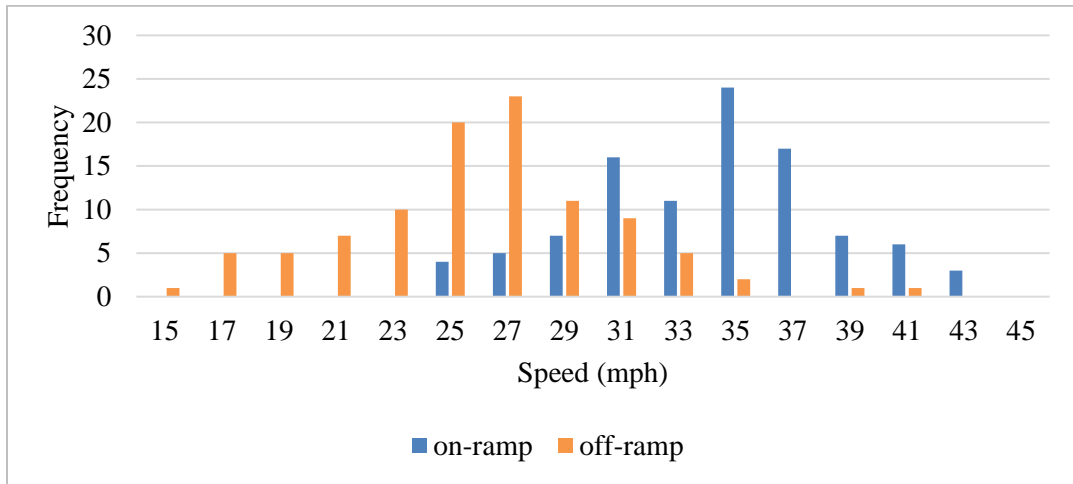


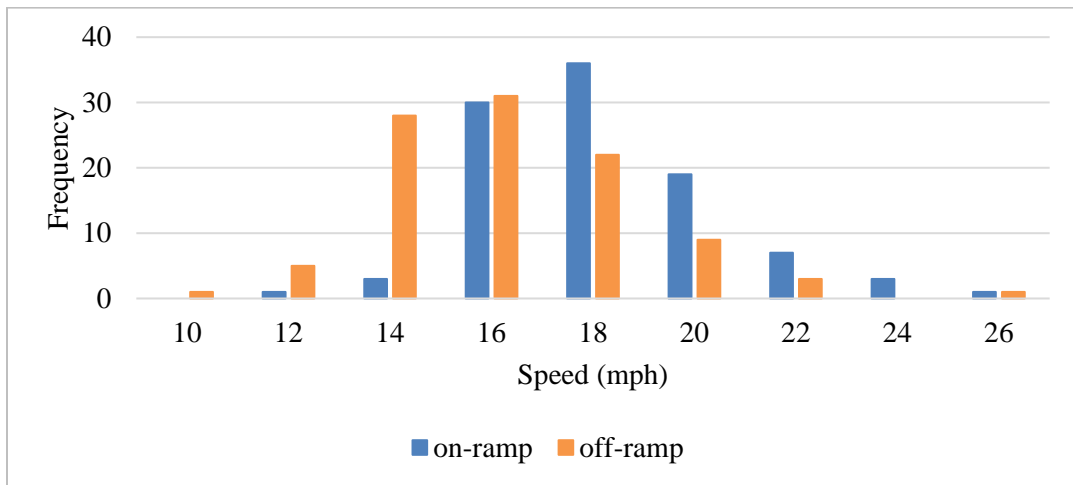
Figure 4.3 Spots where Speeds were Measured on Ramps



(a)



(b)



(c)

Figure 4.4 Speed Distributions at (a) Ramp Terminals, (b) Middle Points of Ramps, and (c) Tangent of Ramp Curves

Table 4.2 Speed Characteristics at Three Spots of Ramps

Location	Speed	On-ramp (mph) V_{1ww}	Off-ramp (mph) V_{1rw}
Terminal	85th	18.0	10.0
	Mean	16.1	9.8
	Max	28.0	27.0
	Min	10.0	7.0
Location	Speed	On-ramp (mph) V_{2ww}	Off-ramp (mph) V_{2rw}
Middle of Straight Segment	85th	38.0	30.0
	Mean	33.6	25.6
	Max	42.0	41.0
	Min	25.0	15.0
Location	Speed	On-ramp (mph) V_{3ww}	Off-ramp (mph) V_{3rw}
Tangent of Curves	85th	20.0	18.0
	Mean	17.7	15.8
	Max	25.0	25.0
	Min	11.0	10.0

4.3 Analysis of Sound and Vibrations

The data of sound and vibrations was collected from the test track in NCAT, using the sound level meter and accelerometer, at 6 speeds (10, 15, 20, 25, 35, and 45 mph). Five samples were collected under each speed in each direction. In total, 312 samples were collected including those at ambient conditions. According to the previous work (Yang et al. 2018), only the maximum value of sound and vibration along the time domain was investigated, which might ignore important characteristics of the sound or vibration generated by each pattern. For example, only the maximum sound and vibration levels were compared for the same speed between WW and RW directions, which might not represent the total amount of sound and vibration received by drivers in the real world. As such, in the verification tests, the sound was further evaluated in the form of the waveform in the time domain and spectrum analysis of vibrations was applied by using the fast Fourier transform (FFT).

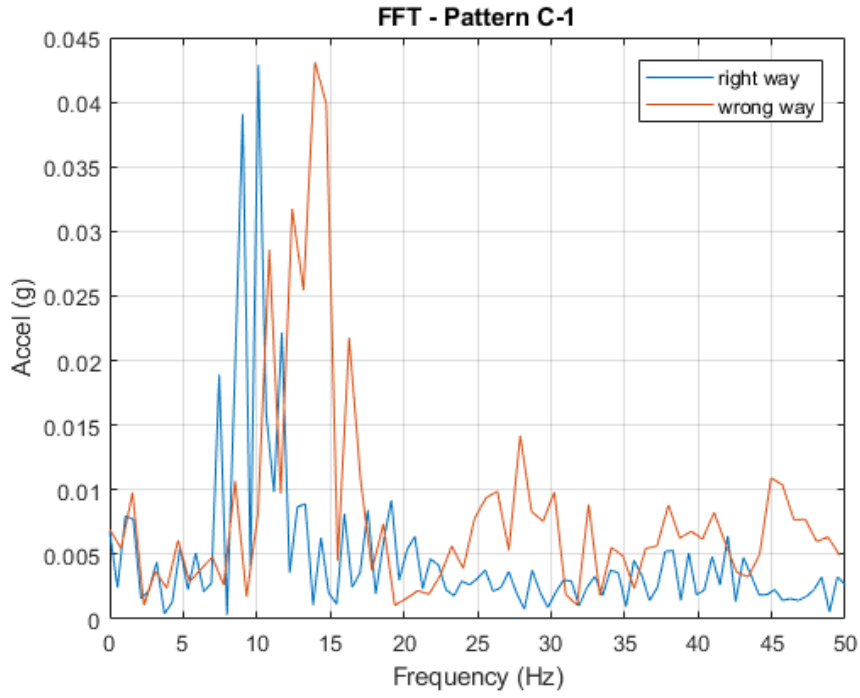
Pattern C

Figure 4.5 illustrates the waveform of sound generated by DRS Pattern C when it is installed at the middle point of a straight and long off-ramp segment. The X-axis is the time which is in reference to the time when the front wheels first encounter the strip. The Y-axis represents the sound level with the unit of dBA. RW drivers were assumed to drive around 25 mph, while WW drivers were accelerating to an approximate speed of 35 mph. As shown in **Figure 4.5-a**, the WW driver would receive a 10 dBA louder sound on average than the RW driver. According to spectrum analysis (**Figure 4.5-b**), the WW driver would receive more vibrations at three sets of strips (C1=1-ft spacing, C2=2-ft spacing, and C5=5-ft spacing) than RW drivers in terms of

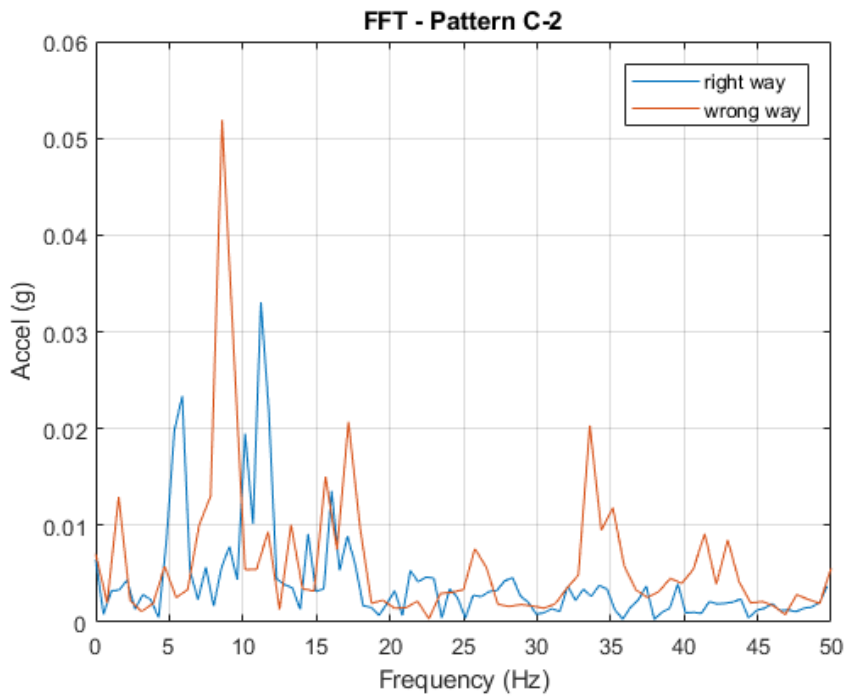
frequency and amplitude. It can be observed that WW driver would receive vibrations with higher frequencies and larger amplitude in general.



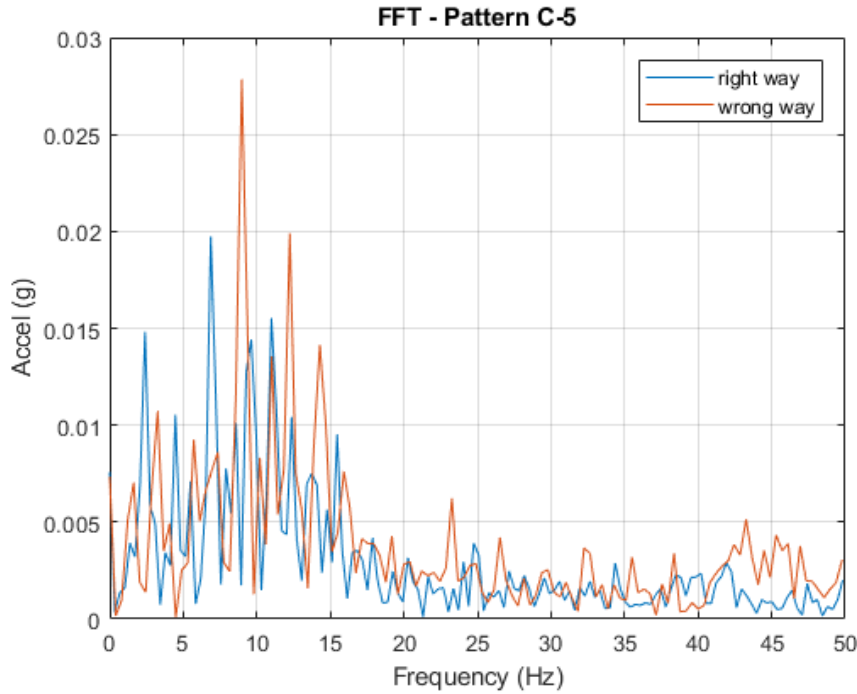
(a)



(b)



(c)



(d)

Note: RW speed = 25 mph and WW speed = 35 mph.

Figure 4.5 Analysis of Sound and Vibrations Generated by Pattern C

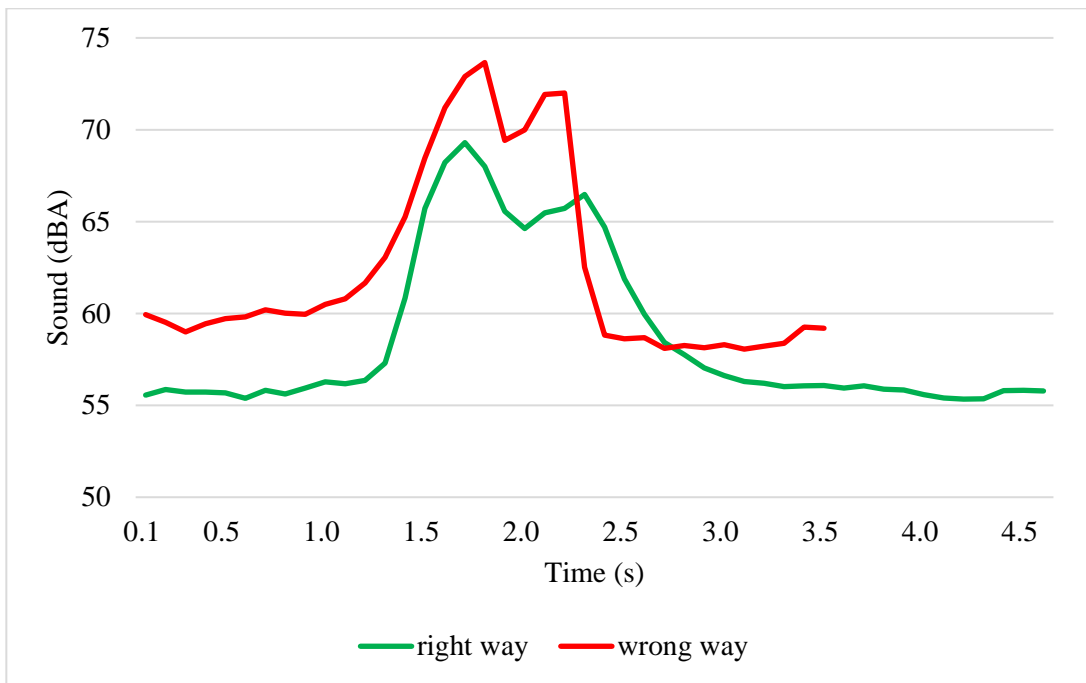
Pattern D3

The waveform on sound levels in Pattern D3, as shown in **Figure 4.6-a**, indicated that the WW drivers could hear an average 10% louder sound than RW drivers. WWD speed was estimated to be 15 mph, and RW driving speed was approximately 10 mph when DRS is installed close to the terminal of an off-ramp. In **Figure 4.6-b**, RW drivers would receive the vibration at around a peak of 8 Hz, while WW drivers would receive the vibration concentrating around a frequency of 13 Hz, which also implied that the WW driver would receive a more severe vibration.

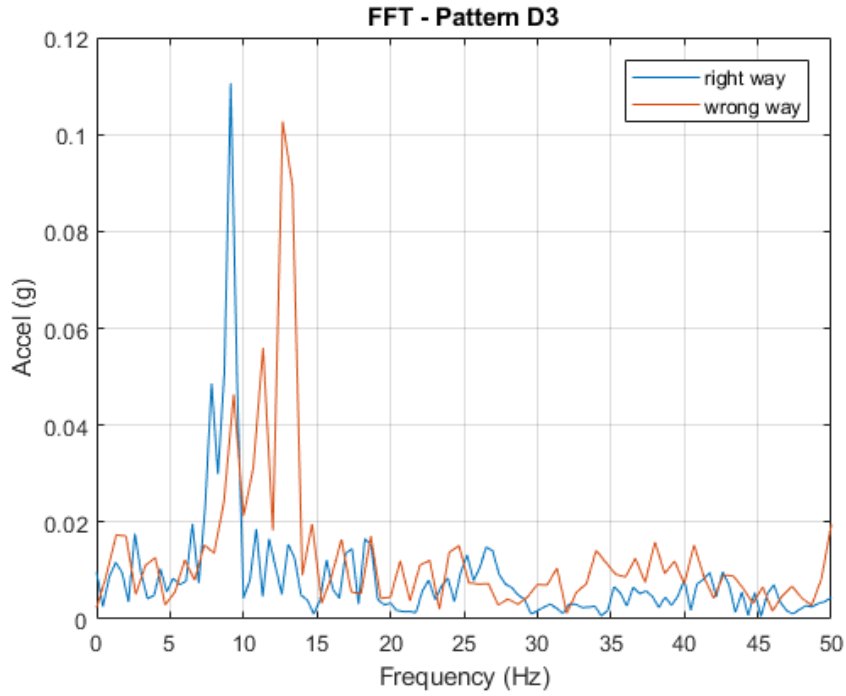
Pattern E.1

Pattern E.1 is designed to be installed before the curve on the off-ramp to provide visual attentiveness of a curve ahead. From the speed data collected on the sharp curves with a turning

radius of 106 ft, the mean speed ahead of the curve was nearly 15 mph on the off-ramp and approximately 20 mph on the on-ramp. **Figure 4.7** presents the sound waveform and FFT plot on vibration. The WW driver can hear a louder sound and feel more severe vibration in terms of both frequency and amplitude. An average sound level increase of 2 dBA can be observed for WW drivers. RW drivers will have peaks of vibration frequencies of 3, 5, 7, and 11 Hz. WW drivers can experience vibrations at peaks of 7, 15, 30, and 37 Hz with larger amplitudes than those from the RW direction. During field tests, drivers could hear a significantly louder sound and feel a much stronger vibration when driving in the WW direction than in the RW direction.



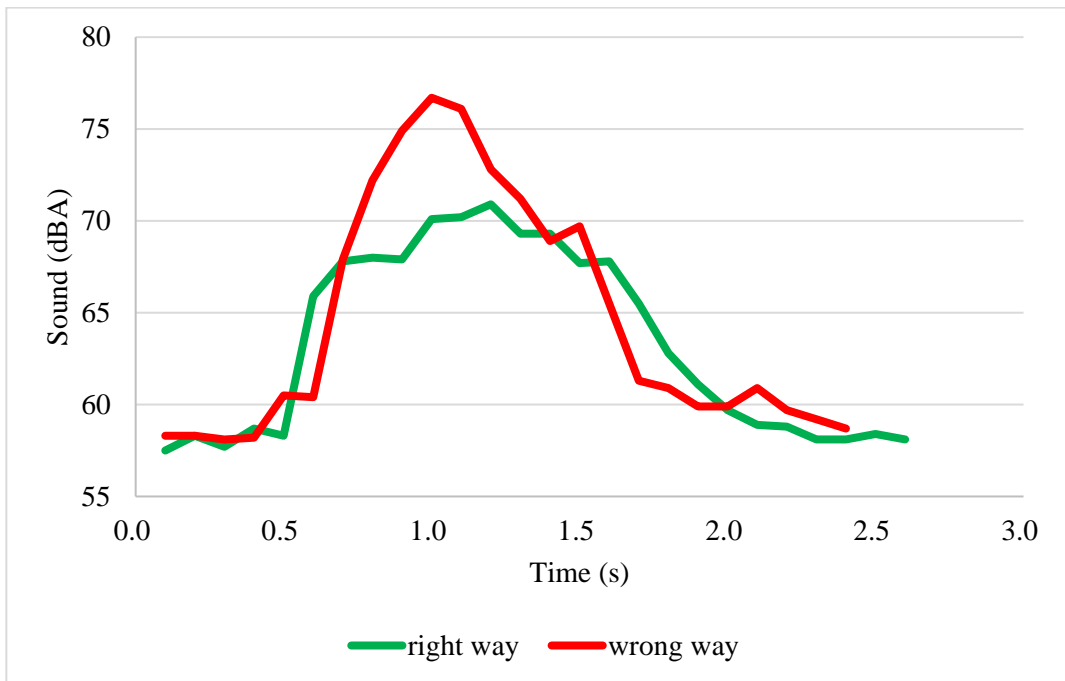
(a)



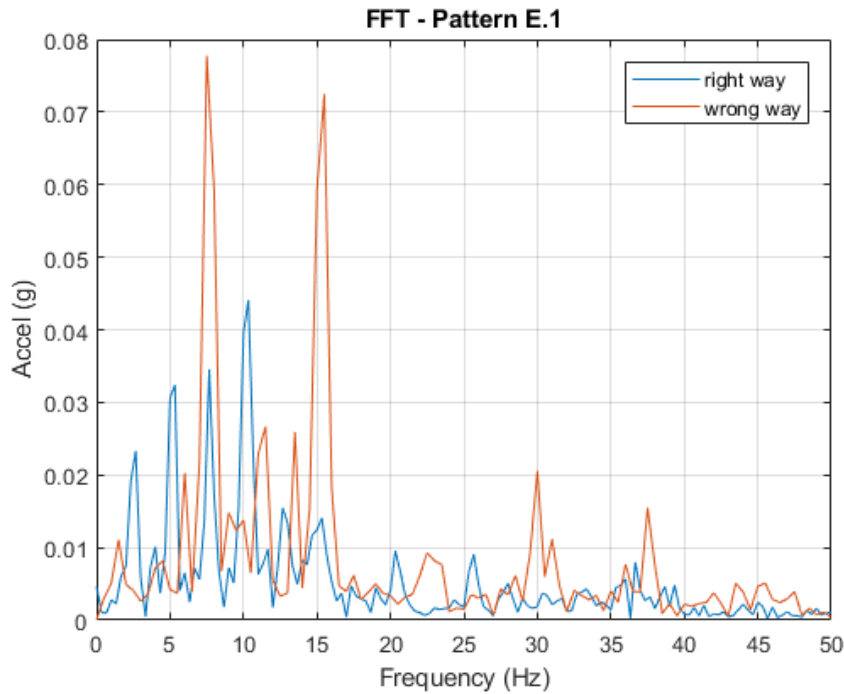
(b)

Note: RW speed = 10 mph and WW speed = 15 mph.

Figure 4.6 Analysis of Sound and Vibrations Generated by Pattern D3



(a)



(b)

Note: RW speed = 10 mph and WW speed = 15 mph.

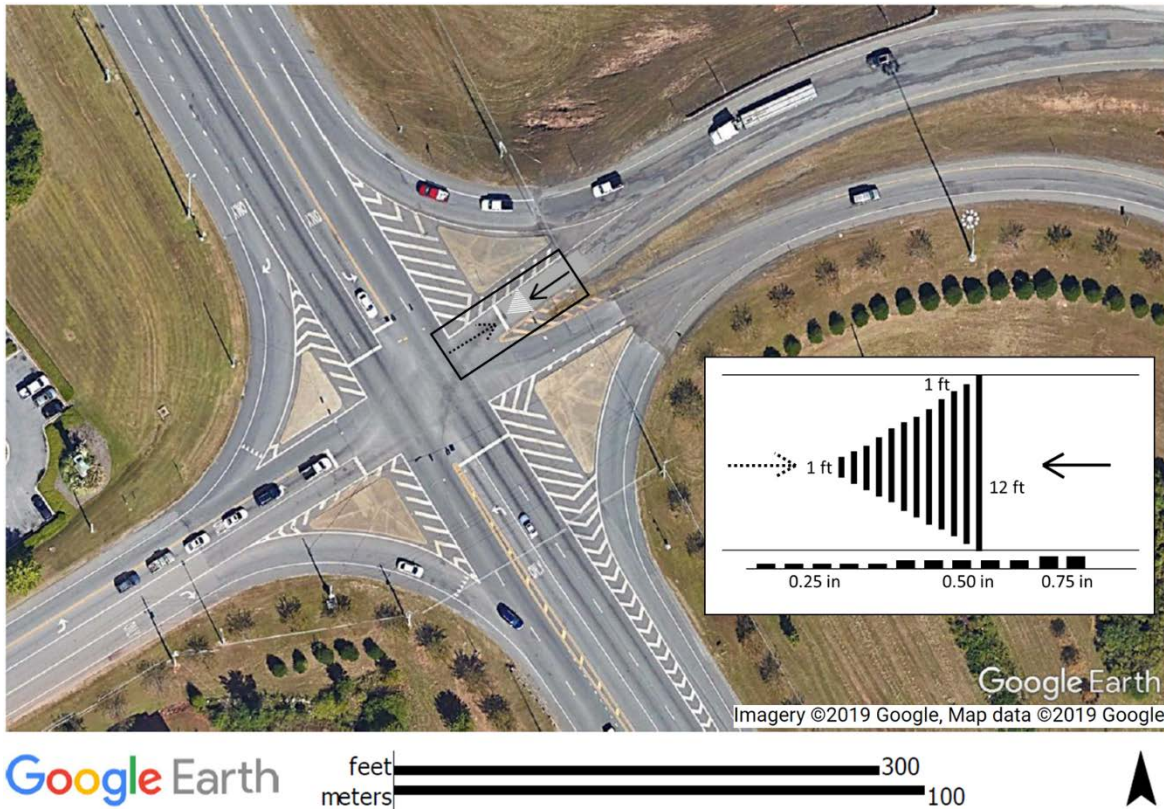
Figure 4.7 Analysis of Sound and Vibrations Generated by Pattern E.1

4.4 Recommendations from Verification Tests Results

According to the verification test results, the recommendations for implementing the three final types of DRS are summarized as follows. Three example locations were selected for each scenario.

Figure 4.8 shows an off-ramp terminal that is close to the on-ramp entrance at Exit 58 of I-85. Drivers who are not familiar with this location, especially at night or under poor illumination conditions, could drive WW onto the freeway. In this case, Pattern D3 can be implemented with the thickest strip as the stop bar, which could be painted red retroreflective on the edge facing

potential WW drivers. Based on the results, WW drivers would receive louder sound and more severe vibrations.

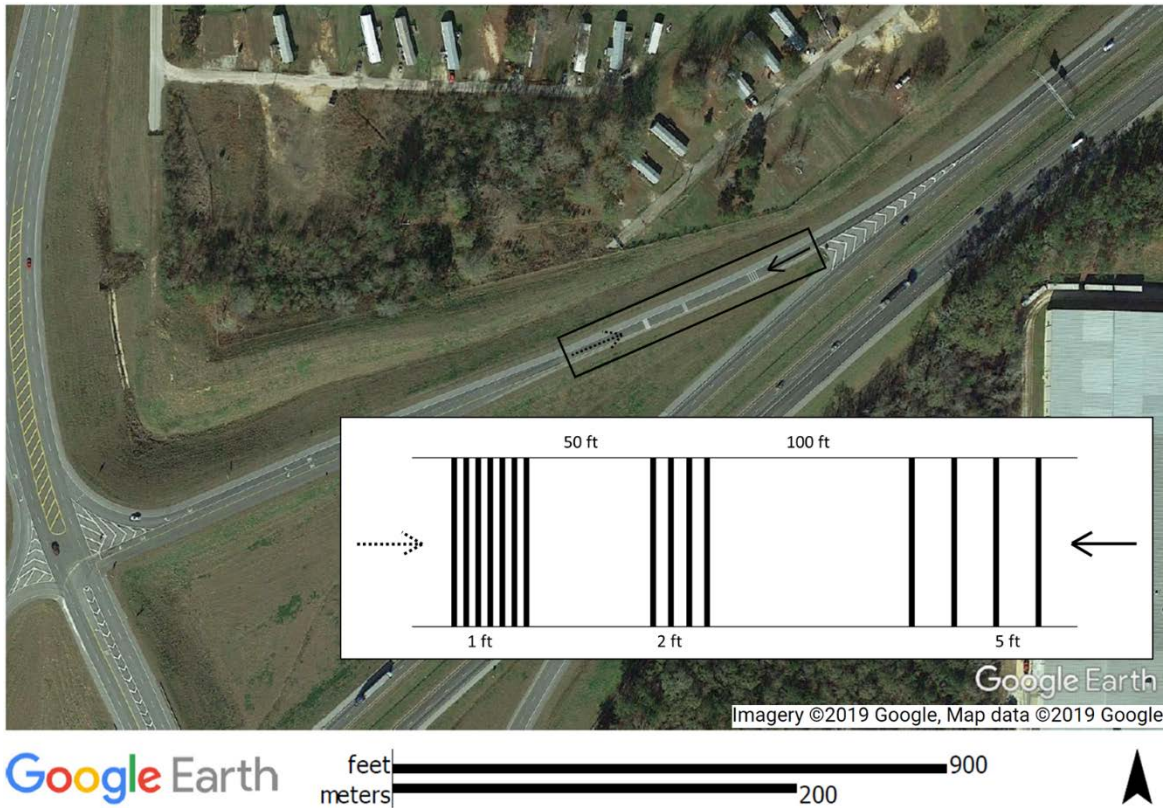


Note: Solid Arrow = RW Direction; Dashed Arrow = WW Direction.

Figure 4.8 Proposed Implementation of Pattern D3

Figure 4.9 presents an example of a potential implementation of Pattern C in the middle of a straight long segment of off-ramps at Exit 50 of I-85. Based on the verification results, the WW drivers can hear an average of 10 dBA louder sound than RW drivers. Further, WW vibrations have higher frequencies and larger amplitudes. Moreover, WW drivers will perceive a different rhythm of sound and vibration due to the diverse spacing among the three sets of strips. In this example location, this pattern is expected to produce louder sound and more severe vibration at the beginning when WW drivers drive through the first set of strips with dense spacing (1 ft). RW

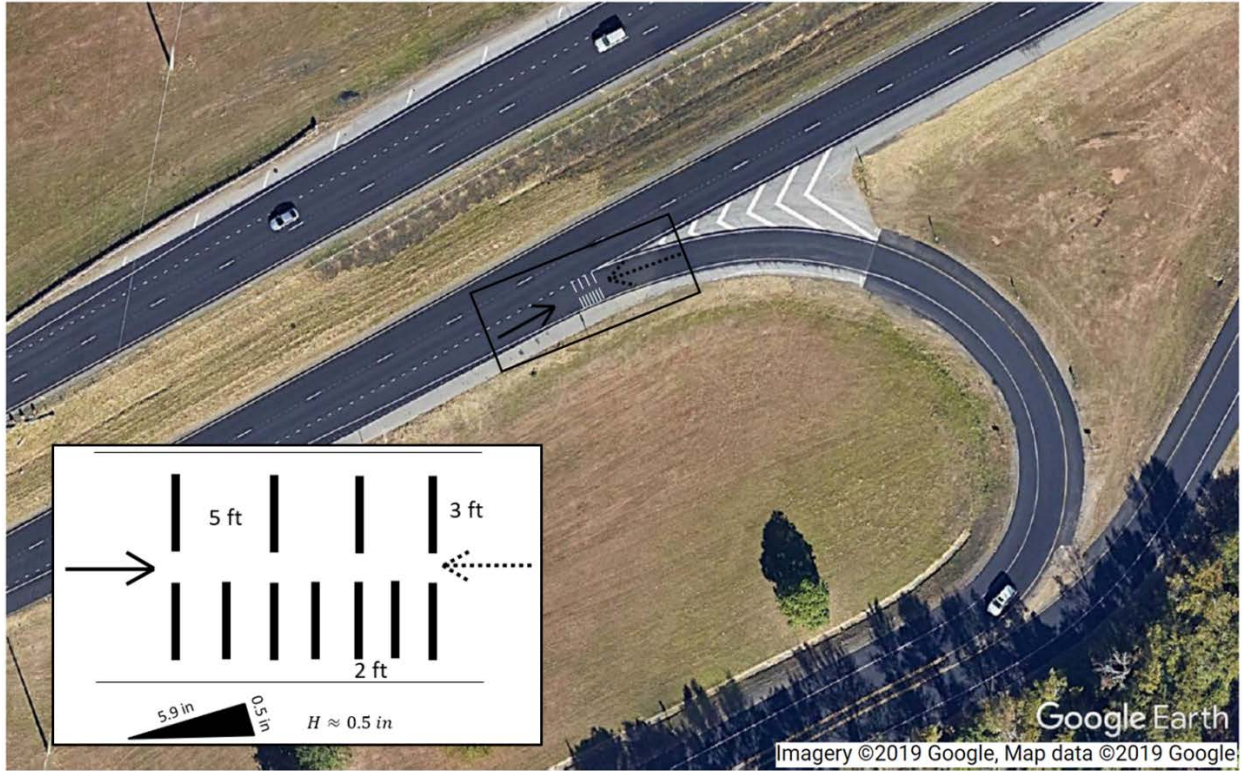
drivers would experience the increasing loudness of sound and severity of vibration, which can be an advanced alert for the intersection ahead to slow them down.



Note: Solid Arrow = RW Direction; Dashed Arrow = WW Direction.

Figure 4.9 Proposed Implementation of Pattern C

In addition to deterring the WWD, Pattern E.1, as shown in **Figure 4.10**, can provide visual attentiveness of the curve ahead and slow down RW driving at Exit 60 of I-85. Pattern E.1 was recommended to be installed on the tangent segment before the ramp curve. Field test experience suggests that this pattern can provide the most recognizable increase of sound and vibration to WW drivers.



Google Earth



Note: Solid Arrow = RW Direction; Dashed Arrow = WW Direction.

Figure 4.10 Proposed Implementation of Pattern E.1

Chapter 5. Field Implementation Results

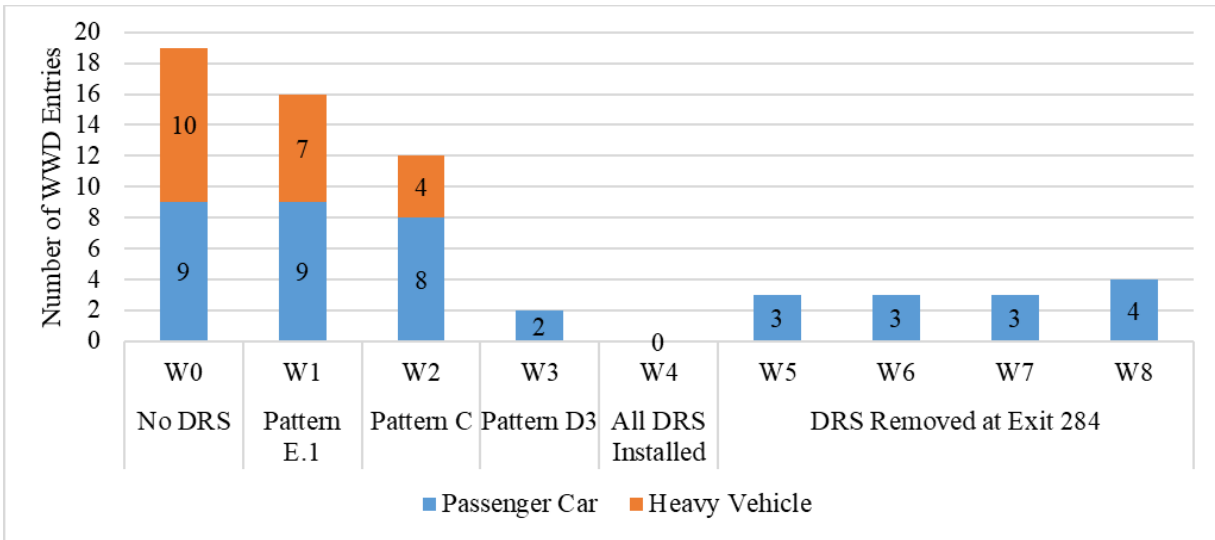
This chapter presents the results from the field implementation of DRS. The experimental implementation was to quantify the impacts of DRS on deterring WWD and RW vehicles' speeds and driving behavior.

5.1 Impacts of DRS on Number of WWD Incidents and WWD Distances

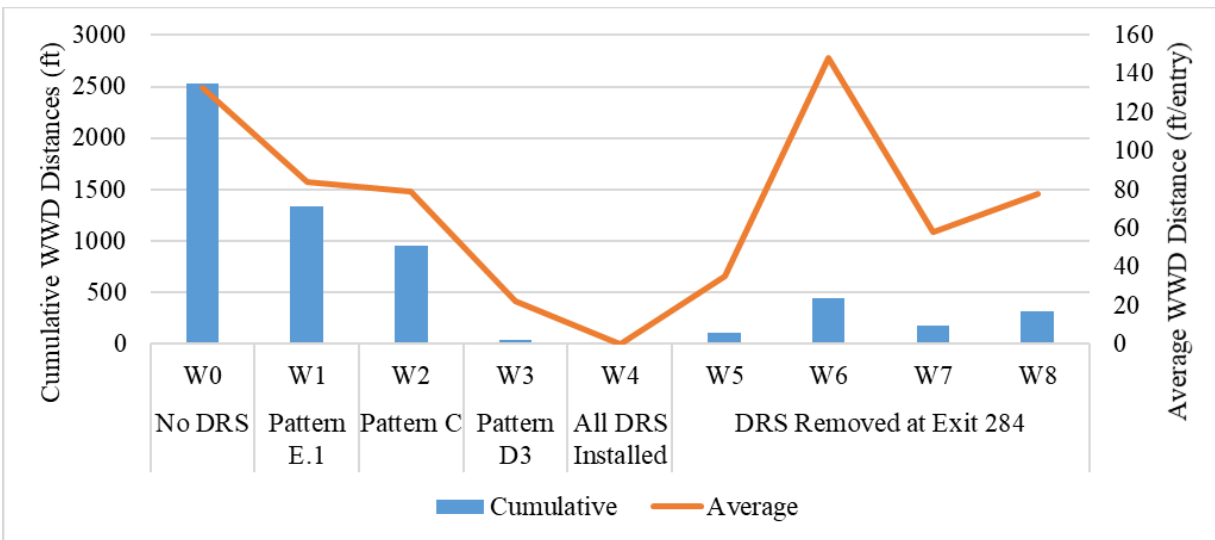
Figure 5.1-a summarizes the frequencies of WWD incidents at the two study locations during different weekend periods (W0 to W8). WWD vehicles were classified as either passenger cars or heavy vehicles (e.g., semitrailer trucks, RVs, pickup trucks with trailers). There was a downward trend in the number of WWD incidents after the installation of DRS. A total of 19 WWD incidents was initially recorded at the two study locations during the weekend of W0, including 10 heavy vehicles (HV) and 9 passenger cars. After implementing Pattern E.1 at W1, the number of WWD incidents (16 incidents) remained similar because most WW drivers turned around before Pattern E2. The number of WWD incidents decreased to 12 after installing Pattern C at W2. After implementing Pattern D3, only 2 WW incidents occurred during the weekend of W3. Three WWD incidents occurred after W4. The majority of these incidents happened at Exit 284 where DRS were removed. Moreover, it should be noted that no heavy vehicles made a WW entry after the installation of Pattern D3 (W3). The potential reason for the significant reduction of WWD incidents by HV could be the visual cue provided by DRS, especially Pattern D3. Typically, the eye height of a HV driver is higher than a passenger car driver when seated. This provides HV drivers with farther/clearer vision than the other drivers, which result in noticing the DRS patterns as well as the off-ramp terminal earlier. Consequently, the potential of WWD caused by insufficient sight distance could be minimized for HV drivers.

In addition to the frequency of WW incidents, the WWD distance was another criterion to evaluate the effectiveness of each DRS pattern. The WWD distance was measured from the stop bar or yield line at the off-ramp terminal to the location where a WW driver fully stopped. Two types of WWD distance were estimated. One was the cumulative WWD distance (the sum of distances traveled by all WW drivers), the other the average distance per WW entry. As shown in **Figure 5.1-b**, both the cumulative and average WWD distances present decreasing trends before the resurfacing project at Exit 284. WWD distances at W3 and W4 were proved to be significantly different from W0, according to *t*-tests with *p*-values less than 0.05 at the significance level of 0.05.

From W5 to W8, all WWD vehicles at Exit 208 stopped and self-corrected after going the WW less than 20 ft by DRS Pattern D3. As the total number of WWD incidents remain low after the resurfacing project at Exit 284, the cumulative WWD distance does not have a significant increase. However, the average WWD distance shows an increasing trend after DRS were removed. **Table 5.1** presents the changes in WW incident frequency and WWD distances at Exit 284 during three different time periods: (1) before installing DRS, (2) after installing DRS, and (3) after removing DRS. The average number of WWD incidents reduced from an average of 10.3 in 72 hours to 0.5, and then increased to 3.3 after DRS were removed. It should be noted that the average WWD distance (77.3 ft) has been reduced to 25 ft after installing DRS, but then increased to 79.7 ft after all the DRS were removed from Exit 284. The maximum driving distance also shows the same trend with and without DRS. The data indicate that DRS can not only deter potential WW drivers from entering the off-ramp, but also reduce their driving distances; therefore, reduce the risk of WWD incidents/crashes. After resurfacing and removing DRS, WW incident frequency and WWD distances significantly increased, though resurfacing the ramps may slow drivers down and provide them with better visibility.



(a)



(b)

Figure 5.1 WWD (a) Frequencies and (b) Distances before and after DRS Installations

Table 5.1 Comparisons of WW Incidents before and after Installing DRS at Exit 284

	Before installing all the DRS (W0-W2)	After installing all the DRS (W3-W4)	After removing all the DRS (W5- W8)
Number of WW incidents per weekend (72 hours)	10.3	0.5	3.3
Maximum WWD distance (ft.)	800	25	400
Average WWD distance (ft.)	77.3	25.0	79.7

By reviewing the video data, it was found that though the off-ramp traffic volumes had the seasonal effects (lower volumes in the winter), the left-turn volumes from the crossroad to the on-ramp were consistent. At Exit 208, the mean left-turn volume was 929 veh/day with a standard deviation of 34 veh/day. While at Exit 284, the daily average number of left-turn vehicles was 1156 with a standard deviation of 29 veh/day. Thus, daily WWD incident rate was calculated and statistically analyzed. As indicated in **Table 5.2**, there was 1.7 WW incidents per day before DRS installation (W0-W2) and 0.6 after (W3-W10). However, the average numbers of WW incidents per day before and after DRS implementation are not significantly different based on *t*-tests at the significance level of 0.05, though the reduction is nearly 65%. The counts of WW incidents at Exit 284 had the similar decreasing trend before the resurfacing project. After the installation of all DRS patterns, the average number of WW incidents per day was significantly reduced by 95%, from 3.6 to 0.2 per day. The average number of WW incidents per day then significantly increased to 1.4 per day with the removal of DRS. For the cross-sectional comparison between two locations, as listed in **Table 5.2**, the average numbers of WW incidents per day showed no statistical

difference between two locations before (W0-W2) and after DRS installation (W3-W4). From W5 to W10, an average of 0.7 WW incidents per day was observed at Exit 208 while 1.4 at Exit 284. With a *p*-value less than 0.05, the average number of WW incidents per day at Exit 284 was significantly higher than that at Exit 208 because of the removal of DRS.

The average WWD distance was 163 ft per entry before the installation of DRS. It was significantly reduced by 82% to 30 ft per entry after the installation of DRS according to **Table 5.3**. At Exit 284, an average WWD distance of 75 ft per entry was recorded before the installation of DRS. It was significantly reduced to 15 ft per entry after the installation of DRS. After removing the DRS, the average WWD distance significantly increased to 126 ft per entry, which showed no statistical difference with the condition before the installation of DRS. With no statistical difference found, the cross-sectional analysis between Exits 208 and 284 manifests the average WWD distances were large before the installation of DRS (W0-W2) at both locations. The average WWD distances were greatly lowered by DRS from W3 to W4. The cross-sectional analysis also indicates that the average WWD distances after W5 between these two locations are significantly different. Without DRS at Exit 284, the average WWD distance is almost 4 times higher than that at Exit 208 where DRS remain in the field.

Table 5.2 Statistical Analysis of Number of WWD Incidents

Studies	Comparison Group 1		Comparison Group 2		<i>t</i> -stat	<i>p</i> -value
	Phase	Mean (per day)	Phase	Mean (per day)		
Before- and-After ^a	Exit 208 Before DRS Implementation (W0-W2)	1.7	Exit 208 After DRS Implementation (W3-W8)	0.6	1.74	0.09
	Exit 284 Before DRS Implementation (W0-W2)	3.6	Exit 284 After DRS Implementation (W3-W4)	0.2	4.87	0.02
	Exit 284 After DRS Implementation (W3-W4)	0.2	Exit 284 DRS Removed from the Field (W5-W8)	1.4	-2.36	0.03
	Exit 284 Before DRS Implementation (W0-W2)	3.6	Exit 284 DRS Removed from the Field (W5-W8)	1.4	2.60	0.03
Cross- Sectional ^b	Exit 208 Before DRS Implementation (W0-W2)	1.7	Exit 284 Before DRS Implementation (W0-W2)	3.6	-1.78	0.11
	Exit 208 After DRS Implementation (W3-W4)	0.2	Exit 284 After DRS Implementation (W3-W4)	0.2	0.00	0.5
	Exit 208 DRS Remain in the Field (W5-W8)	0.7	Exit 284 DRS Removed from the Field (W5-W8)	1.4	-2.45	0.03

Note: ^a*t*-tests; ^bpaired *t*-tests

Table 5.3 Statistical Analysis of Average WWD Distances

Studies	Comparison Group 1		Comparison Group 2		<i>t</i> -stat	<i>p</i> -value
	Phase	Mean (ft/entry)	Phase	Mean (ft/entry)		
Before- and-After ^a	Exit 208 Before DRS Implementation (W0-W2)	163	Exit 208 After DRS Implementation (W3-W8)	30	2.42	0.01
	Exit 284 Before DRS Implementation (W0-W2)	75	Exit 284 After DRS Implementation (W3-W4)	15	1.99	0.03
	Exit 284 After DRS Implementation (W3-W4)	15	Exit 284 DRS Removed from the Field (W5-W8)	126	-3.09	< 0.01
	Exit 284 Before DRS Implementation (W0-W2)	75	Exit 284 DRS Removed from the Field (W5-W8)	126	-0.21	0.12
Cross- Sectional ^a	Exit 208 Before DRS Implementation (W0-W2)	163	Exit 284 Before DRS Implementation (W0-W2)	75	1.45	0.08
	Exit 208 After DRS Implementation (W3-W4)	7	Exit 284 After DRS Implementation (W3-W4)	15	-0.52	0.35
	Exit 208 DRS Remain in the Field (W5-W8)	34	Exit 284 DRS Removed from the Field (W5-W8)	126	-2.74	0.01

Note: ^a*t*-tests

Details of WWD incidents (**Table 5.4**) were also collected, including date and time, locations where WW drivers stopped, and potential effective countermeasures.

Pattern E.1

Pattern E.1 was installed at W1. During the one-week before period, only one WW driver was recorded to travel all the way to the freeway mainline and never return. No other such critical event happened in the four after periods. Only one semitrailer truck stopped and turned around at the middle of the ramp curve right before Pattern E.1 when there was no off-ramp RW traffic at Exit 208 in the W1. More data is needed to evaluate the effectiveness of the Pattern E.1 in deterring WWD incidents.

Pattern C

At Exit 208, a total of five WWD incidents (**Table 5.4** No. 1-5) happened during the three after periods (W2, W3, and W4). Two of them stopped and turned around at the 2-ft spacing strip group of Pattern C. WW drivers were apparently alerted by Pattern C and noticed the WW signs. Pattern C and WW signs were identified as potential effective countermeasures. The other three WW incidents were stopped and turned around by the DNE sign and dual WW arrows. At Exit 284, three out of seven WWD incidents (**Table 5.4** No. 6-12) were affected by Pattern C. The remaining four WW drivers turned around before Pattern C by RW traffic or other traffic control devices, such as a divided roadway sign or DNE sign. To conclude, Pattern C had an impact on over 40% of WWD self-corrections at Exit 208 and Exit 284.

Pattern D3

After implementing Pattern D3, only six WWD incidents occurred during from W3 to W8 for a total of 432 hours at each location, respectively (**Table 5.4** No. 13-18). These incidents were deterred by Pattern D3. WW vehicles stopped and immediately turned around at Pattern D3 or

immediately after D3. Pattern D3 had an impact on all the WWD self-corrections at the two study locations.

Table 5.4 Records of WW Incidents (W1-W8) at Exit 208

No.	Date & Time	Locations where WW Drivers Stopped	Potentially Effective Countermeasures
1	2018/12/14 10:09	in front of the dual WW arrows	dual WW arrows
2	2018/12/14 13:23	middle of the ramp curve	Pattern E.1
3	2018/12/21 11:42	before the second set of Pattern C	Pattern C; WW signs
4	2018/12/22 23:10	just passed the channelized island	DNE sign
5	2018/12/23 11:26	in front of the dual WW arrows	dual WW arrows
6	2018/12/24 6:44	in front of the dual WW arrows	dual WW arrows
7	2018/12/24 8:23	just passed the second set of Pattern C	Pattern C; WW signs
8	2019/1/13 2:48	at Pattern D3	Pattern D3; DNE sign
9	2019/8/10 22:19	before Pattern D3	Pattern D3; DNE sign
10	2019/9/28/ 5:13	at Pattern D3	Pattern D3; WW sign
11	2019/9/28/ 23:54	at Pattern D3	Pattern D3; WW sign
12	2019/12/15 3:05	before Pattern D3	Pattern D3; DNE sign

Table 5.5 Records of WW Incidents (W1-W8) at Exit 284

No.	Date & Time	Locations where WW Drivers Stopped	Potentially Effective Countermeasures
1	2018/12/14 17:14	in front of WW arrows	off-ramp traffic
2	2018/12/14 17:14	in front of WW arrows	off-ramp traffic
3	2018/12/14 17:14	just passed the channelized island	off-ramp traffic
4	2018/12/14 18:51	at the second WW sign	WW sign
5	2018/12/14 20:31	just passed the channelized island	WW sign; WW arrows
6	2018/12/14 20:31	just passed the channelized island	WW sign; WW arrows
7	2018/12/14 21:15	hesitated before the stop bar	WW sign; WW arrows
8	2018/12/15 15:04	just passed the channelized island	DNE sign
9	2018/12/15 17:34	just passed the stop bar	WW sign; WW arrows
10	2018/12/15 17:35	in front of dual WW arrows	WW sign; WW arrows
11	2018/12/15 18:21	just passed the channelized island	DNE sign
12	2018/12/15 19:12	hesitated before the stop bar	WW sign; WW arrows
13	2018/12/16 15:23	just passed the channelized island	DNE sign
14	2018/11/5 13:30	just passed the channelized island	off-ramp traffic
15	2018/12/21 12:09	just passed the yield line	DNE sign
16	2018/12/21 20:06	just passed the first set of Pattern C	Pattern C; WW sign
17	2018/12/22 13:32	just passed the yield line	off-ramp traffic
18	2018/12/22 21:32	at the second set of Pattern C	Pattern C; WW sign
19	2018/12/22 22:55	at the third set of Pattern C	Pattern C
20	2018/12/22 22:57	just passed the yield line	Divided roadway sign

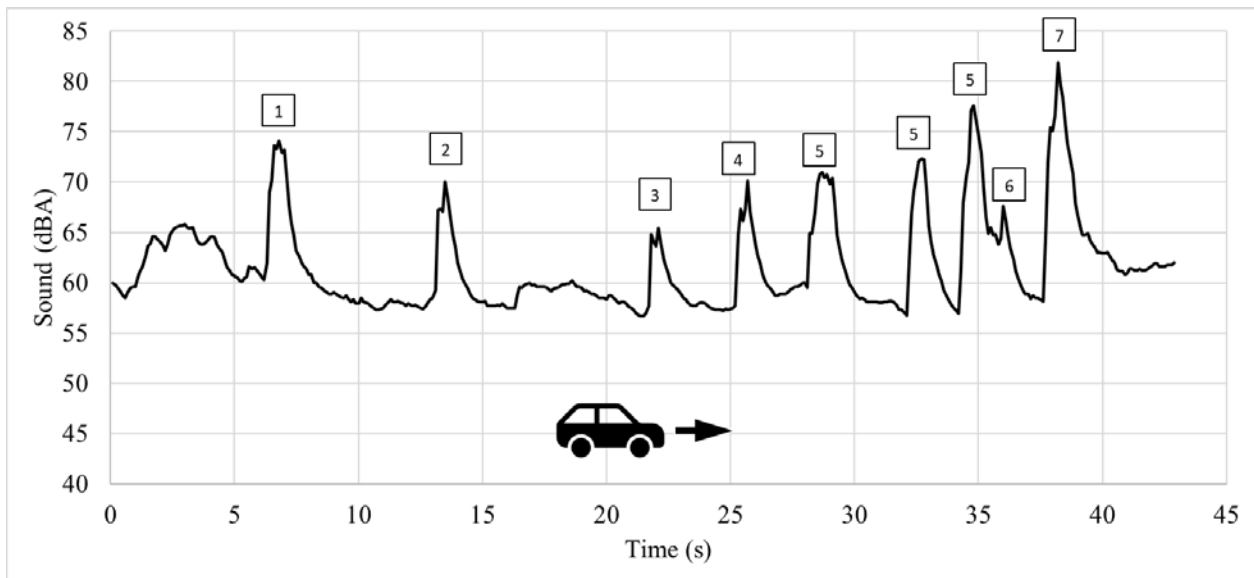
21	2018/12/23 15:50	hesitated before stop bar	Divided roadway sign
22	2019/1/13 21:56	just passed Pattern D3	Pattern D3; WW sign
23	2019/8/9 1:37	before the first WW sign	WW sign
24	2019/8/10 22:48	just passed the second WW sign	WW sign
25	2019/8/30 2:57	before the first WW sign	WW signs
26	2019/9/1 23:11	at the first WW sign	WW signs; Off-ramp traffic
27	2019/9/27 21:15	at the first WW sign	WW signs
28	2019/9/29 1:31	before the first WW sign	WW signs; Off-ramp traffic
29	2019/9/29 23:02	at the first WW sign	WW signs
30	2019/12/13 22:25	at the first WW sign	WW signs
31	2019/12/13 23:19	at the first WW sign	WW signs; Off-ramp traffic
32	2019/12/14 20:48	at the second WW sign	WW signs; Off-ramp traffic
33	2019/12/15 2:27	just passed the second WW sign	Off-ramp traffic

5.2 Analysis of Sound and Vibrations caused by DRS

Interior Sound

Interior sound data were collected through field driving tests. Due to the limitations of temporary ramp closures, the field driving tests were only conducted at Exit 208 on I-65. Both RW and WW interior sound data were acquired under seven speed categories, including 10, 15, 20, 25, 30, 35, and 40 mph. To gather the RW sound data, one researcher drove a full-size passenger car from the deceleration lane to the off-ramp terminal on the closed ramp, then drove in the reverse direction to obtain the WW sound data. **Figure 5.2** presented the sample RW sound data along the

off-ramp at a constant speed of 20 mph. Initially, from 0 to 5 s, some noises resulted from the vehicle acceleration. At 7 s, the first peak was generated by passing Pattern E.1. A second peak was created by passing the WW arrow at 14 s. However, the first lane-use arrow was not hit. Then, the vehicle passed the following WW and lane-use arrows at 22 and 26 s. Afterward, passing Pattern C generated three sound peaks. The dual WW arrows led to a consequential peak. The last peak was produced by passing Pattern D3.



Note: a) 1 = Pattern E.1; 2 = WW arrow; 3 = WW arrow; 4 = lane-use arrow; 5 = Pattern C; 6 = dual WW arrows; 7 = Pattern D3. b) Speed = 20 mph.

Figure 5.2 Sample RW Sound Data along the Off-Ramp

The time-series technique was used to visualize the sound data. It was applied to obtain an understanding of sound level which changes over the entire trip, including the peaks when vehicles pass the DRS. *T*-tests at the significance level of 0.05 were also used to discern significant differences between the average RW and WW sound levels.

According to the NC-350 speed data, the average RW speed was 30 mph and WW 35 mph before the ramp curve close to the freeway mainlines. **Figure 5.3-a** presents the RW and WW

sound of Pattern E.1. This DRS pattern created a 15 dBA louder sound for RW drivers and 20 dBA more for WW drivers than in the ambient conditions. The mean value of WW sound was 71.74 dBA, which was almost 5 dBA higher than the RW effective value (66.94 dBA). The p -value of the t -test (significance level = 0.05) was 0.012, which indicated that RW and WW sound levels were significantly different in means.

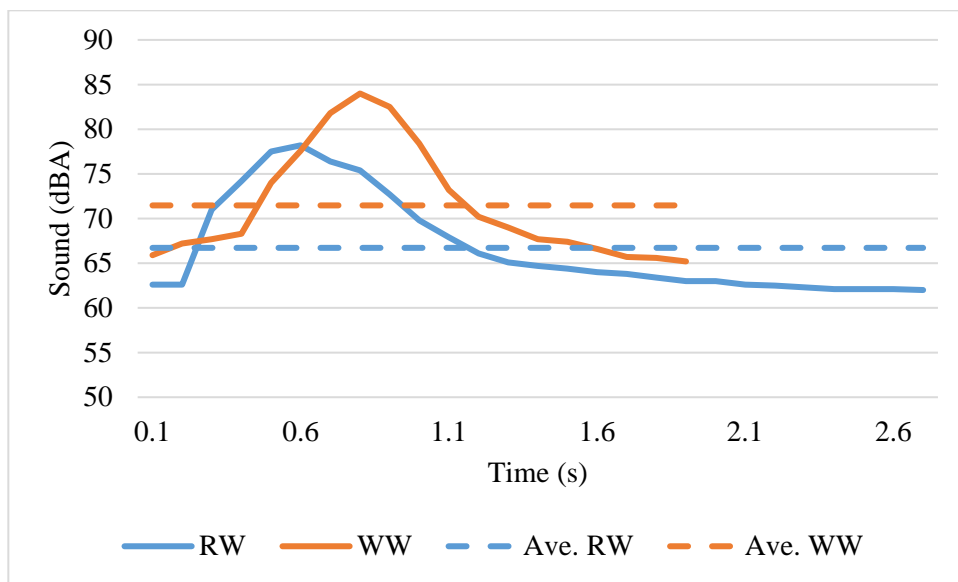
Figure 5.3-b shows the RW and WW sound of Pattern C. As shown in **Figure 5.3-b-1**, based on the speed data collected by NC-350, the average RW speed was 30 mph and WW 35 mph when vehicles passed the strips of 5-ft spacings. RW drivers were able to perceive a maximum of 10 dBA louder sound than ambient conditions. While WW drivers can receive 17 dBA louder sound than ambient conditions. Moreover, RW drivers can hear a sound 65.33 dBA and WW 69.34 dBA on average. Thus, WW drivers can obtain 4 dBA louder sound. Based on a t -test with a significant level of 0.05, p -value of 0.03 implied that a significant difference existed between the average RW and WW sound levels.

Figure 5.3-b-2 presents the RW and WW sound generated by 2-ft-spacing strips of Pattern C. The RW drivers drove at 25 mph and WW 35 mph on average. When against ambient conditions, strips produced 15 dBA louder sound for RW drivers and 17 dBA more for WW drivers at most. The mean values also signified that WW drivers (72.49 dBA) would get a 5 dBA louder sound than RW drivers (67.36 dBA). The t -test (significance level = 0.05) result revealed the average WW sound level was significantly different from the RW one with a p -value of 0.03.

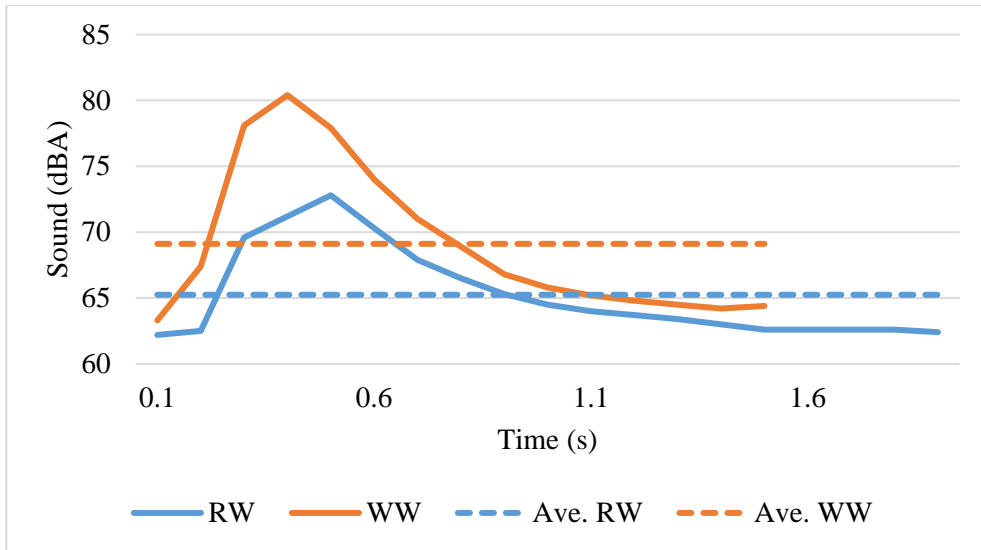
The RW and WW sound produced by 0.30-m spacing strips of Pattern C is shown in **Figure 5.3-b-3**. The speed sensor recorded an average speed of 20 mph for RW drivers and captured the WW speed of 35 mph. In comparison with the ambient status, a maximum of 17 dBA louder sound was caused by strips for RW drivers and 20 dBA for WW drivers. Mean values also suggested that

WW drivers (70.73 dBA) would receive an increased 5-dBA sound as opposed to RW drivers (65.93 dBA). A p -value of 0.02 (t -test with a significant level of 0.05) manifested the significant difference between the average RW and WW sound levels.

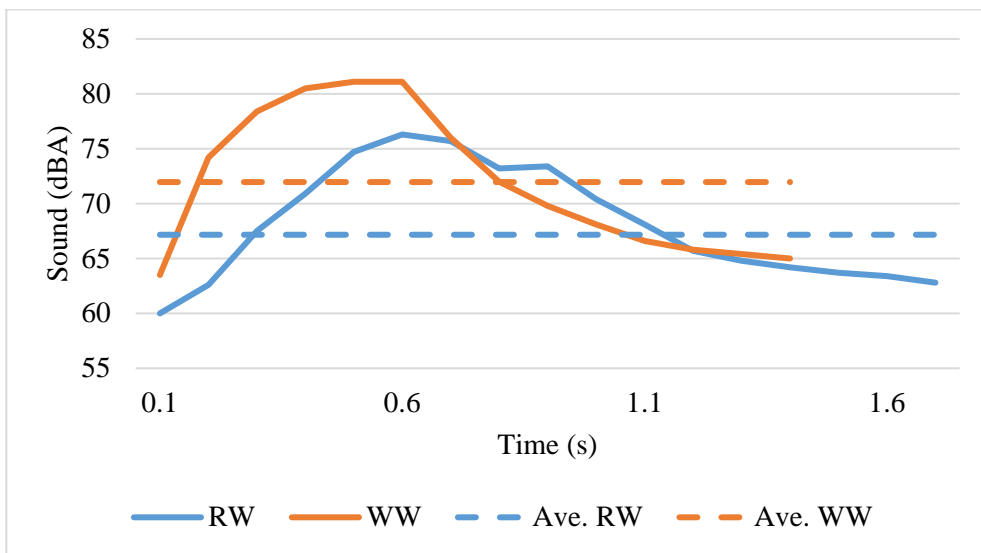
Figure 5.3-c demonstrates the RW and WW sound levels when a vehicle passes Pattern D3. The RW speed was 10 mph and WW 25 mph. Compared with ambient circumstances, RW drivers were able to obtain a 13 dBA louder sound at most. While WW drivers would perceive 20 dBA more. Additionally, WW drivers can obtain 70.50 dBA sound on average, which is 13 dBA more than the mean RW sound (57.5 dBA). The t -test (significant level = 0.05) result showed that the average RW and WW sound levels were significantly different by a p -value less than 0.01.



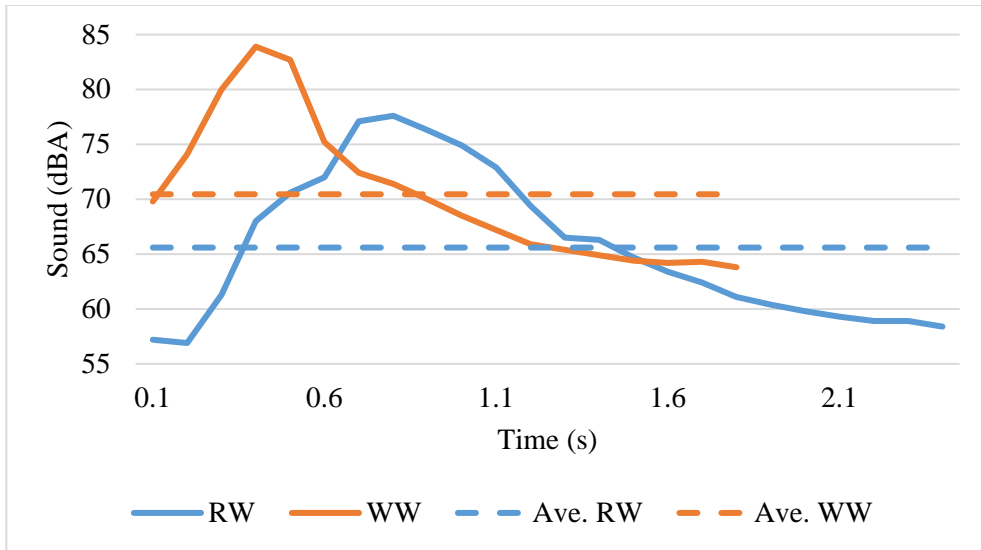
(a) Pattern E.1



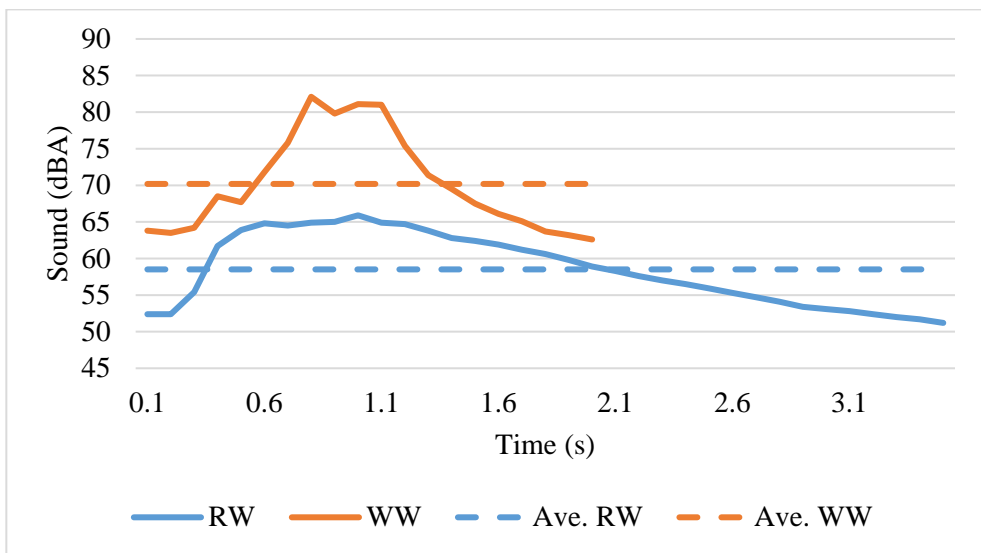
(b-1) Pattern C: 5-ft-spacing strips



(b-2) Pattern C: 2-ft-spacing strips



(b-3) Pattern C: 1-ft-spacing strips



(c) Pattern D3

Figure 5.3 RW and WW Sound of (a) Pattern E.1, (b) Pattern C, and (c) Pattern D3

Exterior Sound

When a vehicle traveler over rumble strips, exterior sound is a source of disturbance and has been the cause of complaints from roadside residents. The findings in this section can help directing the usage of the DRS in consideration of noise disturbances at adjacent properties, by

comparing the increase in noise levels with the required thresholds of noise levels. As shown in **Figure 5.4**, a sound-level meter was positioned 25 ft from the center of the travel lane, according to a study on evaluating centerline rumble strip noises (Sexton 2014). The sound meter was also placed 5 ft above the lane surface, which helped to reduce the effects of ground surfaces on sound propagation (i.e., “ground effects”).



Figure 5.4 Data Collection of Exterior Sound Caused by DRS

The exterior sound data was collected near the DRS under the ambient status (named “ambient” in **Table 5.6**) and conditions when vehicles were passing the DRS (named “vehicle”). The ambient status was considered as long as no vehicle was on the off-ramp travel lane. For example, it was also counted as ambient status if other vehicles were using the nearby freeway mainline, on-ramp, or crossroad. To eliminate the overlapping sound effects, a total of 100 free-flow vehicles was sampled for each DRS pattern (Pattern E.1 and D3) or every strip group (Pattern C). To evaluate the average exterior sound increment caused by the DRS, the “ambient” data was collected for the same duration of acquiring the “vehicle” data.

Table 5.6 summarizes the exterior sound levels caused by the DRS. At Exit 208, the ambient condition at Pattern E.1 ranged from 55 to 75 dBA. Because it was close to the freeway mainline, the sound level was 75 dBA at a maximum when mainline vehicles passed by. The sound level was from 68 to 79 dBA when a vehicle passed Pattern E.1. The average sound level indicates that Pattern E.1 generated an extra 8.9 dBA sound to the environment.

Pattern C was located on the segment between the off-ramp curve and terminal, which was close to neither the freeway mainlines nor the crossroad. Thus, the maximum ambient sound level was 65 dBA. The reduced spacings of strips led to the increasing sound levels generated by three strip groups. It also resulted in a sound increment. Therefore, the 5-ft-spacing strips generated an additional 3.2 dBA to the surroundings, with 5.1 and 9.7 dBA by the 2 and 1-ft strip groups, respectively.

Pattern D3 was placed at the ramp terminal, so that the ambient sound was a bit louder, compared with Pattern C. However, vehicles typically made complete stops at the stop bar and accelerated onto the crossroad. In this way, the exterior sound level was completely covered by and relied on the engine noise. Therefore, the sound increment caused by Pattern D3 was negligible.

Likewise, results were similar at Exit 284, except for the overall louder sound due to the larger traffic volumes. To summarize, Pattern E.1 can produce 9 dBA extra sound to the environment. Pattern C generated almost 10 dBA additional sound by the 5-ft-spacing strips, 5 dBA by the 2-ft ones, and 3 dBA by the 1-ft ones. The exterior sound impact of Pattern D3 was also negligible.

Table 5.6 Exterior Sound Levels Caused by DRS

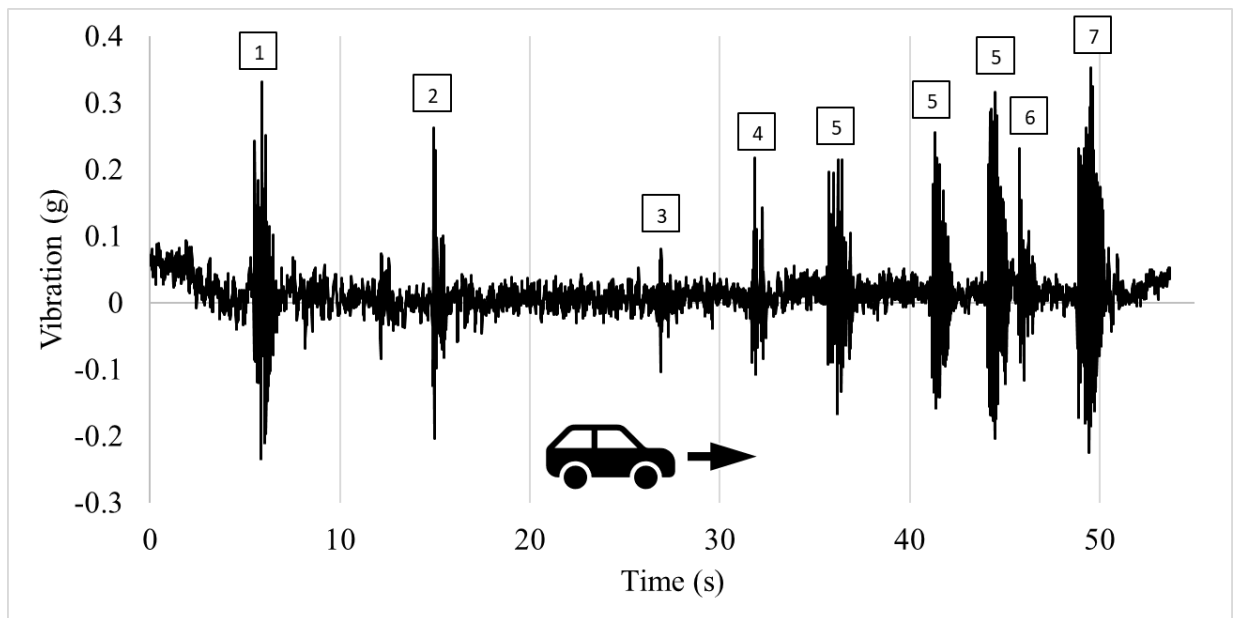
Location	Pattern		Ambient (dBA)	Vehicle (dBA)	Mean Increment (dBA)
Exit 208 I-65, AL	E.1		55-75	68-79	8.9
	C	5-ft	55-65	58-68	3.2
		2-ft		60-70	5.1
		1-ft		65-74	9.7
	D3		55-67	engine noise	negligible
Exit 284 I-65, AL	E.1		62-77	70-77	8.5
	C	5-ft	60-67	62-70	2.9
		2-ft		66-72	5.6
		1-ft		70-75	9.2
	D3		65-70	engine noise	negligible

Note: “Ambient” = Sound level when no vehicle passes DRS; “Vehicle” = Sound level when one vehicle passes DRS.

Interior Vibrations

Interior vibration data was also acquired from field driving tests at Exit 208 on I-65, AL. Seven speed categories, i.e., 10, 15, 20, 25, 30, 35, and 40 mph, were tested for both RW and WW directions. The RW vibration data was collected from the deceleration lane to the off-ramp

terminal on the closed ramp. The WW data was obtained from driving in the reverse direction. **Figure 5.5** displays the sample RW vibration data along the off-ramp at a constant speed of 20 mph. There was a time lag between recording the sound data and triggering the vibration data collection. Hence, noises were caused by vehicle acceleration before 6 s. At 7 s, the vehicle started passing Pattern E.1, so that the first signal was generated. A second signal was created by passing the WW arrow at 15 s. As previously mentioned, the first lane-use WW arrow was not hit. Afterward, the vehicle passed the following WW and lane-use arrows at 27 and 32 s. Then, three signals were produced by Pattern C, followed by a consequential one from the dual WW arrows. Pattern D3 contributed to the last vibration signal.



Note: a) 1 = Pattern E.1; 2 = WW arrow; 3 = WW arrow; 4 = lane-use arrow; 5 = Pattern C; 6 = dual WW arrows; 7 = Pattern D3. b) Speed = 20 mph.

Figure 5.5 Sample RW Vibration Data along the Off-Ramp

RMS amplitudes of vibrations were employed to present the equivalent constant values. *F*-tests at the significance level of 0.05 were then used to check whether there was a significant difference in variance between RW and WW vibrations.

According to the NC-350 speed data, the average RW speed was 30 mph and WW 35 mph when vehicles passed Pattern E.1. The effective amplitude of WW vibrations was 0.106 g (g: standard gravity; $1\text{ g} = 32\text{ ft/s}^2$), which was 0.027 g higher than the RW direction (0.079 g). The p -value from the f -test at the significance level of 0.05 was less than 0.01, which showed that the variances of RW and WW vibrations were significantly different. **Figure 5.6** presents the RW and WW spectrums of Pattern E.1. The RW vibrations had peaks of 2 and 13 Hz, while the WW direction had peak vibrations at 2, 16, 32, and 47 Hz. In short, WW drivers can perceive more severe vibrations of higher amplitudes and frequencies.

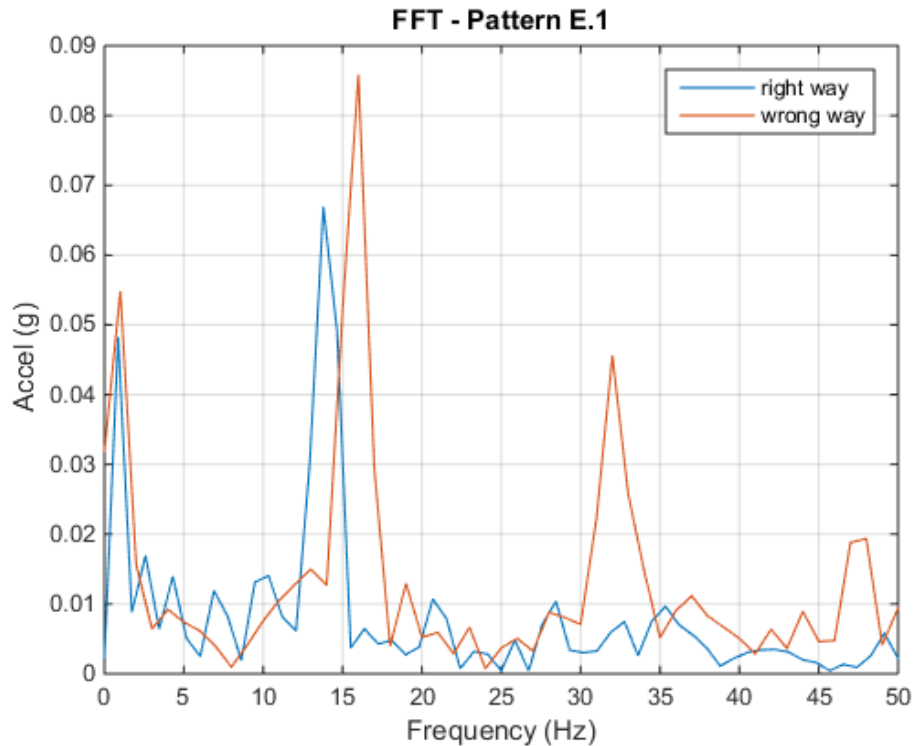


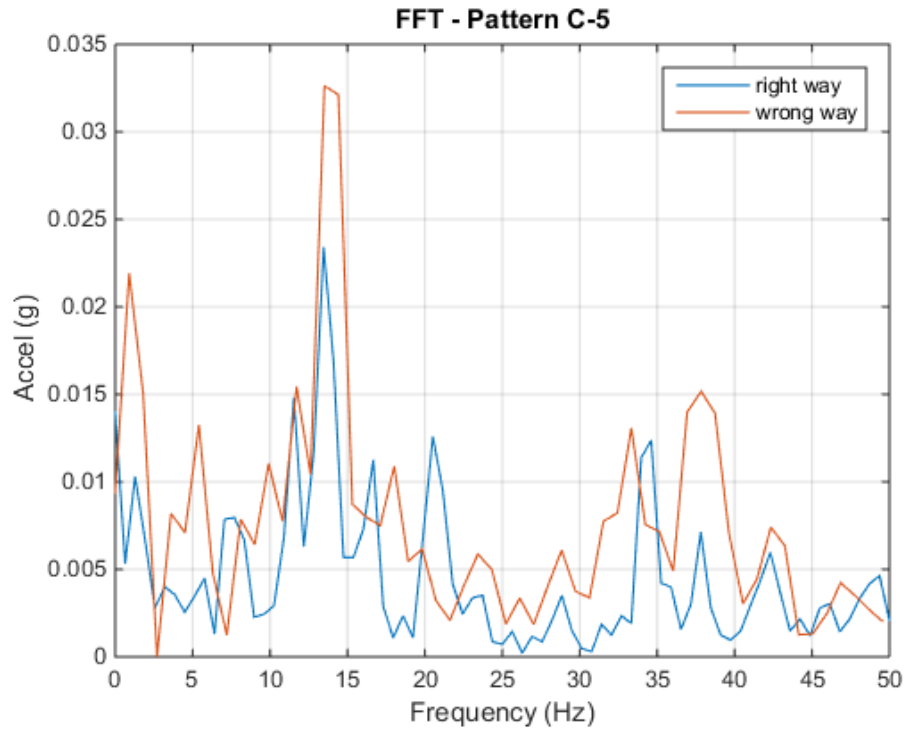
Figure 5.6 RW and WW Spectrums of Pattern E.1

WW vehicles were recorded to have a constant speed of 35 mph while passing the segment where Pattern C was installed. However, RW drivers had decreased average speeds of 30, 25, and 20 mph at the strips of 5-ft, 2-ft, and 1-ft spacings, respectively. Consequently, RW drivers were able to perceive vibrations equivalent to 0.041 g and WW 0.054 g when passing the strips of 5-ft

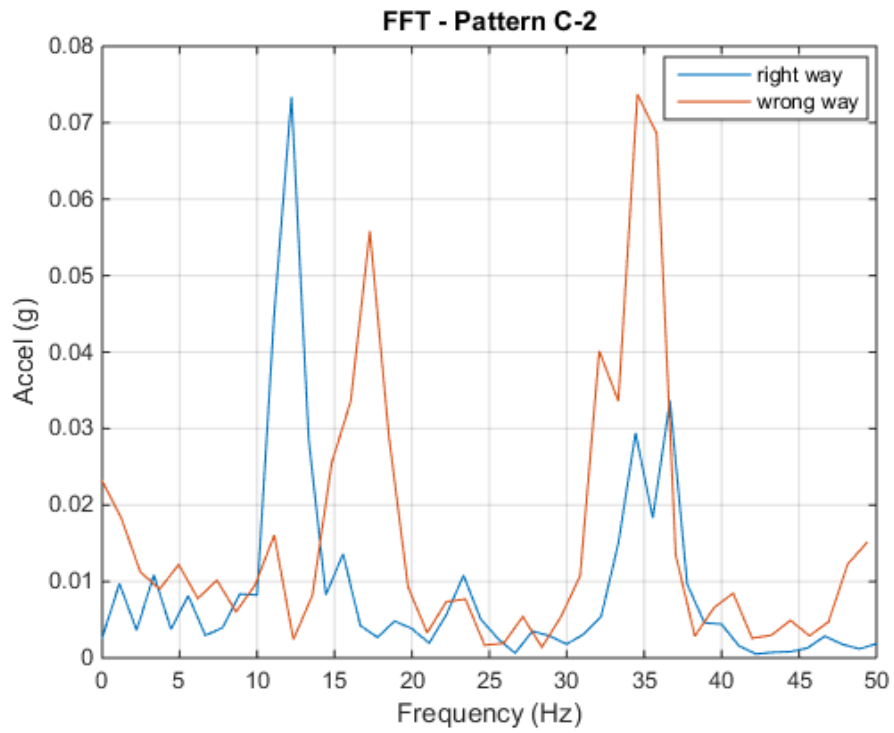
spacings. The RW and WW vibrations were significantly different in variances according to the p -value less than 0.01 from the f -test. As shown in **Figure 5.7-a**, vibrations for RW drivers had peaks of 3, 13, 21, and 35 Hz, while WW vibrations saw peaks of 2, 5, 13, 33, and 37 Hz. Visually, the peaks from RW and WW vibrations were alike due to the close speeds. However, WW vibration peaks had 1.3 times higher amplitudes on average.

The effective WW vibration was 0.117 g , which was 0.040 g more than the RW one (0.077 g) by the 2-ft-spacing strips. The f -test result also showed the significant difference between the variances of RW and WW vibrations. The spectrums of RW and WW vibrations produced by these strips are presented in **Figure 5.7-b**. RW vibrations had peaks of 13 and 35 Hz, while peaks occurred at 17 and 35 Hz in the WW direction. The amplitude of the 13 Hz RW peak was almost 0.02 g higher than the 17 Hz WW peak, while amplitudes of the 35 Hz WW peak were more than twice as high as the RW one.

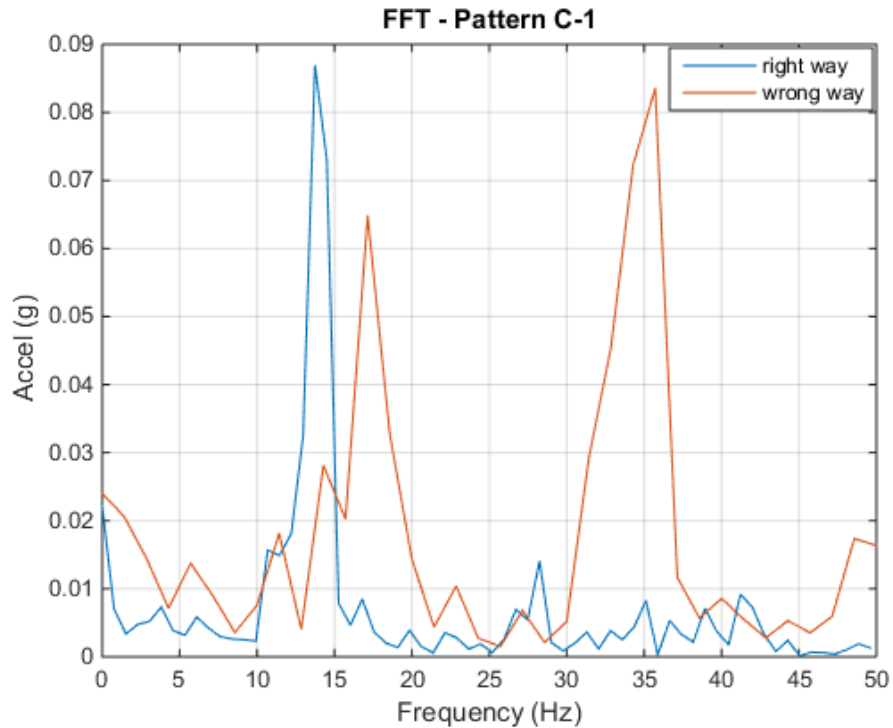
For the 1-ft-spacing strips, RW drivers can get 0.098 g vibrations and WW 0.121 g according to the RMS values. A p -value of 0.02 from the f -test revealed a significant difference between RW and WW vibrations in variances. **Figure 5.7-c** exposed the spectrums of RW and WW vibrations. The RW vibration only had a peak of 14 Hz, while WW had two of 17 and 36 Hz. To sum up, WW drivers can also perceive more severe vibrations by Pattern C regarding the larger amplitudes and higher frequencies.



(a)



(b)



(c)

Figure 5.7 RW and WW Spectrums of Pattern C: (a) 5-ft, (b) 2-ft, and (c) 1-ft Spacing

RW drivers further slowed down until making a complete stop at the stop bar. Thus, the average RW speed was about 10 mph at Pattern D3. In contrast, WW drivers considered the off-ramp terminal as the on-ramp entrance, which resulted in their entering speed being recorded around 25 mph. Consequently, RW drivers can perceive vibrations equivalent to 0.044 g and WW 0.089 g. As shown in **Figure 5.8**, vibrations for RW drivers had peaks of 1 and 7 Hz, while WW drivers obtained peaks of 1, 12, and 35 Hz in vibration. Briefly, WW drivers would have twice as many RW vibrations according to the RMS values as well as peaks of higher frequencies.

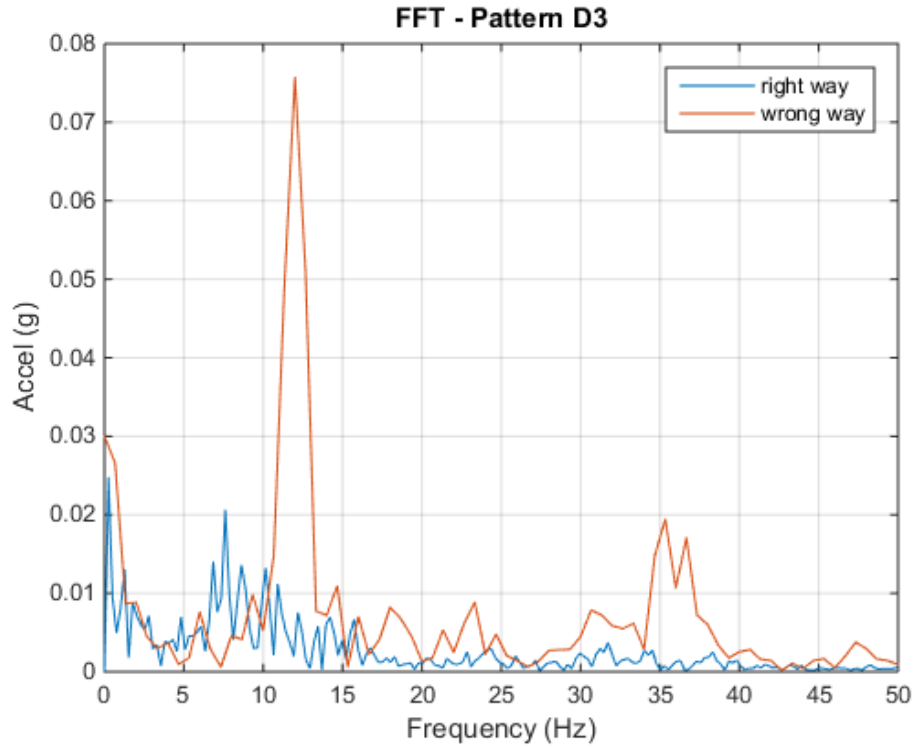


Figure 5.8 RW and WW Spectrums of Pattern D3

5.3 Impacts of DRS on Vehicle Speeds

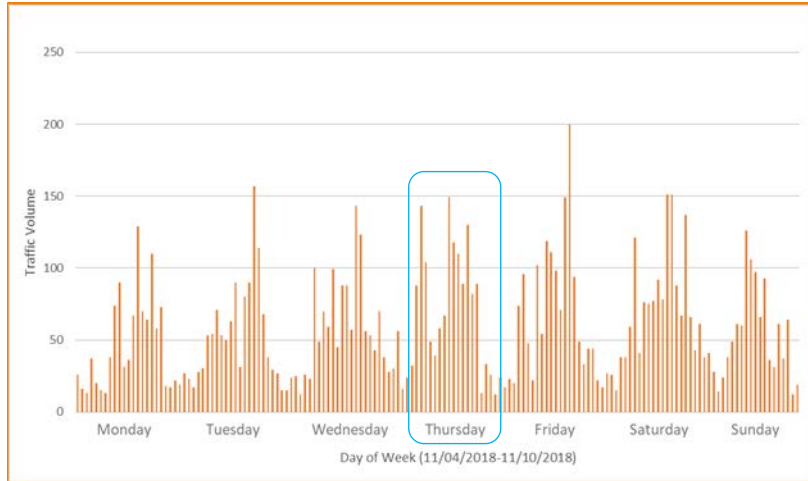
To evaluate the effectiveness on right-way traffic speed of three DRS patterns, speed data were collected for one week from W0 to W3. Raw speed data were filtered and cleaned prior to analysis. Descriptions of variables of the raw data are listed in **Table 5.7**. For the purpose of analyzing the RW vehicle speed, the advice code of 2 was selected. According to *Reference.com* (Reference, 2019), the average length of passenger cars ranges from 14.4 to 16.4 ft in America. Thus, a filter was set to search records between 14 and 17 ft. To eliminate the effects of slow leading vehicles on speeds, gaps greater than 2 s were selected. The 2 s time headway was associated with the space headway of more than 90 ft. This will ensure that the average speeds on the off-ramps were estimated for the free-flow condition. Consequently, boxplots were utilized to detect potential outliers. Outliers were filtered if they were more than the upper limit or less than

the lower limit. For a normal distribution ($\alpha = 0.05$), 0.7% of the data (outliers) was beyond the upper and lower limits. Here, interquartile range (IQR) = upper quartile (Q3) – lower quartile (Q1), lower limit = Q1 – 1.5×IQR, and upper limit = Q3 + 1.5×IQR. Finally, approximately 70% of speed data remained for analysis after filtering and cleaning process.

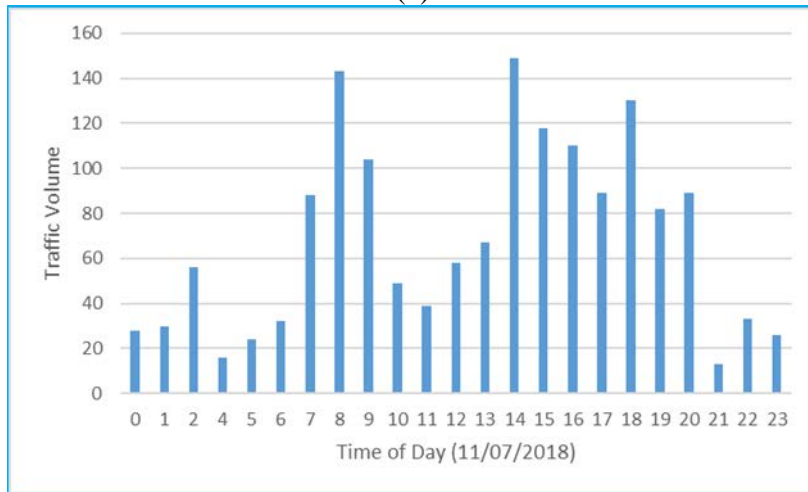
Table 5.7 Variables of Raw Speed Data (Partial)

Variable	Unit	Description
DateTime	Year/month/day/time	Date and time when a vehicle occupied the sensor.
AdviceCode	-	Codes for different records. For example, 2 is the correct direction, 4 stands for the reversed direction, and 128 means that records exceeded the preset filters.
Speed	Mph	Vehicle speed when it passed the sensor.
Length	Ft	Detected vehicle length.
Gap	S	Time headway between recorded vehicles.

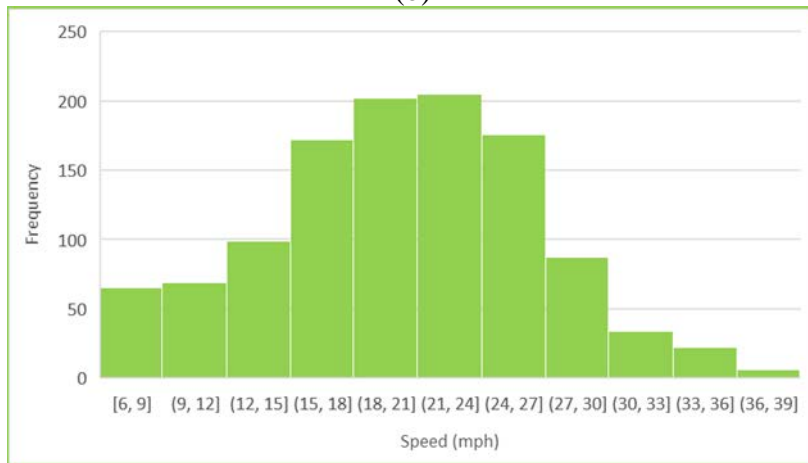
An example of traffic volume and speed data from the sensor #98 during W0 is illustrated in **Figure 5.9**. In **Figure 5.9-a**, daily traffic volumes of a week are presented. Morning and afternoon peaks can also be observed. Roughly, Sunday and Monday had lower traffic volumes, while Friday had the highest afternoon peak. Taking the Thursday data as an example in **Figure 5.9-b**, morning, midday, and afternoon peaks can be found around 8 a.m., 2 p.m., and 6 p.m. Much lower volumes were recorded during the nighttime. **Figure 5.9-c** shows the speed histogram of the day, which follows the normal distribution. Speeds are concentrated within 15 to 27 mph.



(a)



(b)



(c)

Figure 5.9 Sample traffic volume and speed data: (a) week volume; (b) Thursday volume in (a); (c) speed histogram of (b)

Descriptive statistics such as maximum, 85th percentile, mean, minimum, and variance (standard deviation) were first calculated. Details can be found in Appendix B. To compare the average speeds, z -tests were employed. As the speed distributions were normal, both z - (when variances were known) and t -tests can be applied. Z -tests were used when the sample size was large (i.e., greater than 30), while t -tests were utilized with small sample sizes. The significance level of z -tests used in this study was 0.05. Garber and Gadiraju (1989) found that crash rates increased by 0.3% with a 1 unit increase in speed variance (mph²). In this study, f -tests were applied to compare the before and after speed variances. Also, the driver adoption of the DRS was investigated through changes in speed variances after the implementation.

Average Speeds

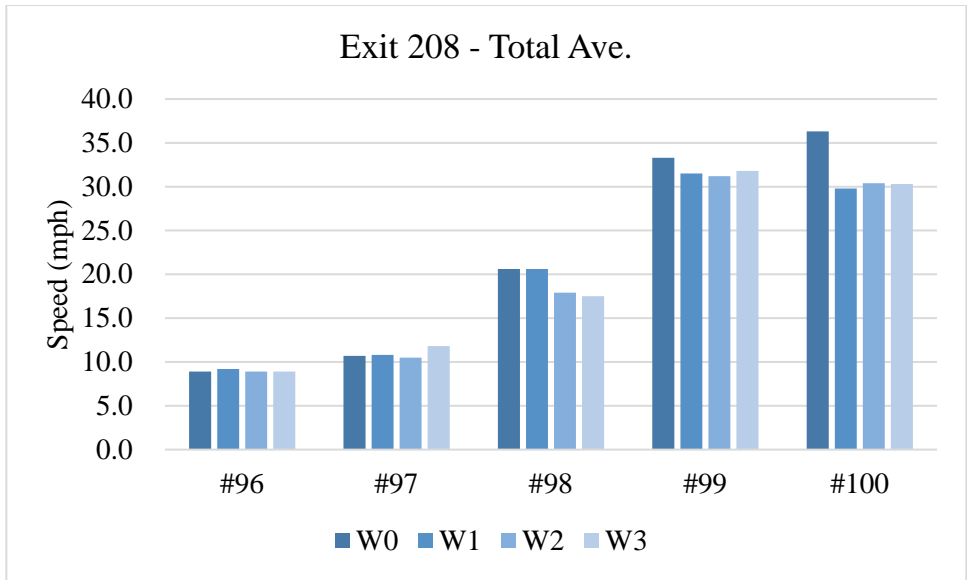
The average speeds of RW vehicles were estimated at each location for each of four study periods (W0-W3). A comparison between the average speed before and after each DRS implementation was conducted to examine if the DRS pattern has an impact on average speed. In addition, the average speed was compared with the posted advisory speeds (25 mph at Exit 208 and 30 mph at Exit 284). As shown in **Figure 5.10-a**, the average speed from sensor #100 significantly decreased by 6.5 mph (from 36.3 to 29.8 mph) at Exit 208 after the installation of Pattern E.1. While at Exit 284 (**Figure 5.10-b**), a significant reduction of 2.3 mph (from 30.3 to 28 mph) in the average speed from sensor #104 was observed after implementing Pattern E.1. Because the average speed in the before period was close to the advisory speed, less reduction in Exit 284 was observed compared with that in Exit 208. Moreover, as shown in **Table 5.8**, it was found that 94% of vehicles exceeded the advisory ramp speed at Exit 208 in the W0 period. This percentage was reduced to 83% by installing Pattern E.1, while the percentage of vehicles that

drove faster than the advisory ramp speed, decreased from 45% to 30% at Exit 284. This finding implied that Pattern E.1 can slow down RW drivers and help them to follow the advisory speed when they were approaching the ramp curve. The possible reason for more reduction in Exit 208 is because the posted advisory speed (25 mph) at Exit 208 is much lower than the average speed of 36.3 mph in the W0 period.

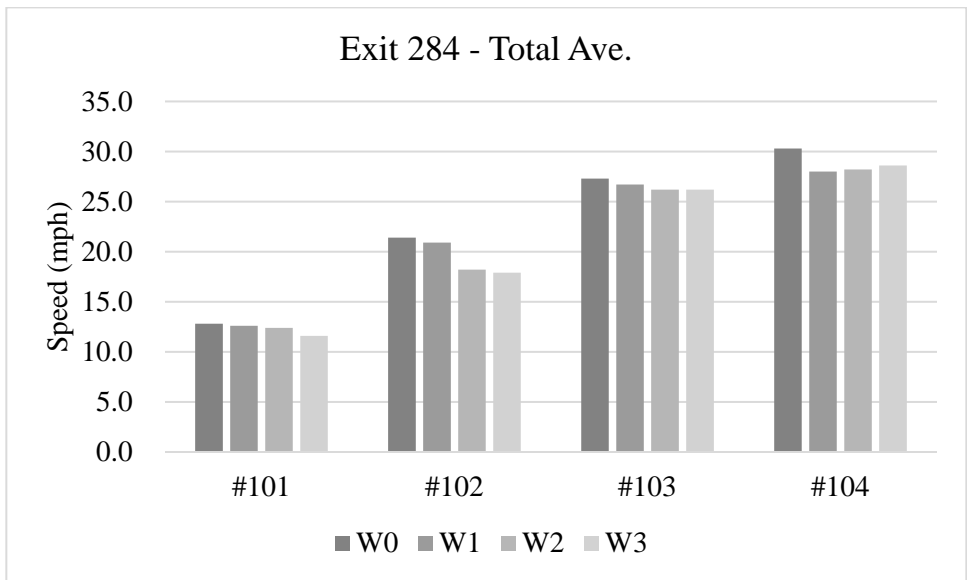
After installing Pattern C, as shown in **Figure 5.10**, significant changes in average speeds between W1 and W2 can be observed from sensors #98 and #102 at Exits 208 and 284, respectively. The same average speed reduction of 2.7 mph occurred at both off-ramps when RW vehicles passed Pattern C.

At Exit 208 (**Figure 5.10-a**), the average right-turn speed slightly increased by 1.3 mph at the stop bar where sensor #97 was located after implementing Pattern D3, while there was no significant change from sensor #96 for left turns. The possible reason is that more right-turning vehicles stopped on Pattern D3 before the stop bar and then accelerated to merge the crossroad traffic. Sensor #97 was installed after the stop bar. The average speed at the yield line (sensor #101 in **Figure 5.10-b**) was significantly reduced by 0.8 mph at Exit 284 because most of vehicles did not make a full stop behind the yield line.

The above significances were tested using z -tests at the significance level of 0.05. Statistical results can be found in **Table 5.9**. Average speeds among the four study periods, which showed no significant difference, are not listed.



(a)



(b)

Figure 5.10 Average Speeds on Southbound Off-Ramps at Exits (a) 208 and (b) 284

Table 5.8 Pattern E.1 Helped Drivers Follow the Advisory Ramp Speed

Time	Traffic Volume		Vehicles (%) Exceed the Advisory Ramp Speed		Note
	Exit 208	Exit 284	Exit 208	Exit 284	
W0	1,347	1,127	1,266 (94%)	507 (45%)	Pattern E.1 wasn't installed
W1	1,291	1,180	1,072 (83%)	354 (30%)	Pattern E.1 was installed

Table 5.9 Z-tests Results of Changes in Average Speeds

Sensor	Comparison Groups ²		<i>p</i> -value ¹
#97	W2	W3	0.02
#98	W1	W2	< 0.01
#99	W0	W1	< 0.01
#100	W0	W1	< 0.01
#101	W2	W3	< 0.01
#102	W1	W2	< 0.01
#104	W0	W1	< 0.01

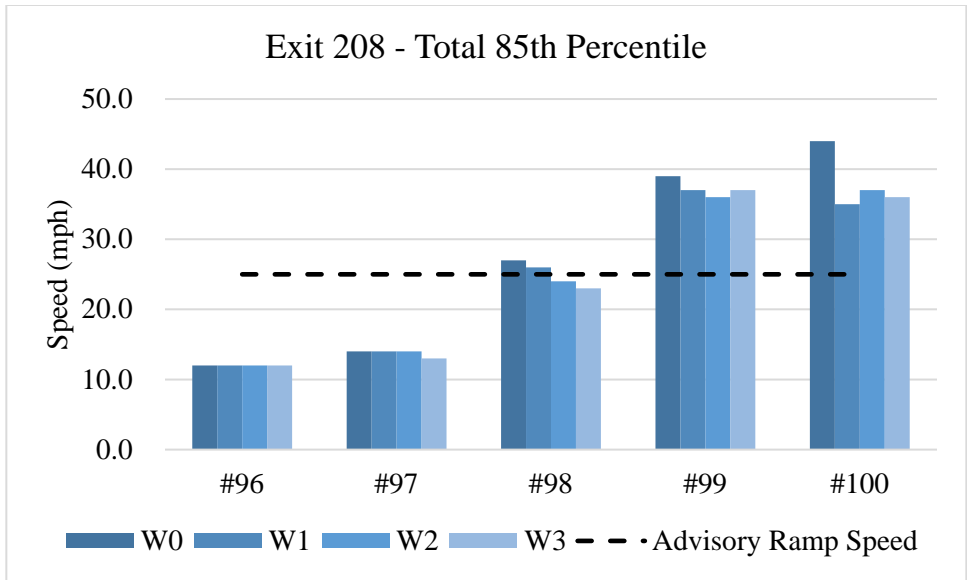
Note: 1) *z*-tests; 2) Adjacent weeks that having no statistical differences were not listed.

85th Percentile Speeds

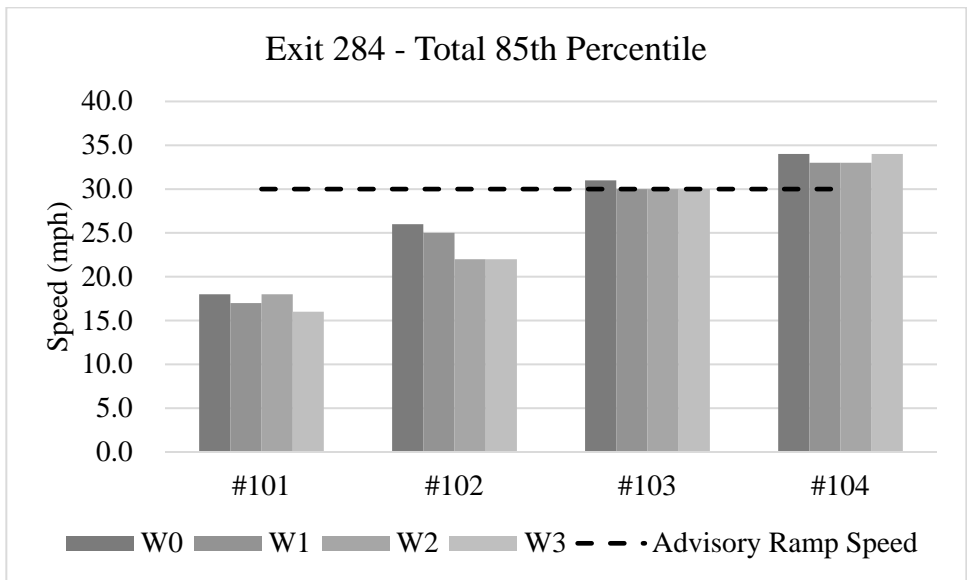
The 85th percentile speeds generally describe the speeds higher than 85 percent of drivers. The upper 15th percentile of this distribution can represent aggressive driving speeds. The MUTCD recommends that the speed limit be within 5 mph of the 85th percentile speed of free-flowing traffic. Adjustments can be made if there are horizontal and vertical curves (possible limited sight distance).

As shown in **Figure 5.11-a**, the advisory ramp speed is 25 mph at Exit 208. The 85th percentile speed when vehicles approached the ramp curve (sensor #100) stabilized at around 35 from 44 mph after implementing Pattern E.1. The 85th percentile speed was reduced from 39 mph to around 35 mph at the location (sensor #99). The results indicated that the majority of drivers reduced their speed by 4 to 9 mph by Pattern E.1. Moreover, changes in upper 15th percentile speeds also implied that Pattern E.1 can help mitigate aggressive driving. As listed in **Table 5.10**, characteristics of the upper 15th percentile speeds when vehicles approached (sensor #100) and exited (sensor #99) the ramp curve, including maximum, mean, minimum, and standard deviation, were reduced after implementing Pattern E.1. With p -values less than 0.05 from z - and f -tests at the significance level of 0.05, their mean and standard deviation proved to have significant decreases.

The advisory ramp speed was 30 mph at Exit 284, as presented in **Figure 5.11-b**. No significant difference of the 85th percentile speed was observed when vehicles entered (sensor #104) and exited (sensor #103) the ramp curve because the initial 85th speed was close to the advisory speed.



(a)



(b)

Figure 5.11 85th Percentile Speeds on Southbound Off-Ramps at Exits (a) 208 and (b) 284

Table 5.10 Characteristics of Upper 15th Percentile Speeds from Sensors #99 and #100 at Exit 208

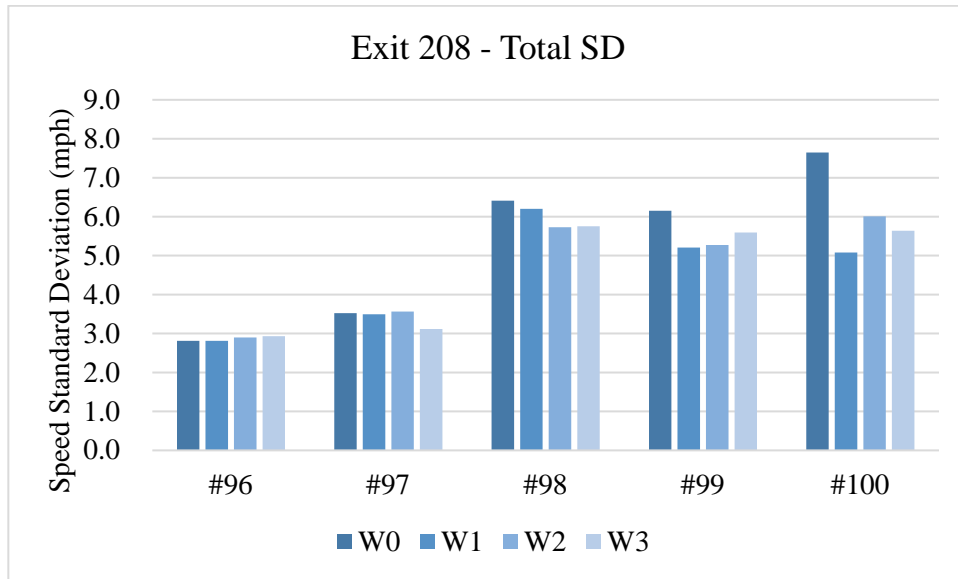
Characteristics (Unit: mph)	Sensor #99				Sensor #100			
	W0	W1	W2	W3	W0	W1	W2	W3
Max	51.0	45.0	45.0	48.0	58.0	44.0	47.0	46.0
Mean	43.0	40.1	39.5	40.7	49.7	38.7	41.5	40.4
Min	40.0	38.0	37.0	38.0	45.0	36.0	38.0	37.0
Standard Deviation	3.1	1.9	2.3	2.6	4.0	2.3	3.0	2.8

Speed Standard Deviations

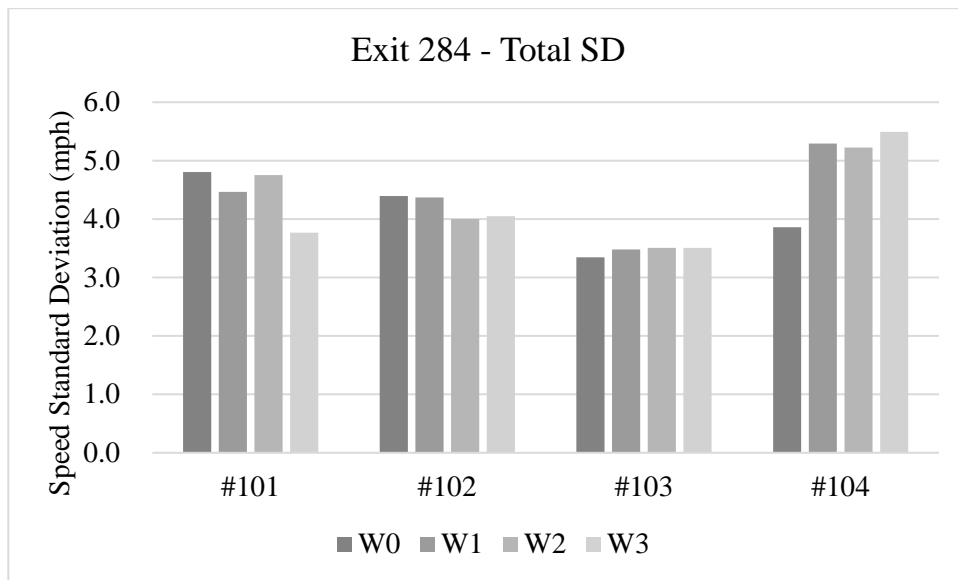
Figure 5.12 presents the standard deviations (SDs) of RW speeds along the off-ramps from W0 to W3 at the two study locations. At Exit 208 (**Figure 5.12-a**), the SDs of RW speed at all five spots showed a decline trend after implementing DRS. In the W1 period after implementing Pattern E.1, SDs from sensors #100 and #99 significantly decreased by 2.5 and 1.0 mph, respectively. From W1 to W2, the SDs from sensor #98 were significantly reduced by 0.5 mph after installation of Pattern C. Further, Pattern D3 led to a decrease of 0.5 mph in SDs for right-turning speed at the stop bar (sensor #97).

At Exit 284 (**Figure 5.12-b**), Pattern D3 led to a decrease of 1.0 mph in the SDs for right-turn speeds at the yield line (sensor #101). Pattern C reduced 0.4 mph in the SDs of average speed in the middle of ramp (sensor #102). However, SDs from sensor #104 significantly increased by 1.4 mph after installing Pattern E.1. Moreover, the SD from sensor #104 significantly increased by 0.9 mph in the W2 period. The possible reason is that average speed of this location was close to the posted advisory speed. Some drivers may further reduce their speeds after implementing the DRS, which increased the speed SDs as a result.

Speed variances were tested using f -tests at the significance level of 0.05. The results are shown in **Table 5.11**. Speed variances between adjacent weeks, which show no significant difference, are not listed.



(a)



(b)

Figure 5.12 Speed Standard Deviations on Southbound Off-Ramps at Exits (a) 208 and (b) 284

Table 5.11 F-test Results of Changes in Speed Variances

Sensor	Comparison Groups ²		p-value ¹
#97	W2	W3	< 0.01
#98	W1	W2	0.03
#99	W0	W1	< 0.01
#100	W0	W1	< 0.01
	W1	W2	< 0.01
#101	W2	W3	< 0.01
#102	W1	W2	< 0.01
#104	W0	W1	< 0.01

Note: 1) *f*-tests; 2) Adjacent weeks that having no statistical differences were not listed.

Driver Adoption of DRS

Because DRS are new traffic control devices, drivers may need time to get used to them. The trends of daily changes in speed SDs were used to evaluate the driver adoption of a certain DRS pattern. The following parts describe the driver adoption process of each DRS pattern as time goes by. Speed SDs at each location were recorded for each day from W0 to W3. The simple moving average method (Interval = 2 days) was applied to track the trend.

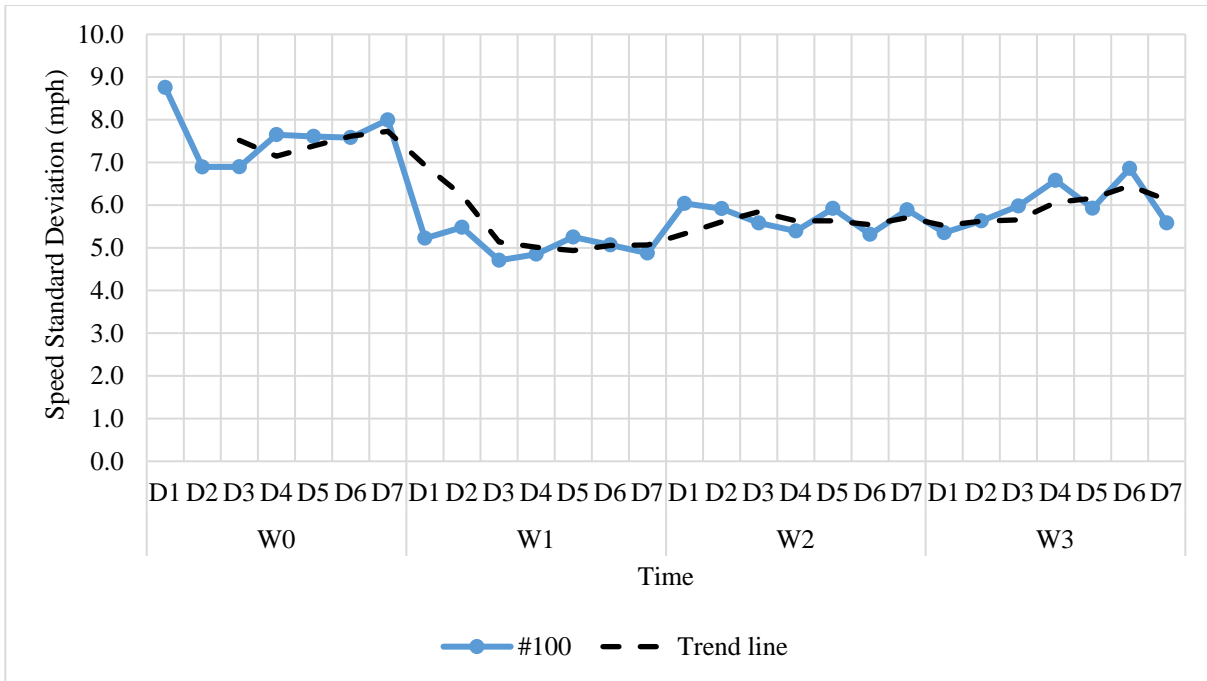
As illustrated in the previous sections, significant changes of speed SDs were identified before vehicles entering the off-ramp curves at both locations after installing Pattern E.1. **Figure 5.13** presents the trends of the driver adoption process. At Exit 208 (**Figure 5.13-a**), an immediate drop of the speed SD was observed on the first day of W1 when Pattern E.1 was installed. It roughly took two days for the speed SD to become stable around 5 mph. After another week, it

had the trend that the speed SD there had increased by 1 mph. Hence, Pattern E.1 was not eventually in effect until the third day. Once drivers got used to it, the speed SD could slightly increase. In contrast, an increasing trend can be found from Day 1 (D1) to Day 3 (D3) during W1 at Exit 284 (**Figure 5.13-b**), which was related to the installation of Pattern E.1. The speed SD then stabilized between 5 and 6 mph. *P*-values of 0.01 (Exit 208) and < 0.01 (Exit 284) from *f*-tests at a significance level of 0.05 indicated that the speed SDs before W1 D1 were significantly higher than that after W1 D3. Therefore, speed differences gradually increased within three days, as drivers became increasingly familiar with the Pattern E.1.

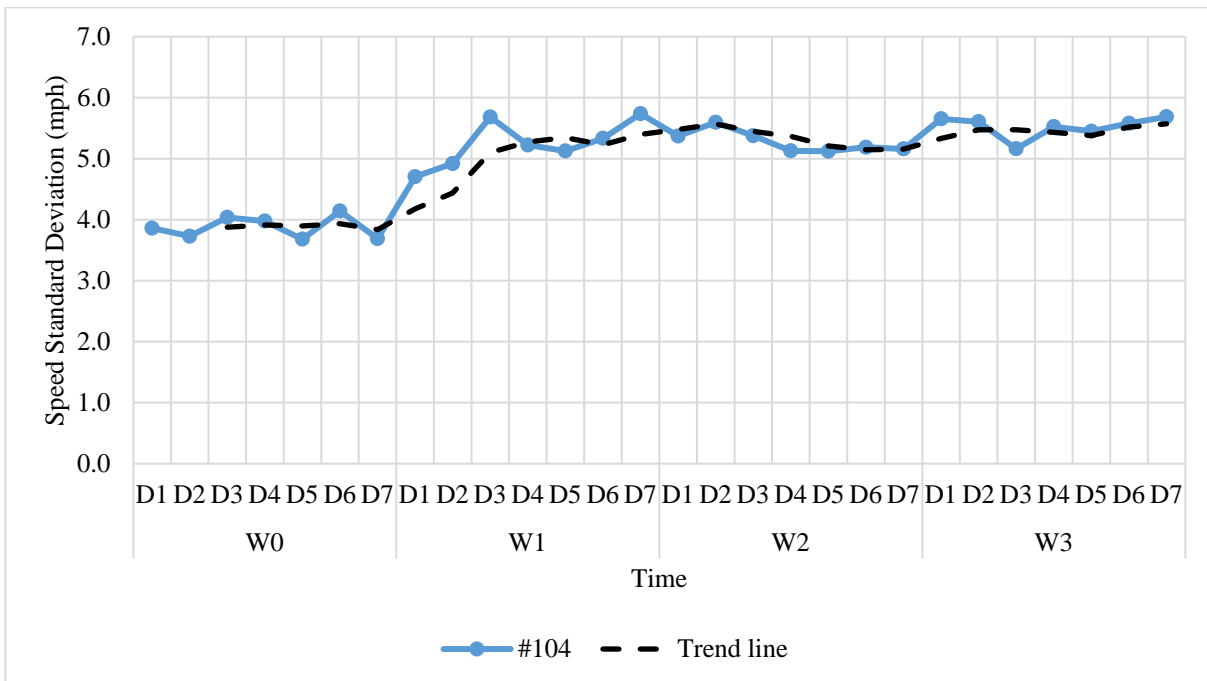
Significant reductions in speed SD at the segment between the ramp curve and terminal were also found after installation of Pattern C. As presented in **Figure 5.14**, the speed SDs gradually decreased after Day 1 (D1) at W2 until becoming stable. The first drop of speed SDs occurred on the second day of W2. Because Pattern C and TRS were alike, drivers easily became accustomed to this DRS pattern. *P*-values of 0.03 (Exit 208) and 0.02 (Exit 284) from *f*-tests at a significance level of 0.05 indicated that the speed SDs before W2 D1 were significantly higher than that after W2 D2.

Pattern D3 helped reduce the speed SDs at both stop and yield-controlled ramp terminals. As presented in **Figure 5.15-a**, the decreasing trend of the speed SD for right-turn vehicles slowed after three days at Exit 208. It indicated that an increased proportion of drivers made complete stops, which resulted in smaller speed differences. The downhill trend also indicated that Pattern D3 could help more drivers make complete stops at the stop bar, even if there is no vehicle on the crossroad. While at the yield-controlled terminal, as shown in **Figure 5.15-b**, it took two days for RW drivers to further lower the speed SDs. Pattern D3 eventually reduced the average speed SD below 5 mph, which may make it safer to merge onto the crossroad by taking more time to choose

a gap. P -values of 0.01 (Exit 208) and 0.01 (Exit 284) from f -tests at a significance level of 0.05 indicated that the speed SDs before W3 D1 were significantly higher than that after W3 D2.

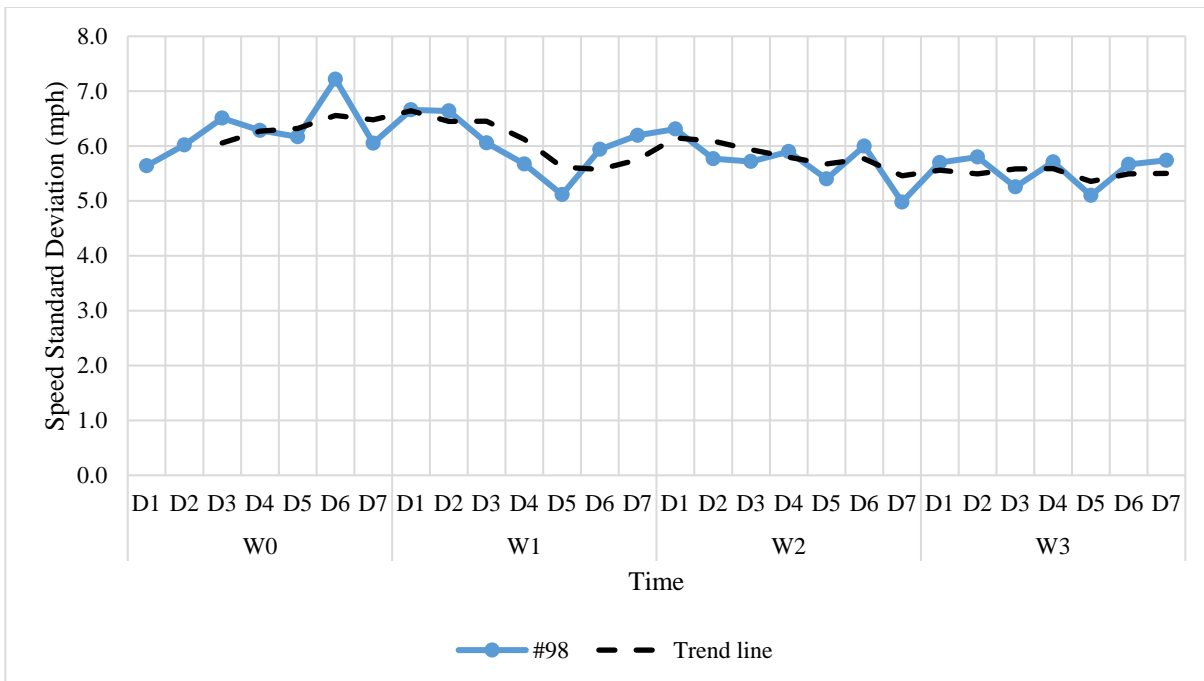


(a)

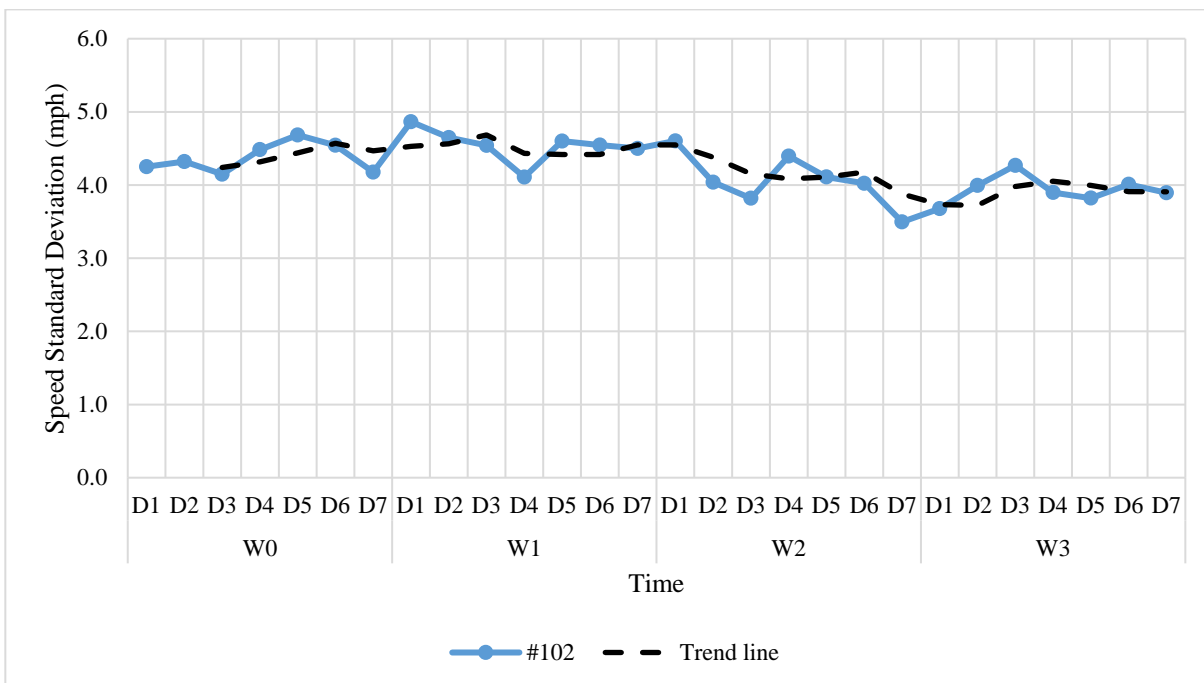


(b)

Figure 5.13 Driver Adoption of Pattern E.1 at Exits (a) 208 and (b) 284

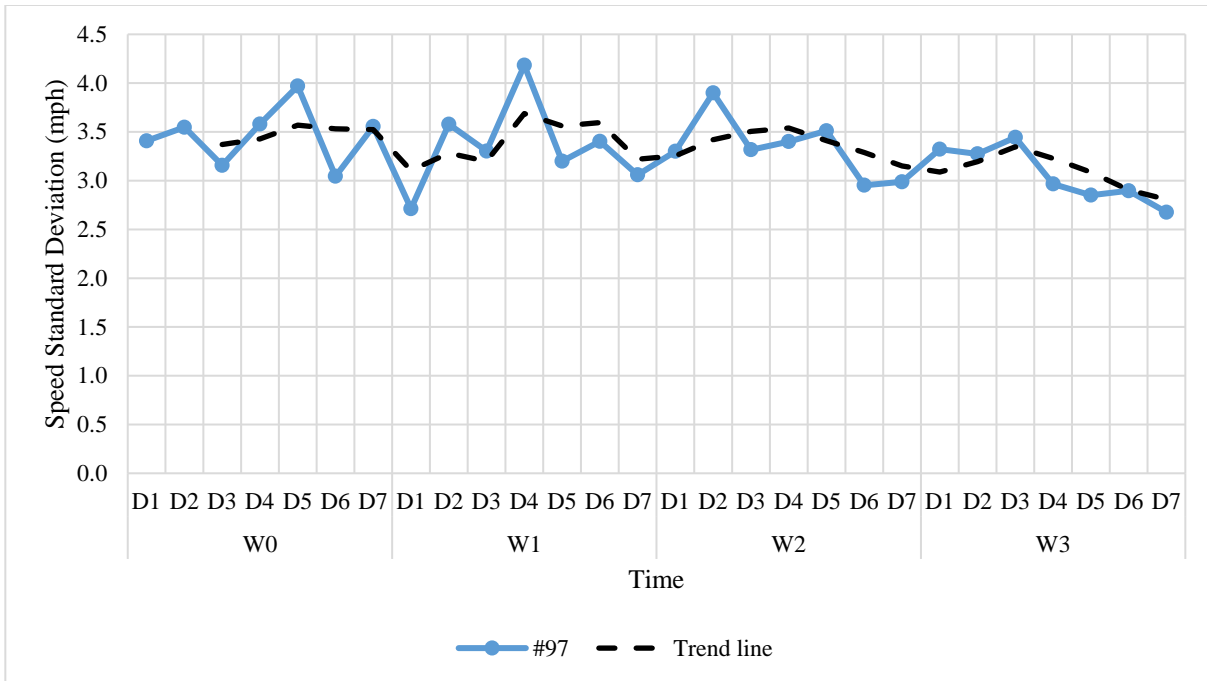


(a)

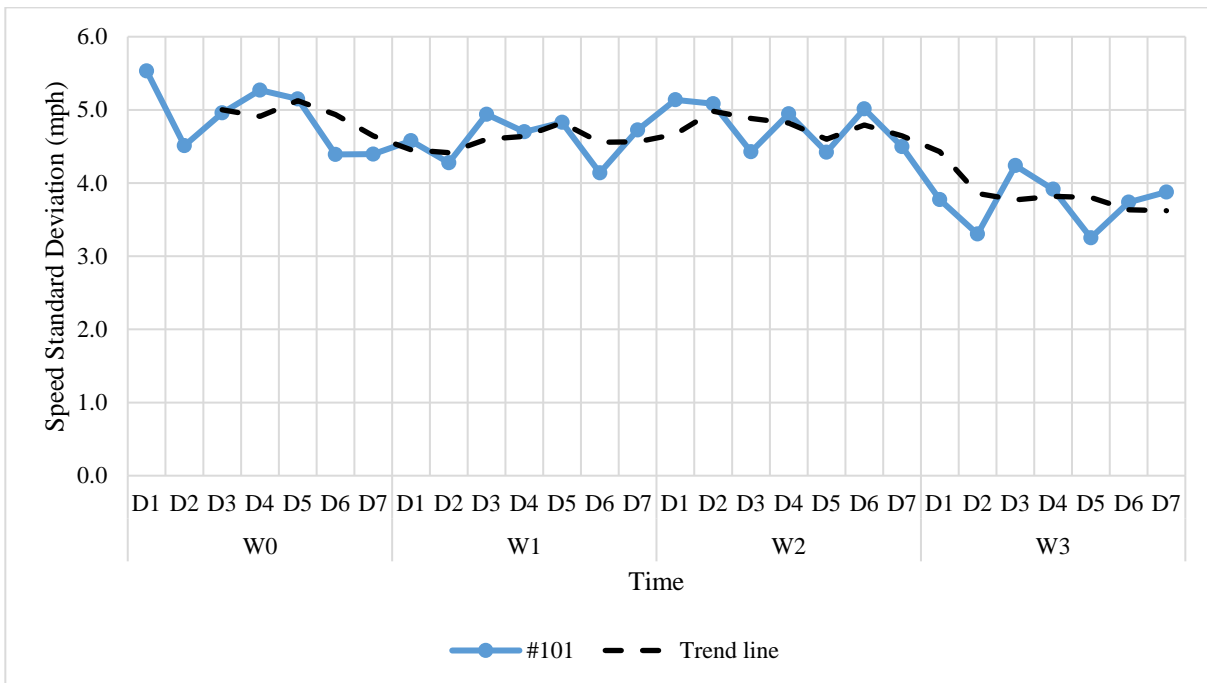


(b)

Figure 5.14 Driver Adoption of Pattern C at Exits (a) 208 and (b) 284



(a)



(b)

Figure 5.15 Driver Adoption of Pattern D3 at Exits (a) 208 and (b) 284

Speed Comparisons between Daytime and Nighttime

This section discusses the potential different impacts of DRS on vehicle speed and driver behavior during daytime and nighttime. Daytime was considered from 7 a.m. to 5 p.m. when it was not completely dark based on videos. About 60% of traffic volume occurred during the daytime. Findings of comparisons of average speed and its SD between daytime and nighttime are summarized as follows.

As previously discussed, Pattern E.1 was able to reduce average speeds when RW vehicles approached the off-ramp curve. As shown in **Table 5.12**, vehicles traveled faster during the daytime than the nighttime before entering the ramp curve according to data from sensors #100 and #104. Also, average speeds decreased more at Exit 208 than Exit 284, according to the speed reductions and their percentages. Pattern E.1, with all white strips, can reduce average speed by 1.8 mph at Exit 284 during the daytime. However, the z -test result indicated that it wasn't significant at the 95% confidence level because the p -value exceeded 0.05. During the nighttime, the average speed at Exit 284 significantly reduced by 2.6 mph, which was more than the reduction during the daytime. Pattern E.1, with one-side yellow strips, at Exit 208 can significantly reduce average speeds by 6.9 and 6.5 mph during daytime and nighttime, respectively.

The SD comparisons listed in **Table 5.13** show that speed SDs at Exit 284 decreased 10% more during daytime than nighttime. However, there was no difference between daytime and nighttime at Exit 208, given the SD reductions over 30%.

Table 5.12 Comparisons of Daytime and Nighttime Average Speeds after Implementing Pattern E.1

Time	Location	Average Speed (mph)		Speed Reduction (mph)	Reduction %	<i>p</i> -value ¹
		W0	W1			
Daytime	Exit 208	37.0	30.1	6.9	19%	< 0.01
	Exit 284	30.8	29.0	1.8	6%	0.06
Nighttime	Exit 208	35.6	29.1	6.5	18%	< 0.01
	Exit 284	29.6	27.0	2.6	9%	0.02

Note: 1) *z*-tests.

Table 5.13 Comparisons of Daytime and Nighttime Speed Standard Deviations after Implementing Pattern E.1

Time	Location	Speed SD (mph)		SD Reduction (mph)	Reduction%	<i>p</i> -value ¹
		W0	W1			
Daytime	Exit 208	7.7	5.1	2.6	34%	< 0.01
	Exit 284	3.8	5.4	-1.6	-42%	< 0.01
Nighttime	Exit 208	7.6	5.1	2.5	33%	< 0.01
	Exit 284	3.8	5.0	-1.2	-32%	< 0.01

Note: 1) *f*-tests.

At the straight long segment between the ramp terminal and curve, the average speed reductions by Pattern C between daytime and nighttime were similar at both locations based on data from sensors #98 and #102, as shown in **Table 5.14**. Compared with the daytime, an extra 3% reduction was observed at Exit 284 during the nighttime. Moreover, the average speed during the

nighttime was higher than that during the daytime before installing Pattern C at Exit 284 (W1). After implementing Pattern C (W2), the average speed was reduced from 21 to around 18 mph throughout the day. Besides slowing down RW vehicles, Pattern C also reduced speed SDs (Table 5.15). In general, larger SD reductions were found at both locations during the nighttime, which were more than 10% of the SDs during W1.

Table 5.14 Comparisons of Daytime and Nighttime Average Speeds after Implementing Pattern C

Time	Location	Average Speed (mph)		Speed Reduction (mph)	Reduction%	<i>p</i> -value ¹
		W1	W2			
Daytime	Exit 208	21.3	18.4	2.9	14%	< 0.01
	Exit 284	20.7	18.3	2.4	12%	< 0.01
Nighttime	Exit 208	19.7	16.9	2.8	14%	< 0.01
	Exit 284	21.1	18.0	3.1	15%	< 0.01

Note: 1) *z*-tests.

Table 5.15 Comparisons of Daytime and Nighttime Speed Standard Deviations after Implementing Pattern C

Time	Location	Speed SD (mph)		SD Reduction (mph)	Reduction%	<i>p</i> -value ¹
		W1	W2			
Daytime	Exit 208	6.1	5.8	0.3	5%	0.03
	Exit 284	4.4	4.1	0.3	7%	0.02
Nighttime	Exit 208	5.9	5.3	0.6	10%	0.01
	Exit 284	4.4	3.9	0.5	11%	0.02

Note: 1) *f*-tests.

The average speeds and speed SDs at the off-ramp terminals did not show any differences between daytime and nighttime after implementing Pattern D3 (**Table 5.16** and **Table 5.17**). The reduction percentage of the average speeds and speed SDs were close in regard to data from sensors #97 and #101.

Table 5.16 Comparisons of Daytime and Nighttime Average Speeds after Implementing Pattern D3

Time	Location	Average Speed (mph)		Speed Reduction (mph)	Reduction%	<i>p</i> -value ¹
		W2	W3			
Daytime	Exit 208	10.7	10.5	0.2	2%	< 0.01
	Exit 284	12.5	11.6	0.9	7%	< 0.01
Nighttime	Exit 208	10.3	10.1	0.2	2%	< 0.01
	Exit 284	12.3	11.6	0.7	6%	< 0.01

Note: 1) *z*-tests.

Table 5.17 Comparisons of Daytime and Nighttime Speed Standard Deviations after Implementing Pattern D3

Time	Location	Speed SD (mph)		SD Reduction (mph)	Reduction%	<i>p</i> -value ¹
		W2	W3			
Daytime	Exit 208	3.7	3.3	0.4	11%	< 0.01
	Exit 284	4.8	3.8	1.0	21%	< 0.01
Nighttime	Exit 208	3.3	2.9	0.4	12%	< 0.01
	Exit 284	4.6	3.6	1.0	22%	< 0.01

Note: 1) *f*-tests.

5.4 Other Findings

Reduction in Left-Turn Confusion

The video camera captured that the new channelization island can confuse left-turn drivers at the off-ramp terminal at Exit 208 on I-65, AL. As shown in **Figure 5.16**, an SUV driver entered a right-turn lane to turn left. The driver may mistakenly consider the new island as a right-in/right-out channelization design. Thus, there was concern that some drivers did not fully understand the purpose of the channelized island at the off-ramp terminal.

A hundred free-flow vehicles were sampled from videos that were recorded during random nonpeak hours on each weekend. Videos taken during daytime or nighttime were considered. **Table 5.18** summarizes the changes in left-turn confusion (defined as left-turn maneuvers from the right-turn lane). Nearly 23% to 28% of left-turn vehicles were confused by the new channelization island before installation of Pattern D3. After implementation of Pattern D3, the percentage was roughly reduced by half. This indicated that the arrow shape of Pattern D3 can help to guide left-turning vehicles to stay in the correct lane.

Table 5.18 Change in Left-Turn Confusions

Time	Left-Turn Vehicles	Right-Turn Vehicles	Number of Left-Turn Confusion	Left-Turn Confusion%	Note
W0	35	65	8	23%	Pattern D3 wasn't installed
W1	40	60	11	28%	
W2	37	63	10	27%	
W3	33	67	4	12%	Pattern D3 was installed
W4	36	64	4	11%	
W5	38	62	6	16%	
W6	30	70	4	13%	
W7	41	59	5	12%	
W8	31	69	3	10%	

(a)



(b)



(c)



Figure 5.16 Example of Left-Turn Confusion Captured at Exit 208

Utilization of the Center Gaps

Center gaps were tested at the removable TRS in a previous study (Meyer 2006). Considering the complaints from motorcyclists on TRS, the 2-ft gap in Patterns E.1 and C allowed motorcycles to travel over the strips without hitting them. As shown in **Figure 5.17**, a motorcycle is utilizing the center gap to pass Pattern C. Additionally, no complaints were heard from road users thus far based on the feedback from ALDOT.

Other than serving motorcycles, the center gap has the potential to help emergency vehicles passing DRS patterns without receiving additional sound and vibrations.



Figure 5.17 Motorcycle Using the Center Gaps to Pass DRS Pattern C

Chapter 6. Guidelines for Implementing DRS

6.1 DRS Implementation Guidelines

DRS is a relatively new traffic control device for drivers to distinguish between the on and off-ramps. Currently, there is no standard or guideline for implementing this device. This study found that DRS has advantages in alerting WW drivers and reducing WWD incidents by providing WW drivers with elevated interior sound and vibrations. Besides, DRS can reduce RW vehicles' speeds. The benefits of implementing DRS is summarized in **Table 6.1**. The following includes recommended guidelines from DRS implementation based on the results of this study. Recommended deployments of DRS and relevant signs and pavement markings are presented in **Figure 6.1**.

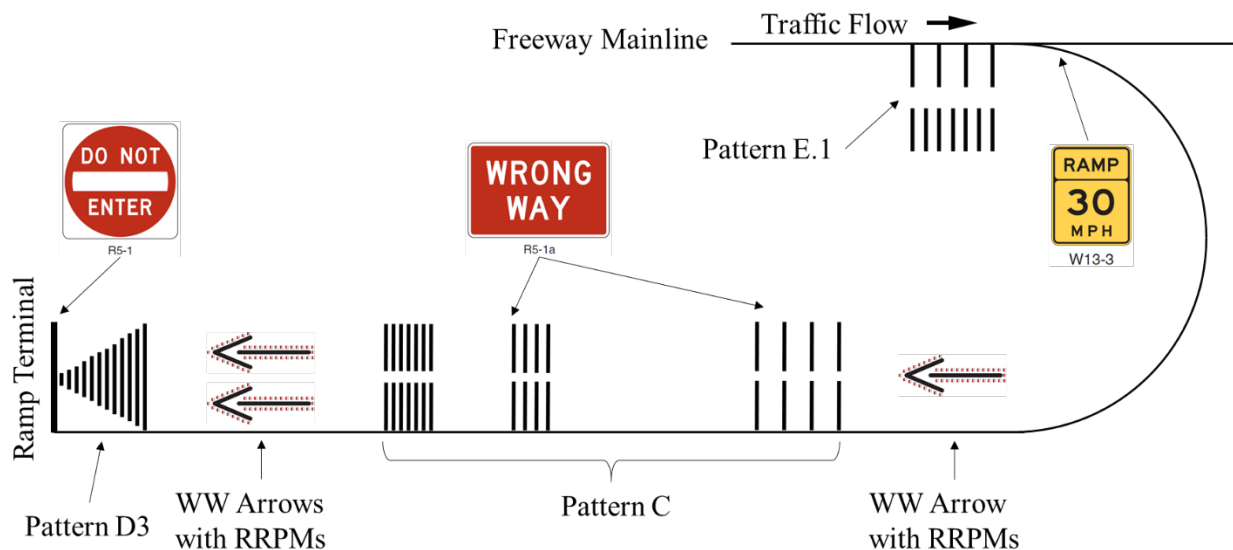


Figure 6.1 Recommended DRS Deployments with Relevant Signs and Pavement Markings

Table 6.1 Summary of Benefits of DRS Implementation

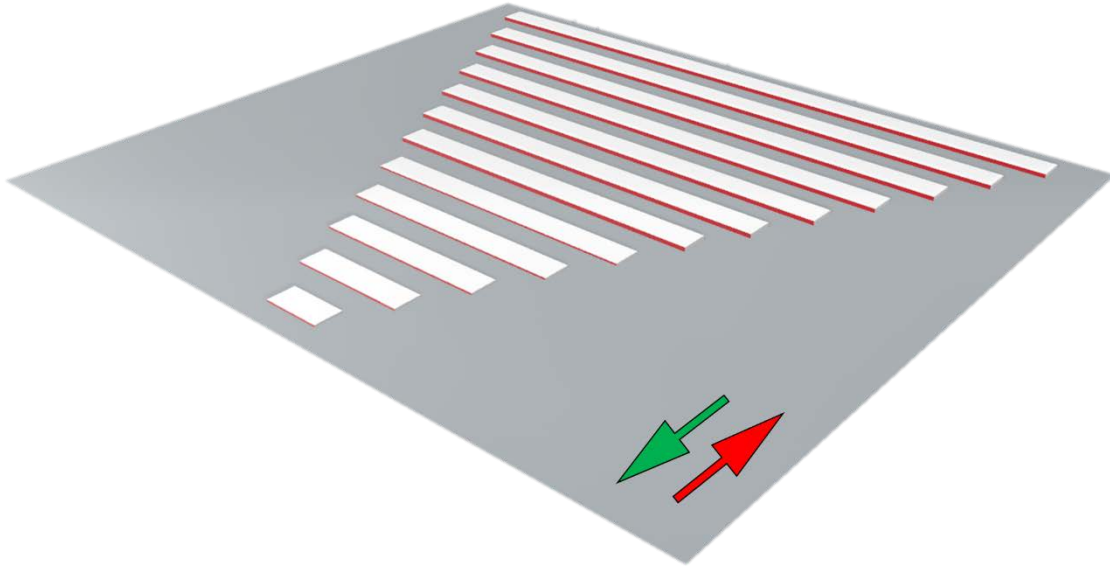
Benefits		Pattern D3	Pattern C (1-ft)	Pattern C (2-ft)	Pattern C (5-ft)	Pattern E.1
Interior Sound (dBA)	RW	58	66	67	65	67
	WW	71	71	72	69	72
	Difference	13	5	5	4	5
	Difference %	22%	8%	7%	6%	7%
Exterior Sound Increase (dBA)		Negligible	10	5	3	9
Vibration (g)	RW	0.04	0.10	0.04	0.04	0.08
	WW	0.09	0.12	0.12	0.05	0.11
	Difference	0.05	0.02	0.08	0.01	0.03
	Difference %	114%	20%	193%	32%	34%
Speed Reduction (mph)	Mean	Negligible	2~3			2~6
	85th	0~1	1~3			1~10
	SD	0.5~1	0.2~1			-1~3
Driver Adoption (day)		2~3				
Impacts on WWD incidents		90% of WWD incidents	40% of WWD incidents			Need more evidence
Other		Guide left-turn vehicles	Visual cue for horizontal curve			
			Center gap designed for motorcycles and emergency vehicles			

Pattern E.1 is recommended to be installed ahead of the advisory ramp speed sign in advance of the sharp horizontal ramp curve. The distance between Pattern E.1 and the advisory ramp speed sign shall be considered based on the sight distance study and engineering judgment. For example, 30 ft was employed in this study that can provide a good sight distance for drivers to see the advisory ramp speed signs and the horizontal curve when passing the DRS. The yellow and white strip colors are in conformance with MUTCD Section 3A.05. The use of yellow strips should be permitted to Pattern E.1. Based on the results of this study, Pattern E.1 with one-side yellow

strips were more effective in reducing the speed SDs. Thus, it is recommended to have yellow strips of Pattern E.1 on the left side of the travel lane.

Pattern C is recommended to be installed at the long straight off-ramp segment between the ramp gore area and terminal. It can alert RW drivers of a need to slow down or stop or to other upcoming changes. It will also alert WW drivers via sound and vibrations to pay attention to WW signs on the roadside. Therefore, it is recommended to have WW signs placed ahead of Pattern C. Lower-mounted WW signs could be an option per MUTCD Section 2B.41. Furthermore, the placement of Pattern C should not be overlapping with other pavement markings. Base on this study, it can be placed between two sets of WW arrows.

It is recommended to deploy Pattern D3 at the off-ramp terminals. This pattern is effective in terms of reducing WW entries by alerting WW drivers with louder sound and more severe vibrations and a clear visual cue. It can work in collaboration with DNE signs. An optional lower mounting height for DNE signs can also be considered, according to MUTCD Section 2B.41. The strips should not be attached to other pavement markings such as stop bars or yield lines. In this study, the 1-ft strip of this pattern was installed 1 ft behind the stop bars and the yield line. As described in MUTCD Section 3B.13, retroreflective markers may be used to supplement wide lateral line markings (e.g., stop bar) and wrong-way arrows. Similarly, red retroreflective paint can be applied onto the WW side of Pattern D3, as shown in **Figure 6.2**.



Note: Green Arrow = Right-Way Direction; Red Arrow = Wrong-Way Direction

Figure 6.2 Pattern D3 with Red Retroreflective Paint

6.2 Cost and Benefit

The cost of materials for each DRS pattern is \$1,500 each with a combined \$2,500 labor cost (\$7,000 for 3 patterns in total). These patterns are recommended to be replaced every 3 to 5 years according to the contractor. So far, it has been over one year since the initial installation and the strips are still in good conditions based on the field inspection.

The primary benefit of DRS is to deter WWD crashes. A WWD crash is more likely to be a fatal crash because of the high chance of head-on collisions. The cost of one fatal crash can be over \$10 million (Harmon et al. 2018). The study locations had confirmed at least one WWD crash in the past decade. Given reducing one WWD crash in ten years, the savings of crash is \$10 million (total societal cost). The cost would be \$14,000 with the initial installation and one maintenance. The benefit/cost ratio (b/c ratio) can be at least 714:1. To conclude, the reward of DRS is huge by

detering WWD crashes. Unlike other costly cameras or sensors, the relatively low cost makes it possible to implement DRS at every off-ramp.

Chapter 7. Conclusions

This research evaluated three DRS patterns (D3, C, and E.1) at two off-ramps in Alabama to mitigate two major issues on freeway off-ramps – WWD and speed control. The closed-course tests first verified the previous results and further identified the proper deployment of DRS in the field. The field implementation tests quantified the impacts of DRS on WWD and RW traffic speeds. The results showed that these DRS patterns can reduce the frequency and distance of WWD. The elevated sound and vibrations generated by DRS can alert WW drivers and potentially improve the effectiveness of other WW-related traffic control devices (e.g., WW signs). The results also indicated that RW vehicles were slowed down by DRS as they trended to closely follow the posted advisory speed. Transportation agencies can utilize these findings to deter WWD and control traffic speeds on freeway off-ramps.

Three DRS patterns were tested and implemented in this research. Pattern D3 is similar to the advance warning markings for speed humps, which has a triangle shape, as the length of the strip gradually increases from 1 to 12 ft. The thickness of the strip for Pattern D3 ranges from 0.25 to 0.5 (0.25 in. for strips from 1 to 5 ft and 0.5 in. for strips from 6 to 12 ft). Pattern C is similar to the traditional TRS but has different spacings. Three groups of strips with spacings of 1, 2, and 5 ft, respectively, were placed apart with 100- and 50-ft spacing. All of the strips had the same thickness of 0.25 in. Pattern E.1 had double strips on the driver side in the WW direction to ensure that WW drivers received elevated sound and vibrations. The width of the strips was 6 in., and the thickness was about 0.25 in.

Southbound off-ramps at Exits 208 and 284 on I-65 in Alabama were selected for implementation based on model prediction results and number of recurring WWD incidents observed in the field. Speed and video data were collected using cameras and magnetic sensors.

Field driving tests were conducted to collect sound and vibration data at various speed categories for both RW and WW drivers. Time-series were applied to analyze sound, while spectrum analysis was used for analyzing vibrations. For these two off-ramps, Pattern D3, which was shaped like an arrow to indicate the right direction, was installed at the off-ramp terminal near the stop bar/yield lines. Pattern C was implemented at the segment between the terminal and the ramp curve. WW drivers were alerted by the increasing sound and vibrations from three strip groups, so that they could pay attention to the standard WW-related signs and pavement arrows. Pattern E.1 was installed on the tangent part before the ramp curve, which can alert a WW driver before entering the freeway mainline and reduce aggressive driving speeds for vehicles exiting the freeway before entering the oncoming curve.

Before-and-after studies were conducted to evaluate the effectiveness of these patterns based on WWD incidents, vehicle speeds, and driver behavior changes. Both numbers of WWD incidents and WWD distances significantly dropped toward zero after implementing the DRS patterns. Though a critical event was rare (e.g., WW vehicle drove all the way to the freeway), one WW vehicle was stopped on the ramp curve by Pattern E.1. Further evaluation will be required to test its effectiveness in countering WW incidents. After deploying Pattern C, WWD frequencies and average WWD traveling distances were reduced by almost by half. According to changes in time frames when most WW incidents occurred, Pattern C significantly reduced the number of WW incidents around afternoon peaks. Pattern D3 was considered the most effective, as it prevented vehicles from entering the off-ramps from crossroads. After implementing Pattern D3, WWD frequencies and distances were reduced to near zero. No WWD vehicles traveled farther than the latest implemented DRS pattern in this study. However, due to the resurfacing project, the

number of WW incidents as well as WWD distances increased again after DRS being removed at Exit 284.

The before-and-after speed analysis suggested that Pattern E.1 can reduce average speed by 2.3 to 6.5 mph depending on the difference between the advisory speed and operational speeds. For the location at Exit 208, when the operational average speed was about 10 mph over the advisory speed, Pattern E.1 could also reduce speed SD by 2.5 mph. For the location at Exit 284, where the operational speed is close to the advisory speed, Pattern E.1 increased the speed SD by 1.4 mph. The results from both locations showed that the average speeds and speed SDs decreased by 2.7 and 0.5 mph, respectively because of the implementation of Pattern C. Pattern D3 helped lower the speed SDs by 0.5 and 1.0 mph at the stopped and yield-controlled terminals, respectively. The trends of changes in speed SDs indicated that two to three days were needed for drivers to become familiar with these new traffic control devices. Speed comparisons between daytime and nighttime illustrated that Pattern C could reduce the speed SD 5% more during the nighttime than the daytime.

While all the DRS patterns generated enough interior sound to alert drivers, WW drivers could perceive louder sound from all three patterns (12 dBA by D3, 5 dBA by Patterns C and E.1). The exterior sound increasements caused by the DRS suggested that Pattern C could produce a maximum of 10 dBA additional noise and Pattern E.1 could produce 9 dBA. However, extra noise caused by Pattern D3 were negligible. DRS patterns generated higher frequencies and larger amplitudes of vibrations for WW drivers. By calculating the RMS values for vibrations, Pattern D3 produced 0.045 *g* more vibrations for WW drivers, while Pattern C generated at least 0.011 *g* more and Pattern E.1 0.027 *g* more.

In addition to the above findings, Pattern D3 showed that it can provide additional guidance for RW left-turn drivers. Confused left-turns at the channelized island were reduced by nearly 50% after installing Pattern D3. Moreover, the center gaps at Patterns C and E.1 provided convenience to motorcyclists.

Chapter 8. Limitations and Future Study

The implementation guidelines of DRS have been adopted by ALDOT as DRS have been planned to be installed on more off-ramps (e.g., Exits 58 and 60 on I-85). No safety concerns or public complaints regarding DRS were heard from the district offices. The ultimate goal of this study is to have DRS widely implemented by transportation agencies and adopted by MUTCD. To that end, limitations and needs of future studies are pointed out as follows.

Due to the time, budget, and permissions of experimental implementation, this study only included two off-ramps to evaluate the effectiveness of DRS on RW and WW traffic. Future studies should expand the sample size by installing DRS on more off-ramps. Before-and-after studies should follow the same procedure described in this study to quantify the impacts of DRS.

A general guideline of implementing DRS on off-ramps was provided in this study. The optimal deployment of DRS patterns and other WW signs or pavement markings needs to be further studied. The research team will conduct a study using the driving simulator to identify the best installation locations of signs, pavement markings, and DRS.

In this study, the effectiveness of DRS on influenced drivers are unknown. Thus, a driving-simulator-based study will be conducted to evaluate the impacts of DRS on severely intoxicated drivers. The research team will determine driver's perception to DRS under different blood alcohol content (BAC) levels and develop guidelines of implementation to reduce the frequency and severity of WWD crashes.

References

- Aarts, L. and I. Van Schagen. (2006). Driving speed and the risk of road crashes: A review. *Accident Analysis & Prevention*, 38(2), 215-224.
- Agent, K. R. and T. Creasey. (1986). *Delineation of Horizontal Curves. Interim Report* (No. UKTRP-86-4). University of Kentucky, Lexington.
- Alabama Department of Transportation (ALDOT). 2020 Alabama Department of Transportation Standard and Special Drawings for Highway Construction (Traffic Stripe).
https://alletting.dot.state.al.us/Docs/Standard_Drawings/2020%20English/70100.pdf.
Accessed June 2019.
- Allaby, P., B. Hellinga, and M. Bullock. (2007). Variable speed limits: Safety and operational impacts of a candidate control strategy for freeway applications. *IEEE Transactions on Intelligent Transportation Systems*, 8(4), 671-680.
- Atiquzzaman, M. and H. Zhou. (2018). Modeling the risk of wrong-way driving entry at the exit ramp terminals of full diamond interchanges. *Transportation Research Record*, 2762(17), 35–47.
- Baisyet, R., and A. Stevens. (2015). Combating wrong way drivers on divided carriageways. In *Proceedings of the Institution of Professional Engineers New Zealand (IPENZ) Transportation Conference, Christchurch, New Zealand* (pp. 22-24).
- Baratian-Ghorghi, F., H. Zhou, M. Jalayer, and M. Pour-Rouholamin. (2015). Prediction of potential wrong-way entries at exit ramps of signalized partial cloverleaf interchanges. *Traffic injury prevention*, 16(6), 599-604.
- Baratian-Ghorghi, F., H. Zhou, and J. Shaw. (2014). Overview of wrong-way driving fatal crashes in the United States. *ITE Journal*, 84(8), 41-47.

- Cain, B., D. Riley, and P.J. McKelvey. (2018). Summary and Initial Findings of the Arizona Department of Transportation Wrong-way Driver Pilot System. The Intelligent Transportation Society of America Annual Meeting. Detroit, MI.
- Campbell, J. L. (2010). *Human factors guidelines for road systems* (Vol. 600). Transportation Research Board, Washington, DC.
- Charlton, S. G. (2004). Perceptual and attentional effects on drivers' speed selection at curves. *Accident Analysis & Prevention*, 36(5), 877-884.
- Chowdhury, Mashrur A., Davey L. Warren, Howard Bissell, and Sunil Taori. (1998). Are the criteria for setting advisory speeds on curves still relevant?. *ITE journal*, 68, 32-45.
- Cirillo, J. A. (1968). Interstate system accident research study II, interim report II. *Public roads*, 35 (3), pp. 71-76.
- Cochran, W. T., James W. Cooley, David L. Favon, Howard D. Helms, Reginald A. Kaenel, William W. Lang, George C. Maling, David E. Nelson, Charles M. Rader, and Peter D. Welch. (1967). What is the fast Fourier Transform?. *Proceedings of the IEEE*, 55(10), 1664-1674.
- Cooner, S. A., A. S. Cothron, and S. Ranft. (2004). *Countermeasures for Wrong-Way Movement on Freeways: Overview of Project Activities and Findings* (FHWA/TX-04/4128-1). Austin, TX: Texas Department of Transportation.
- Copelan, J. E. (1989). *Prevention of wrong way accidents on freeways* (FHWA/CA-TE-89-2). Sacramento: California Department of Transportation
- Corkle, J., M. Marti, and D. Montebello. (2001). *Synthesis on the effectiveness of rumble strips* (No. MN/RC--2002-07). Minnesota Department of Transportation. Minneapolis, MN.

- Elefteriadou, Lily, M. El-Gindy, D. Torbic, P. Garvey, A. Homan, Z. Jiang, B. Pecheux, and R. Tallon. (2000). *Bicycle-tolerable shoulder rumble strips* (No. PTI 2K15). Pennsylvania Transportation Institute. University Park, PA.
- Elvik, R., P. Christensen, and A. Amundsen. (2004). Speed and road accidents - An evaluation of the Power Model. *The Institute of Transport Economics (TOI) Report 740/2004*. Institute of Transport Economics TOI, Oslo.
- Fariello, Brian. (2012). "San Antonio Wrong-Way Driver Task Force."
<http://tti.tamu.edu/conferences/tsc11/program/presentations/traffic-ops-2/fariello.pdf>.
Accessed July 2017.
- Farokhzad, S. (2013). Vibration based fault detection of centrifugal pump by fast fourier transform and adaptive neuro-fuzzy inference system. *Journal of mechanical engineering and technology*, 1(3), 82-87.
- Federal Highway Administration (FHWA). (2000). *Manual on Uniform Traffic Control Devices*. Federal Highway Administration, Washington, DC.
- FHWA. (2009). *Manual on Uniform Traffic Control Devices*. Federal Highway Administration, Washington, DC.
- FHWA Research and Technology. (2014). Rumble Strips. <http://www.fhwa.dot.gov/research/deployment/rumblestrips.cfm>. Accessed September 2017.
- Finley, M. D., Steven P. Venglar, Vichika Iragavarapu, Jeffrey D. Miles, Eun Sug Park, Scott A. Cooner, and Stephen E. Ranft. (2014). *Assessment of the effectiveness of wrong way driving countermeasures and mitigation methods* (No. FHWA/TX-15/0-6769-1). Texas A&M Transportation Institute, Texas.

- Fitzpatrick, K., M. A. Brewer, and A. H. Parham. (2003). *Left-turn and in-lane rumble strip treatments for rural intersections* (No. FHWA/TX-04/0-4278-2,). Texas A&M Transportation Institute, Texas.
- Florida Department of Transportation (FDOT). (2014). *Wrong-Way Vehicle Detection Pilot Project Underway*. News Release, Florida Department of Transportation, Florida.
- Gao, J., Guo, L., Kong, L., Zhang, X., and Yang, Z. (2004). Study on Speed Management of High-Classified highway of China. *Advances in Transportation Studies*, 4.
- Garber, N. J., and R. Gadiraju. (1989). Factors affecting speed variance and its influence on accidents. *Transportation Research Record*, 1213, 64-71. Washington, D.C
- Garber, N. Mashrur, A. Chowdhury, and Ravi Kalaputapu. (1992). *Accident characteristics of large trucks on highway ramps*. AAA Foundation for Traffic Safety, Washington, D.C.
- Gianotti, John. (2015). "Wrong-Way Driver Project." 2015 TPWA Short Course. San Antonio District - TransGuide.
- Goldman, S. (1999). *Vibration spectrum analysis: a practical approach*. Industrial Press Inc.
- Grether, W. F. (1971). Vibration and human performance. *Human factors*, 13(3), 203-216.
- Griffin, M. J. (1986). Evaluation of vibration with respect to human response. *SAE transactions*, 323-346.
- Griffin, M. J. (2007). Discomfort from feeling vehicle vibration. *Vehicle System Dynamics*, 45(7-8), 679-698.
- Guignard, J. C. (1971). Human sensitivity to vibration. *Journal of sound and vibration*, 15(1), 11-16.
- Guignard, J. C. (1975). Noise and vibration. *Foundations of Space Biology and Medicine: Ecological and physiological bases of space biology and medicine*. 2 v, 2, 355.

- Harmon, Tim, Geni Brafman Bahar, and Frank B. Gross. (2018). *Crash costs for highway safety analysis*. No. FHWA-SA-17-071. United States. Federal Highway Administration. Office of Safety.
- Harwood, D.W. Use of Rumble Strips to Enhance Safety. (1993). Synthesis of Highway Practice 191, National Cooperative Highway Research Program, National Academy Press, Washington, D.C.
- Hegy, A., B. De Schutter, and H. Hellendoorn. (2005). Model predictive control for optimal coordination of ramp metering and variable speed limits. *Transportation Research Part C: Emerging Technologies*, 13(3), 185-209.
- Horowitz, A. J., and Thomas Notbohm. (2005). "Testing temporary work zone rumble strips." Midwest Smart Work Zone Deployment Initiative. University of Nebraska-Lincoln, Mid-America Transportation Center. Lincoln, NE.
- Hou, S., Sun, X., and He, Y. (2010). Research on variational rule of operating speed along transverse rumble strip on expressway section. *China Journal of Highway and Transport*, 23(1), 105-110.
- ITS International. (2010). "Wrong Way Detection System Prevents Accidents, Improves Safety." *ITS International*. <http://www.itsinternational.com/sections/cost-benefitanalysis/features/wrong-way-detection-system-prevents-accidents-improves-safety/>. Accessed March 2018.
- Kermit, Mark L. and T. C. Hein. (1962). "Effect of Rumble Strips on Traffic Control and Driver Behavior." In *Highway Research Board Proceedings*, vol. 41.
- Khalilikhah, M., K. Heaslip, and Z. Song. (2015). Can daytime digital imaging be used for traffic sign retroreflectivity compliance?. *Measurement*, 75, 147-160.

- Kloeden, C. N., A. J. McLean, V. M. Moore, and G. Ponte. (1997). *Travelling speed and the rate of crash involvement; Vol. 1: Findings*. Report No. CR, 172. Canberra: Federal Office of Road Safety.
- Kloeden, C. N., G. Ponte, and J. McLean. (2001). *Travelling speed and risk of crash involvement on rural roads*. Australian Transport Safety Bureau, Civic Square, ACT 2608, Australia
- Lank, Christian and Bernhard Steinauer. (2011). "Increasing road safety by influencing drivers' speed choice with sound and vibration." *Transportation Research Record: Journal of the Transportation Research Board* 2248: 45-52.
- Lee, C., F. Saccomanno, and B. Hellinga. (2002). Analysis of crash precursors on instrumented freeways. *Transportation Research Record*, 1784(1), 1-8.
- Lee, C., B. Hellinga, and F. Saccomanno. (2003). Real-time crash prediction model for application to crash prevention in freeway traffic. *Transportation Research Record*, 1840(1), 67-77.
- Lee, C., B. Hellinga, and F. Saccomanno. (2006). Evaluation of variable speed limits to improve traffic safety. *Transportation research part C: emerging technologies*, 14(3), 213-228.
- Lin, P.S., C. Chen, and S. Ozkul. (2018). Testing and evaluation of freeway wrong-way detection systems. Florida Department of Transportation. Retrieved from https://ftp.fdot.gov/file/d/FTP/FDOT%20LTS/CO/research/Completed_Proj/Summary_T/E/FDOT-BDV25-977-40-rpt.pdf. Accessed January 2019.
- Lin, P. W., K. P. Kang, and G.L. Chang. (2004). Exploring the effectiveness of variable speed limit controls on highway work-zone operations. In *Intelligent transportation systems* (Vol. 8, No. 3, pp. 155-168). Taylor & Francis Group.

- Leduc, J. L. K. (2008). *Wrong-way driving countermeasures*. Connecticut General Assembly, Office of Legislative Research.
- Lyles, R. W. (1980). *An evaluation of warning and regulatory signs for curves on rural roads* (No. FHWA/RD-80/009 Final Rpt.). FHWA, US Department of Transportation, Washington, DC.
- Mansfield, N. J. (2004). *Human response to vibration*. CRC press.
- Mansfield, N. J. (2012). Human response to vehicle vibration. *Automotive Ergonomics: Driver-Vehicle Interaction*, 77.
- Maryland Department of Transportation State Highway Administration (SHA). (2011). *Guidelines for Application of Rumble Strips*. Baltimore, MD.
- Meyer, E. (2006). *Guidelines for the application of removable rumble strips* (No. K-TRAN: KU-02-3). Lawrence, KS: Kansas. Dept. of Transportation.
- Miles, Jeffrey, and Melisa Finley. (2007). "Factors that influence the effectiveness of rumble strip design." *Transportation Research Record: Journal of the Transportation Research Board 2030*: 1-9.
- Morioka, M. and M. J. Griffin. (2008). Absolute thresholds for the perception of fore-and-aft, lateral, and vertical vibration at the hand, the seat, and the foot. *Journal of sound and vibration*, 314(1-2), 357-370.
- National Transportation Safety Board (NTSB). (2012). Highway Special Investigation Report: Wrong-Way Driving (NTSB/SIR-12/01). Washington, DC.
- Oh, C., J. Oh, S. Ritchie, and M. Chang. (2001). Real-time estimation of freeway accident likelihood. Presented at 80th Annual Meeting of the Transportation Research Board, CD-ROM, Washington, D.C.

- Outcalt, William. (2001). *Bicycle friendly rumble strips* (No. CDOT-DTD). Colorado Department of Transportation. Denver, CO.
- Pour-Rouholamin, M. and H. Zhou. (2016). Analysis of driver injury severity in wrong-way driving crashes on controlled-access highways. *Accident Analysis & Prevention*, 94, 80-88.
- Pour-Rouholamin, M., H. Zhou, J. Shaw, and P. Tobias. (2015). "Current practices of safety countermeasures for wrong-way driving crashes." *TRB 94th Annual Meeting Compendium of Papers*. DOI: 10.13140/2.1.1050.6564.
- Puvanachandran, V. M. (1995). Effect of Road Curvature on Accident Frequency: Determining Design Speeds to Improve Local Curves. *Road and Transport Research*, Vol 4, pp. 76-83.
- Reference. (2019). "What Is the average length of a car?" *Reference*, IAC Publishing, www.reference.com/vehicles/average-length-car-2e853812726d079d. Accessed August 2018.
- Retting, R. A., H.W. McGee, and C. M. Farmer. (2000). Influence of experimental pavement markings on urban freeway exit-ramp traffic speeds. *Transportation research record*, 1705(1), 116-121.
- Rich, Sarah. (2012). "Preventing Wrong-Way Driving Gets a Tech Assist." *Government Technology*. <http://www.govtech.com/public-safety/Preventing-Wrong-Way-Driving-Gets-a-Tech-Assist-.html>. Accessed July 2018.
- Rinde, E. A. (1978). *Off-ramp surveillance: Wrong-way driving*. Department of Transportation, State of California.
- Rose, D. (2011). Wrong-way vehicular detection proof of concept. Paper presented at the 18th World Congress on Intelligent Transport Systems. Orlando, FL.

- Sabato, A. and C. Niezrecki. (2016). Rumble strips noise emission effects on urban road traffic. In *INTER-NOISE and NOISE-CON Congress and Conference Proceedings* (Vol. 252, No. 2, pp. 184-191). Institute of Noise Control Engineering.
- Schrock, Steven, Kevin Heaslip, Ming-Heng Wang, Romika Jasrotia, and Robert Rescot. (2010). "Closed-course test and analysis of vibration and sound generated by temporary rumble strips for short-term work zones." *Transportation Research Record: Journal of the Transportation Research Board* 2169: 21-30.
- Sexton, T. V. (2014). *Evaluation of current centerline rumble strip design (s) to reduce roadside noise and promote safety* (No. WA-RD 835.1). Olympia, WA: Washington Dept. of Transportation.
- Simpson, S. A. (2013). *Wrong-way vehicle detection: proof of concept* (No. FHWA-AZ-13-697). Arizona. Dept. of Transportation.
- Solomon, D. (1964). Crashes on main rural highways related to speed, driver and vehicle. *Bureau of Public Roads. US Department of Commerce. United States Government Printing Office, Washington DC.*
- Stokes, R. W., M.J. Rys, and E.R. Russell. (1996). Motorist Understanding of Selected Warning Signs. *ITE Journal*, 66(8), 36-41.
- Taylor, M. C., D. A. Lynam, and A. Baruya. (2000). *The effects of drivers' speed on the frequency of road accidents*. TRL Report, No. 421. Transport Research Laboratory TRL, Crowthorne, Berkshire.
- Texas Department of Transportation (TxDOT). (2006). *Standard Sheets for Edgeline, Centerline and Transverse Rumble Strips*. Austin, TX. Retrieved from <https://www.dot.state.tx.us/insdot/orgchart/cmd/cserve/standard/toc.htm>.

- TxDOT. (2011). "Engineering Analysis of the Installation of Spike Strips and Other Destructive Devices in Freeway Exit Ramps." *TransGuide, TxDOT Intelligent Transportation Systems website*.
<http://www.transguide.dot.state.tx.us/sat/wwd/content/EngineeringAnalysisSpikeStrips.pdf>
f. Accessed June 2018.
- Torbic, D., L. Elefteriadou, and M. El-Gindy. (2001). Development of rumble strip configurations that are more bicycle friendly. *Transportation research record*, 1773(1), 23-31.
- Torbic, D. J., J.M. Hutton, C. D. Bokenkroger, K. M. Bauer, D. W. Harwood, D. K. Gilmore, J. M. Dunn, J. J. Ronchetto, E. T. Donnell, H. J. Sommer III, and P. Garvey. (2009). NCHRP report 641: Guidance for the design and application of shoulder and centerline rumble strips. *Transportation Research Board of the National Academies, Washington, DC*.
- TransCore. (2008). *White paper: Wrong-way detection system procurement*. Houston, Texas: Harris County Toll Authority.
- Van den Hoogen, E. and S. Smulders. (1994). Control by variable speed signs: results of the Dutch experiment. In *Seventh International Conference on Road Traffic Monitoring and Control, 1994*. (pp. 145-149). IET.
- Vaswani, N. K. (1973). *Measures for preventing wrong-way entries on highways* (No. VHRC 72-R41). Virginia Transportation Research Council.
- Virginia Department of Highways and Transportation (VDOT). (1983). An Evaluation of the Effectiveness of Rumble Strips. Traffic and Safety Division Evaluation (No. 81-5). Richmond, VA.

- Watts, G. R. (1977). *The Development of Rumble Areas as a Driver-Alerting Device*.
Supplementary Report 291. Transport and Road Research Laboratory, Crowthorne, United Kingdom.
- Willey, J. (2011). New system to catch wrong-way drivers. ABC Houston, TX Local News.
- Williams, C. (2007). District 3 ITS Project Update. Florida Department of Transportation, Florida.
<http://www.ce.siu.edu/faculty/hzhou/ww/paper/District3%20ITS%20Engineer.pdf>.
Accessed May 2018.
- Xing, J. (2013). Characteristics and countermeasures against wrong-way driving on motorways in Japan. In *20th ITS World Congress ITS Japan*.
- Xue, C., H. Zhou, D. Xu, and P. Liu. (2019). Field Verification of Directional Rumble Strips to Deter Wrong-Way Freeway Driving. *Journal of Transportation Engineering, Part A: Systems*, 145(8), 04019031.
- Xue, C. and D. Xu. (2019). Factors Influencing Crash Severity at Rural Horizontal Curves in Maine. *Institute of Transportation Engineers. ITE Journal*, 89(5), 36-41.
- Yang, Y., Sun, X., and He, Y. (2010). Effectiveness of rumble strips on freeways. In *ICCTP 2010: Integrated Transportation Systems: Green, Intelligent, Reliable* (pp. 425-433).
- Yang, L., H. Zhou, L. Zhu, and H. Qu. (2016). Operational effects of transverse rumble strips on approaches to high-speed intersections. *Transportation research record*, 2602(1), 78-87.
- Yang, L., H. Zhou, and L. Zhu. (2018). New Concept Design of Directional Rumble Strips for Deterring Wrong-Way Freeway Entries. *Journal of Transportation Engineering, Part A: Systems*, 144(5), 04018010.

- Zador, P. L., H. S. Stein, P. H. Wright, and J. W. Hall. (1987). Effects of chevrons, post-mounted delineators, and raised pavement markers on driver behavior at roadway curves. *Transportation Research Record 1114*, pp. 1-10. Washington, D.C.
- Zegeer, C., R. Stewart., D. Reinfurt, F. Council, T. Neuman, E. Hamilton, T. Miller, and W. Hunter. (1991). *Cost-effective geometric improvements for safety upgrading of horizontal curves* (Report DOTRD-90-021). FHWA, U.S. Department of Transportation, Washington, D.C.
- Zhou, H., J. Zhao, R. Fries, M. Gahrooei, L. Wang, and B. Vaughn. (2012). *Investigation of Contributing Factors Regarding Wrong-Way Driving on Freeways*. Urbana, IL: Illinois Center for Transportation/Illinois Department of Transportation.
- Zhou, H., C. Xue, L. Yang, and A. Luo. (2018). Directional rumble strips for reducing wrong-way-driving freeway entries (CTS 18-04). Minneapolis, MN: Roadway Safety Institute, University of Minnesota.
- Zhou, H. and C. Xue. (2019). Field Implementation of Direction Rumble Strips for Deterring Wrong-Way Entries (CTS 19-22). Minneapolis, MN: Roadway Safety Institute, University of Minnesota.
- Zhou, H. and M. P. Rouholamin. (2014a). Guidelines for reducing wrong-way crashes on freeways (FHWA-ICT-14-010). Urbana, IL: Illinois Center for Transportation/Illinois Department of Transportation.
- Zhou, H. and M. P. Rouholamin. (2014b). Proceedings of the 2013 National Wrong-Way Driving Summit. *Illinois Center for Transportation Series No. 14-009*. Urbana, IL: Illinois Center for Transportation/Illinois Department of Transportation.

Zhou, H. and M. Atiquzzaman. (2019). Logistic regression models to predict wrong-way driving risk at freeway off-ramp terminals. Alabama Department of Transportation.

<http://eng.auburn.edu/files/centers/hrc/aldot-wwd-predictive.pdf>. Accessed June 2019.

Appendix A: Summary of Wrong-Way Incidents

Table A.1 WW Incidents during W0 Weekend at Exit 208 on I-65, AL

Exit 208	Speed from Sensors (mph)				Distance traveled (ft)	Note	Classification	Potential Countermeasure
	96/97	98	99	100				
2018/11/2 18:56	23	11	-	-	55	just passed dual large WW arrows	pickup truck (with trailer)	dual large WW arrows
2018/11/3 4:09	24	-	-	-	50	in front of dual large WW arrows	pickup truck	dual large WW arrows
2018/11/3 22:38	25	-	-	-	50	in front of dual large WW arrows	SUV	dual large WW arrows
2018/11/3 22:44	23	35	-	-	270	around concrete barrier	pickup truck	single small WW arrow
2018/11/4 7:03	26	10	-	-	55	just passed dual large WW arrows	SUV	dual large WW arrows
2018/11/4 8:25	25	33	-	-	240	before concrete barrier	RV	off-ramp traffic
2018/11/4 19:27	25	-	-	-	35	just passed channelized island	semitrailer truck	dual large WW arrows
2018/11/5 5:19	27	36	30	-	650	middle of ramp curve	passenger car	on-ramp traffic

Table A.2 WW Incidents during W0 Weekend at Exit 284 on I-65, AL

Exit 284	Speed from Sensors (mph)				Distance Traveled (ft)	Note	Classification	Potential Countermeasure
	101	102	103	104				
2018/11/2 19:00	22	-	-	-	15	just passed stop bar	passenger car	DNE sign
2018/11/2 19:23	21	25	29	33	800	all the way to the freeway	passenger car	N/A
2018/11/3 1:08	-	-	-	-	-	hesitated before yield line	pickup truck	DNE sign
2018/11/3 5:28	23	-	-	-	55	in front of WW arrow	passenger car	WW sign; dual WW arrows
2018/11/3 11:58	32	-	-	-	65	in front of WW arrow	pickup truck	WW sign; dual WW arrows
2018/11/3 15:41	-	-	-	-	40	hesitated in front of WW arrow	SUV	WW sign; dual WW arrows
2018/11/4 4:21	-	-	-	-	-	hesitated before yield line	pickup truck	DNE sign
2018/11/4 19:14	-	-	-	-	-	hesitated before stop bar	pickup truck	Divided roadway sign
2018/11/4 20:10	22	-	-	-	30	just passed stop bar	passenger car	Divided roadway sign
2018/11/5 2:01	27	-	-	-	100	at WW arrow	passenger car	WW sign; dual WW arrows
2018/11/5 13:30	25	-	-	-	15	just passed channelized island	pickup truck	WW sign; dual WW arrows

Table A.3 WW Incidents during W1 Weekend at Exit 208 on I-65, AL

Exit 208	Speed from Sensors (mph)				Distance Traveled (ft)	Note	Classification	Potential Countermeasure
	96/97	98	99	100				
2018/12/14 10:09	23	10	-	-	50	in front of dual large WW arrows	passenger car	dual large WW arrows
2018/12/14 13:23	26	33	29	-	650	middle of ramp curve	semitrailer truck	Pattern E.1

Table A.4 WW Incidents during W1 Weekend at Exit 284 on I-65, AL

Exit 284	Speed from Sensors (mph)				Distance Traveled (ft)	Note	Classification	Potential Countermeasure	
	101	102	103	104					
2018/12/14 17:14	23	-	-	-	65	in front of dual WW arrows	group of 3	passenger car	off-ramp traffic
2018/12/14 17:14	23	-	-	-	55	in front of dual WW arrows		pickup truck	off-ramp traffic
2018/12/14 17:14	20	-	-	-	15	just passed channelized island		passenger car	off-ramp traffic
2018/12/14 18:51	20	16	-	-	205	at 2nd WW sign	passenger car	WW sign	
2018/12/14 20:31	20	-	-	-	15	just passed channelized island	group of 2	passenger car	WW sign; dual WW arrows
2018/12/14 20:31	15	-	-	-	10	just passed channelized island		SUV	WW sign; dual WW arrows
2018/12/14 21:15	-	-	-	-	-	hesitated before stop bar	pickup truck	WW sign; dual WW arrows	
2018/12/15 15:04	15	-	-	-	15	just passed channelized island	SUV	DNE sign	
2018/12/15 17:34	25	-	-	-	15	just passed stop bar	passenger car	WW sign; dual WW arrows	
2018/12/15 17:35	24	-	-	-	55	in front of dual WW arrows	van	WW sign; dual WW arrows	
2018/12/15 18:21	26	-	-	-	20	just passed channelized island	pickup truck	DNE sign	
2018/12/15 19:12	-	-	-	-	-	hesitated before stop bar	pickup truck	WW sign; dual WW arrows	
2018/12/16 15:23	23	-	-	-	15	just passed channelized island	pickup truck	DNE sign	
2018/12/16 18:16	27	26	-	-	155	middle of WW signs	passenger car	WW sign; dual WW arrows	

Table A.5 WW Incidents during W2 Weekend at Exit 208 on I-65, AL

Exit 208	Speed from Sensors (mph)				Distance Traveled (ft)	Note	Classification	Potential Countermeasure
	96/97	98	99	100				
2018/12/21 11:42	23	15	-	-	95	before 2nd set of Pattern C	passenger car	Pattern C; WW sign
2018/12/22 23:10	17	-	-	-	35	just passed channelized island	semitrailer truck	DNE sign
2018/12/23 11:26	24	-	-	-	50	in front of dual large WW arrows	SUV	dual large WW arrows
2018/12/24 6:44	25	-	-	-	50	in front of dual large WW arrows	passenger car	dual large WW arrows
2018/12/24 8:23	20	26	-	-	110	just passed 2nd set of Pattern C	semitrailer truck	Pattern C; WW sign

Table A.6 WW Incidents during W2 Weekend at Exit 284 on I-65, AL

Exit 284	Speed from Sensors (mph)				Distance Traveled (ft)	Note	Classification	Potential Countermeasure
	101	102	103	104				
2018/12/21 12:09	15	-	-	-	10	just passed yield markings	minivan	DNE sign
2018/12/21 20:06	19	22	-	-	130	just passed 1st set of Pattern C	SUV	Pattern C; WW sign
2018/12/22 13:32	14	-	-	-	10	just passed yield markings	pickup truck	off-ramp traffic
2018/12/22 21:32	18	25	-	-	170	at 2nd set of Pattern C	passenger car	Pattern C; WW sign; off-ramp traffic
2018/12/22 22:55	21	32	23	-	280	at 3rd set of Pattern C	passenger car	Pattern C; off-ramp traffic
2018/12/22 22:57	15	-	-	-	10	just passed yield markings	passenger car (police)	Divided roadway sign
2018/12/23 15:50	-	-	-	-	-	hesitated at the entrance	passenger car	Divided roadway sign

Table A.7 WW Incidents during W3 Weekend at Exit 208 on I-65, AL

Exit 208	Speed from Sensors (mph)				Distance Traveled (ft)	Note	Classification	Potential Countermeasure
	96/97	98	99	100				
2019/1/13 2:48	21	-	-	-	13	at Pattern D	SUV	Pattern D; DNE sign; off-ramp traffic

Table A.8 WW Incidents during W3 Weekend at Exit 284 on I-65, AL

Exit 284	Speed from Sensors (mph)				Distance Traveled (ft)	Note	Classification	Potential Countermeasure
	101	102	103	104				
2019/1/13 21:56	25	-	-	-	30	just passed Pattern D	passenger car	Pattern D; WW sign

Table A.9 WW Incidents during W5 Weekend at Exit 208 on I-65, AL

Exit 208	Distance Traveled (ft)	Note	Classification	Potential Countermeasure
2019/8/10 3:08	15	at Pattern D	passenger car	Pattern D; WW arrows

Table A.10 WW Incidents during W5 Weekend at Exit 284 on I-65, AL

Exit 284	Distance Traveled (ft)	Note	Classification	Potential Countermeasure
2019/8/9 1:37	10		passenger car	WW signs
2019/8/10 22:48	80		SUV	WW signs

Table A.11 WW Incidents during W6 Weekend at Exit 208 on I-65, AL

Exit 208	Distance Traveled (ft)	Note	Classification	Potential Countermeasure
2019/8/30 3:08	15	at Pattern D	passenger car	Pattern D; WW arrows

Table A.12 WW Incidents during W6 Weekend at Exit 284 on I-65, AL

Exit 284	Distance Traveled (ft)	Note	Classification	Potential Countermeasure
2019/8/30 2:57	30		passenger car	WW signs
2019/9/1 23:11	400		passenger car	WW signs; Off-ramp traffic

Table A.13 WW Incidents during W7 Weekend at Exit 284 on I-65, AL

Exit 284	Distance Traveled (ft)	Note	Classification	Potential Countermeasure
2019/9/27 21:15	20		passenger car	WW signs
2019/9/29 1:31	30		passenger car	WW signs; Off-ramp traffic
2019/9/29 23:02	35		SUV	WW signs

Table A.14 WW Incidents during W8 Weekend at Exit 284 on I-65, AL

Exit 284	Distance Traveled (ft)	Note	Classification	Potential Countermeasure
2019/12/13 22:25	21		passenger car	WW signs
2019/12/13 23:19	65		passenger car	WW signs; Off-ramp traffic
2019/12/14 20:48	102		SUV	WW signs; Off-ramp traffic
2019/12/15 2:27	124		pickup truck	Off-ramp traffic

Appendix B: Speed Characteristics

Table B.1 Speed Characteristics at W0 (unit: mph)

Sensor	Mean	85 th	Max	Min	Variance	Standard Deviation
#96	8.9	12.0	17.0	5.0	7.9	2.8
#97	10.7	14.0	21.0	5.0	12.4	3.5
#98	20.6	27.0	37.0	6.0	41.1	6.4
#99	33.3	39.0	51.0	16.0	37.8	6.2
#100	36.3	44.0	58.0	16.0	58.5	7.6
#101	12.8	18.0	27.0	5.0	23.1	4.8
#102	21.4	26.0	34.0	10.0	19.3	4.4
#103	27.3	31.0	37.0	18.0	11.2	3.3
#104	30.3	34.0	40.0	21.0	14.9	3.9

Table B.2 Speed Characteristics at W1 (unit: mph)

Sensor	Mean	85 th	Max	Min	Variance	Standard Deviation
#96	9.2	12.0	19.0	5.0	7.9	2.8
#97	10.8	14.0	22.0	6.0	12.2	3.5
#98	20.6	26.0	37.0	6.0	36.4	6.0
#99	31.5	37.0	45.0	18.0	27.1	5.2
#100	29.8	35.0	44.0	17.0	25.8	5.1
#101	12.6	17.0	25.0	5.0	20.0	4.5
#102	20.9	25.0	33.0	9.0	19.1	4.4
#103	26.7	30.0	36.0	17.0	12.1	3.5
#104	28.0	33.0	41.0	15.0	28.0	5.3

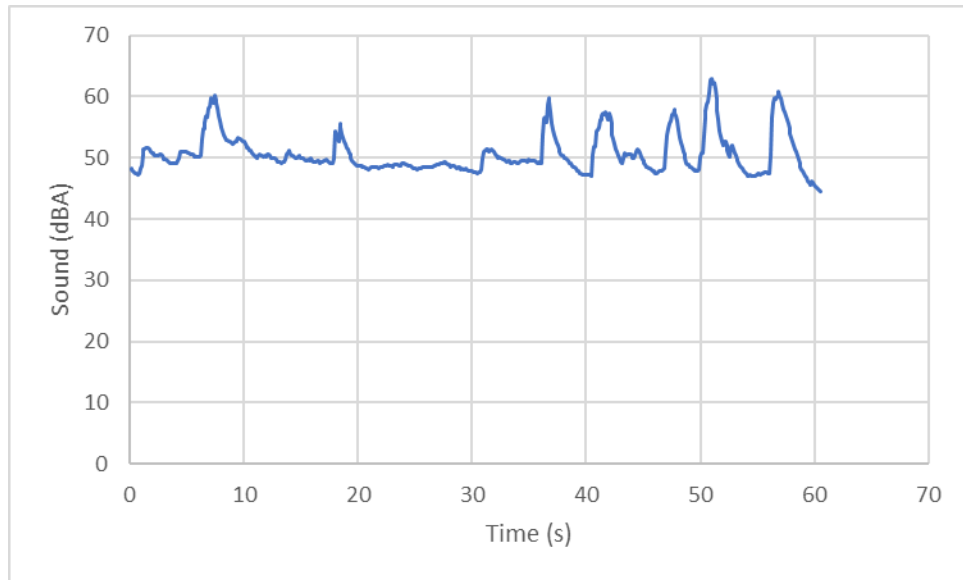
Table B.3 Speed Characteristics at W2 (unit: mph)

Sensor	Mean	85 th	Max	Min	Variance	Standard Deviation
#96	8.9	12.0	19.0	5.0	8.4	2.9
#97	10.5	14.0	22.0	6.0	12.7	3.6
#98	17.9	24.0	34.0	5.0	32.8	5.7
#99	31.2	36.0	45.0	18.0	27.8	5.3
#100	30.4	37.0	47.0	15.0	36.1	6.0
#101	12.4	18.0	26.0	5.0	22.6	4.8
#102	18.2	22.0	28.0	9.0	16.0	4.0
#103	26.2	30.0	36.0	17.0	12.3	3.5
#104	28.2	33.0	42.0	15.0	27.3	5.2

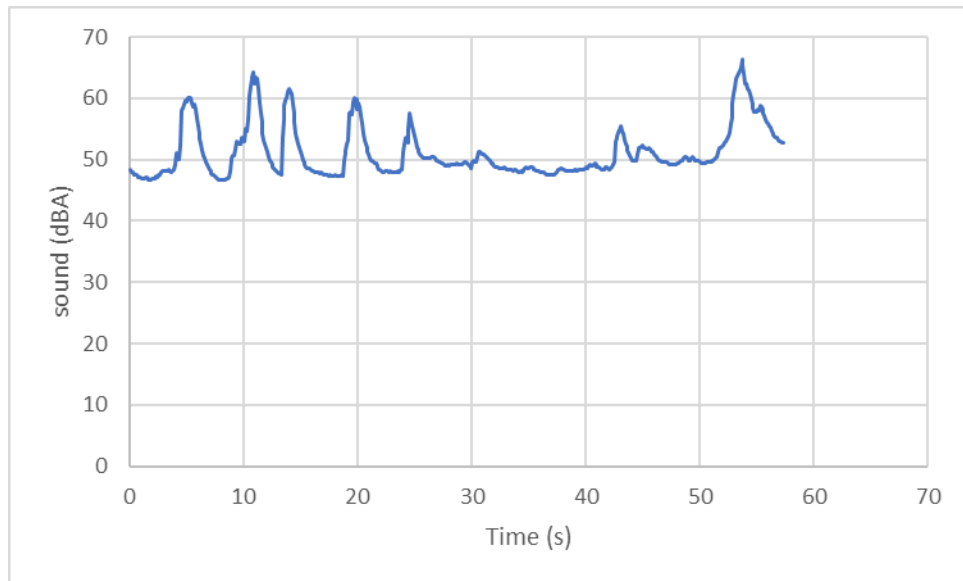
Table B.4 Speed Characteristics at W3 (unit: mph)

Sensor	Mean	85 th	Max	Min	Variance	Standard Deviation
#96	8.9	12.0	19.0	5.0	8.6	2.9
#97	11.8	13.0	19.0	5.0	9.7	3.1
#98	17.5	23.0	34.0	5.0	33.1	5.8
#99	31.8	37.0	48.0	16.0	31.3	5.6
#100	30.3	36.0	46.0	16.0	31.8	5.6
#101	11.6	16.0	21.0	5.0	14.2	3.8
#102	17.9	22.0	29.0	7.0	16.4	4.0
#103	26.2	30.0	36.0	17.0	12.3	3.5
#104	28.6	34.0	43.0	15.0	30.2	5.5

Appendix C: Sound and Vibration Profiles

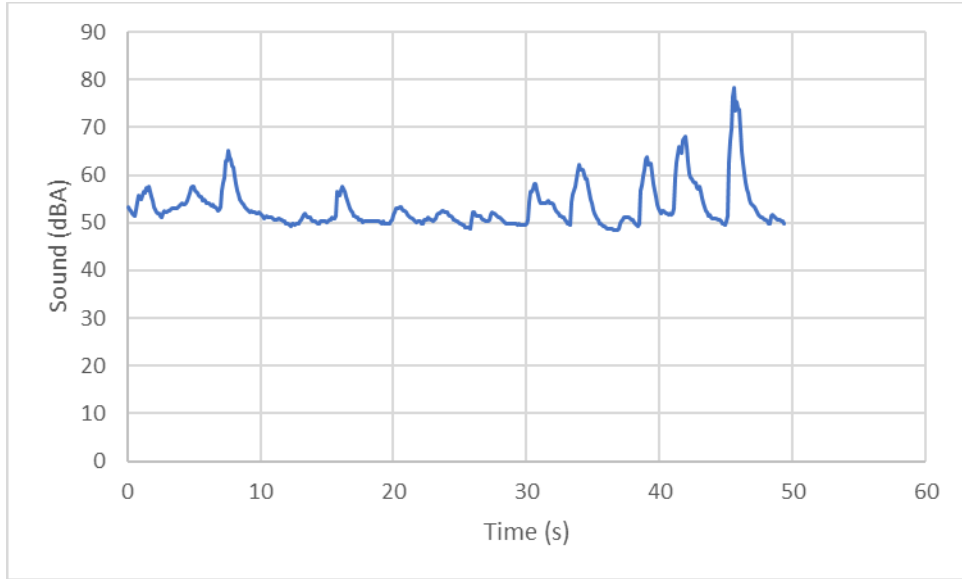


(a)

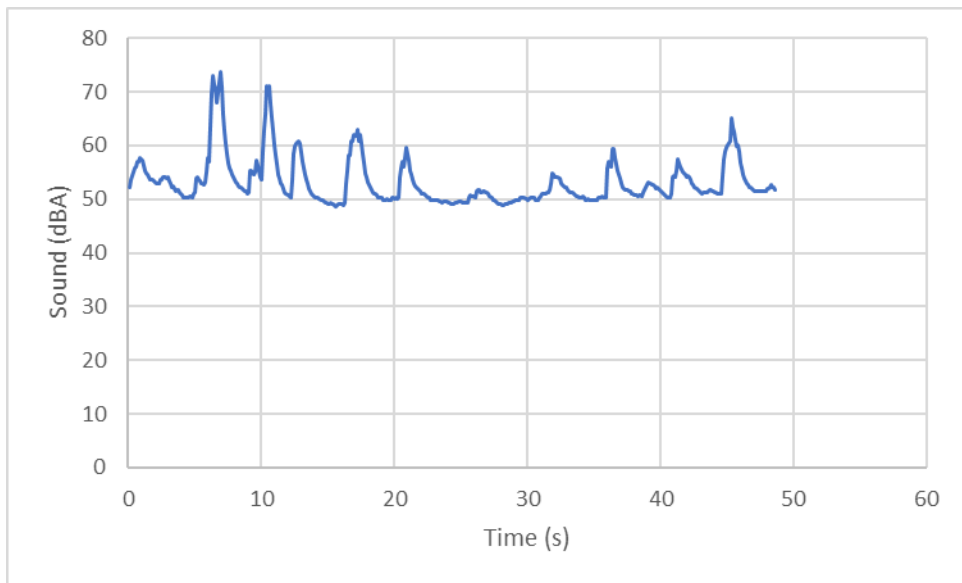


(b)

Figure C.1 Sound Profile at 10 mph (a: RW; b: WW)

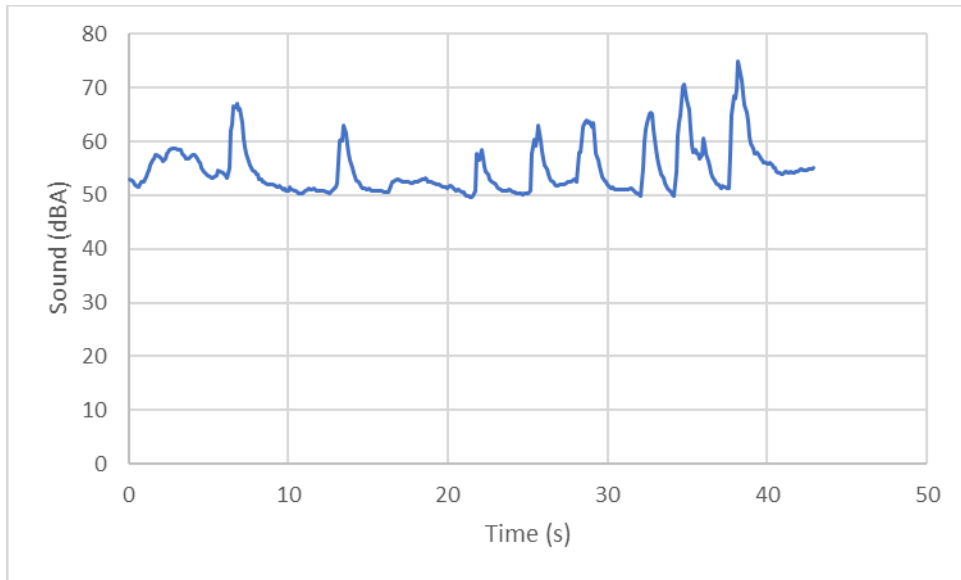


(a)

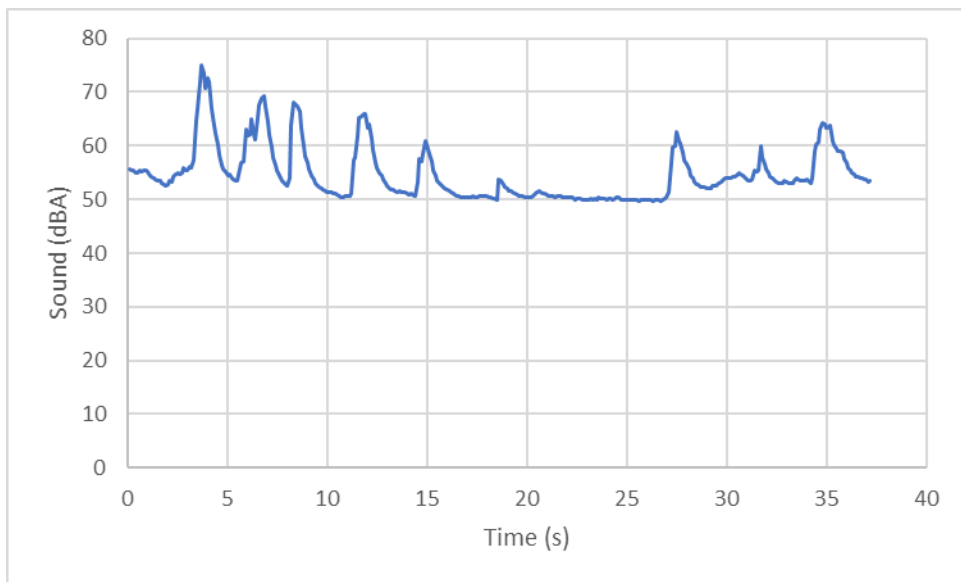


(b)

Figure C.2 Sound Profile at 15 mph (a: RW; b: WW)

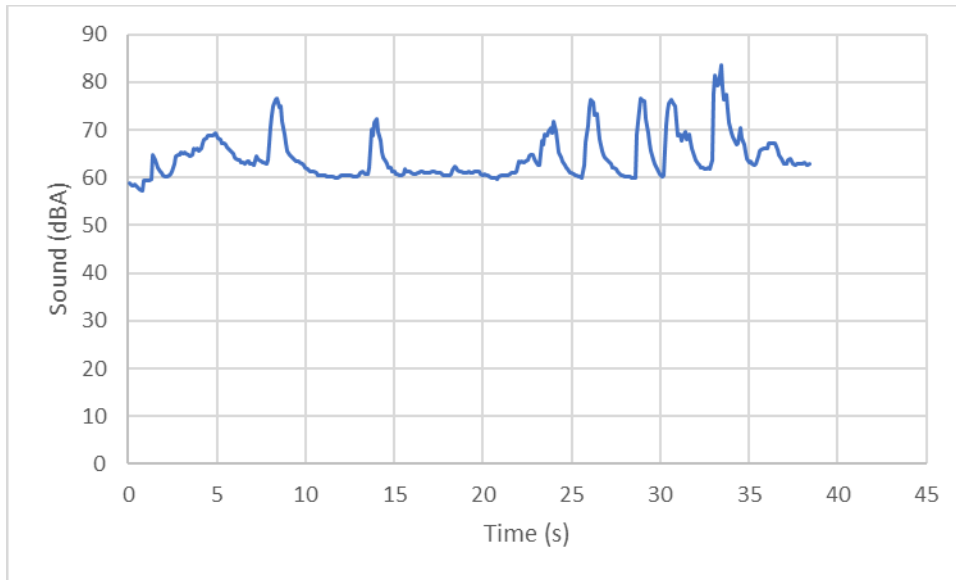


(a)

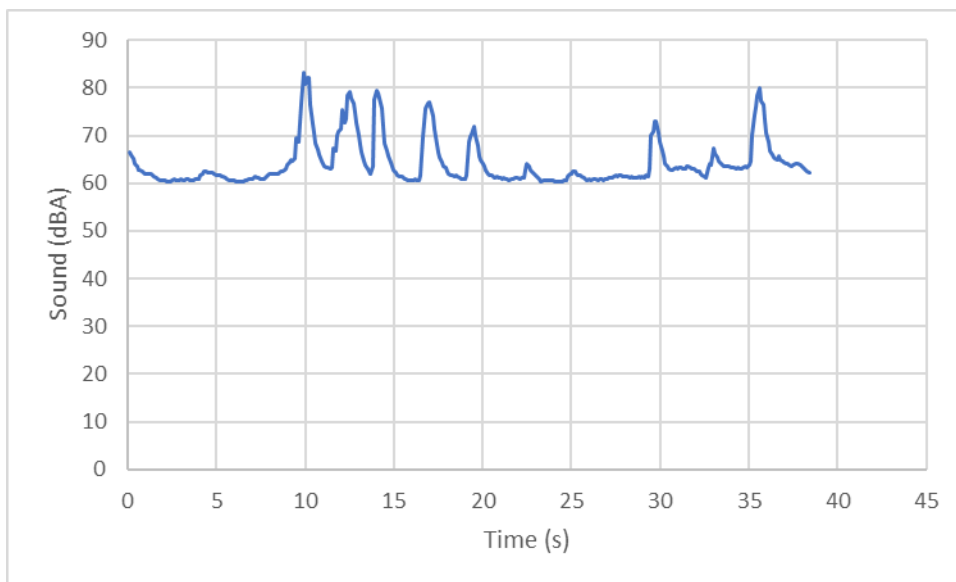


(b)

Figure C.3 Sound Profile at 20 mph (a: RW; b: WW)

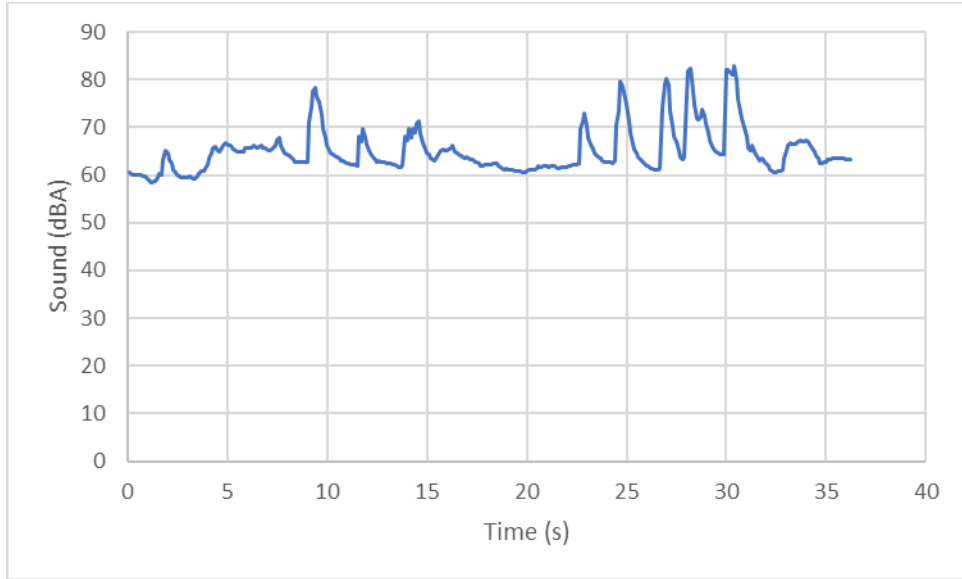


(a)

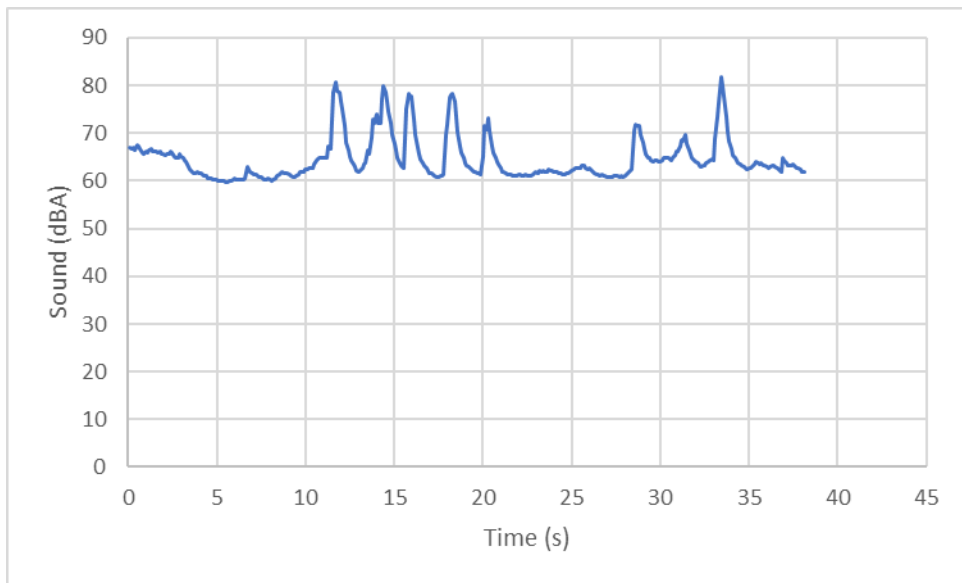


(b)

Figure C.4 Sound Profile at 25 mph (a: RW; b: WW)

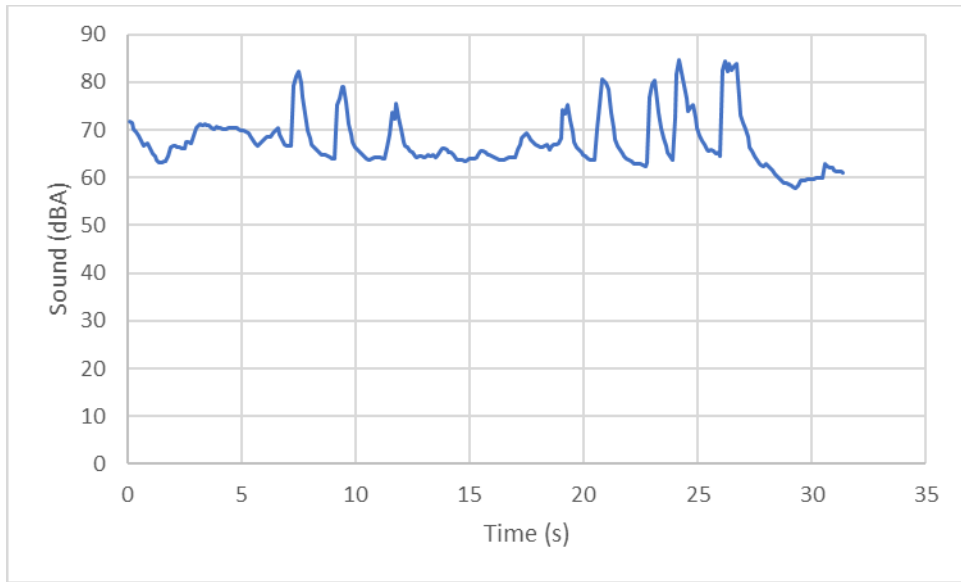


(a)

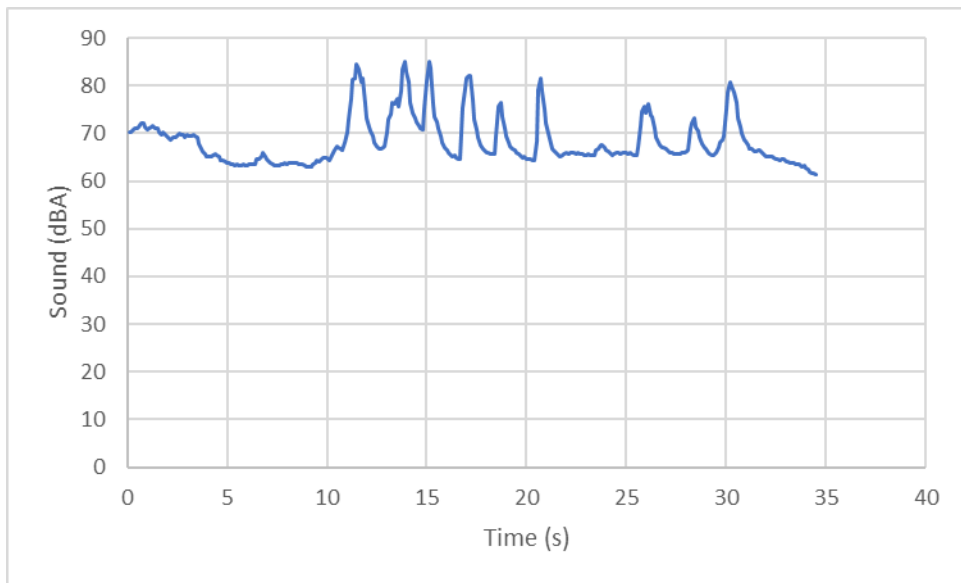


(b)

Figure C.5 Sound Profile at 30 mph (a: RW; b: WW)

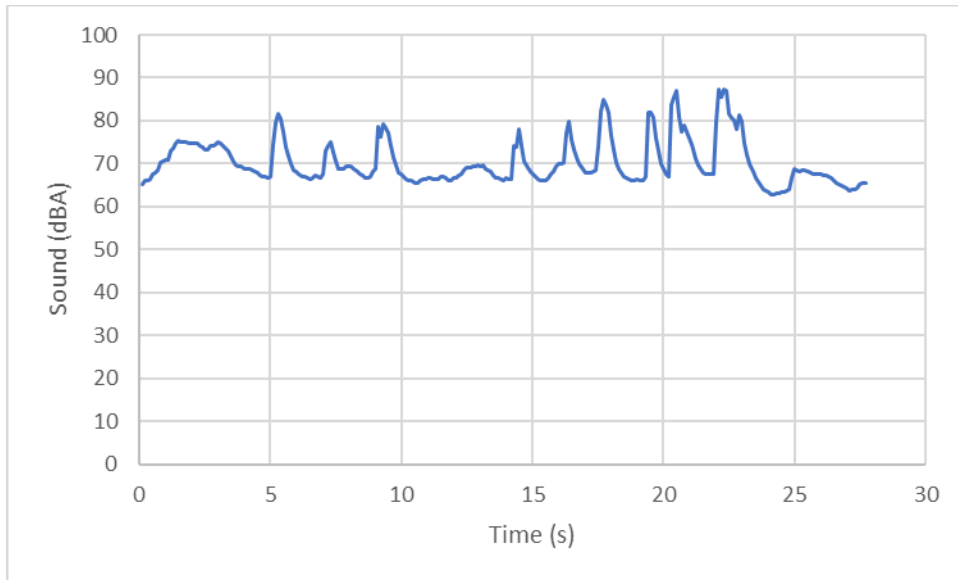


(a)

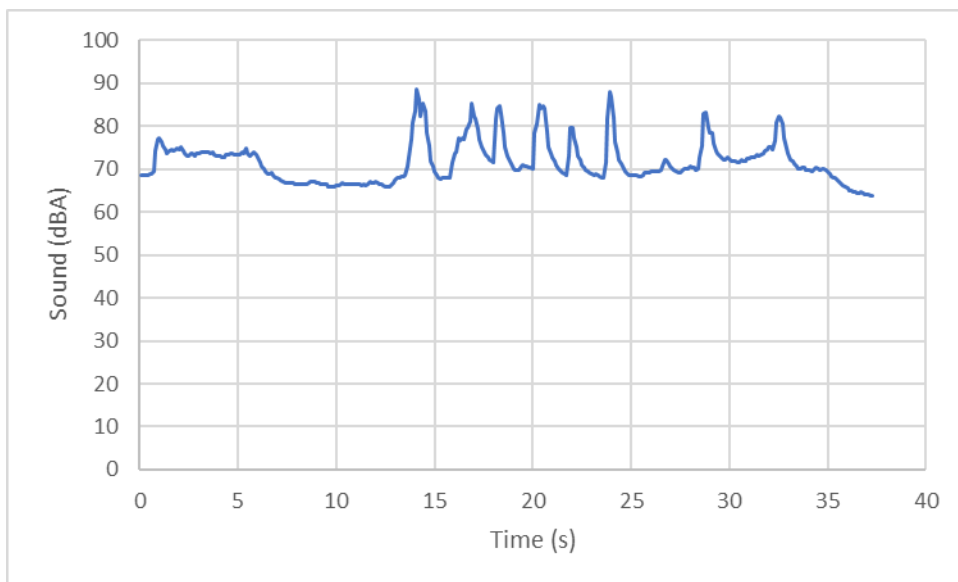


(b)

Figure C.6 Sound Profile at 35 mph (a: RW; b: WW)



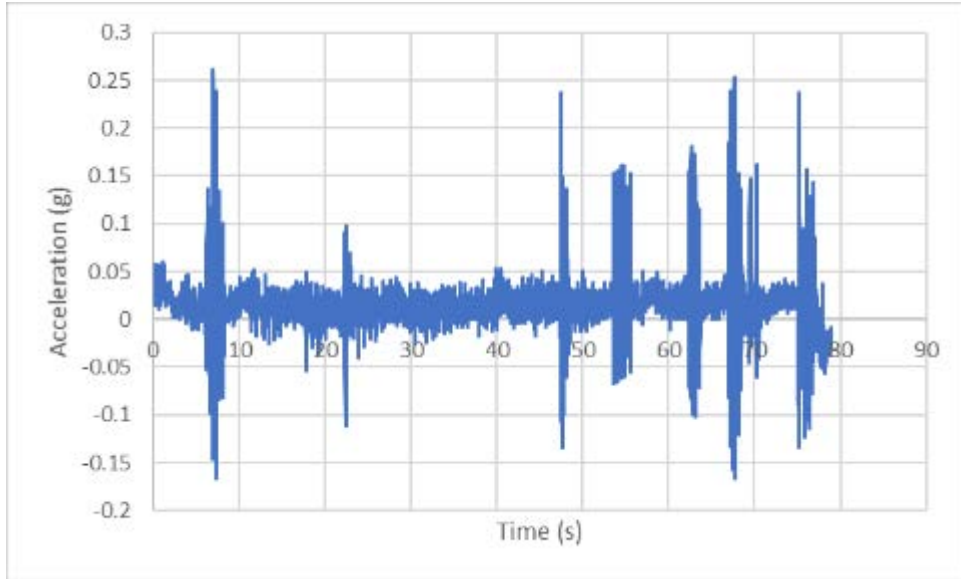
(a)



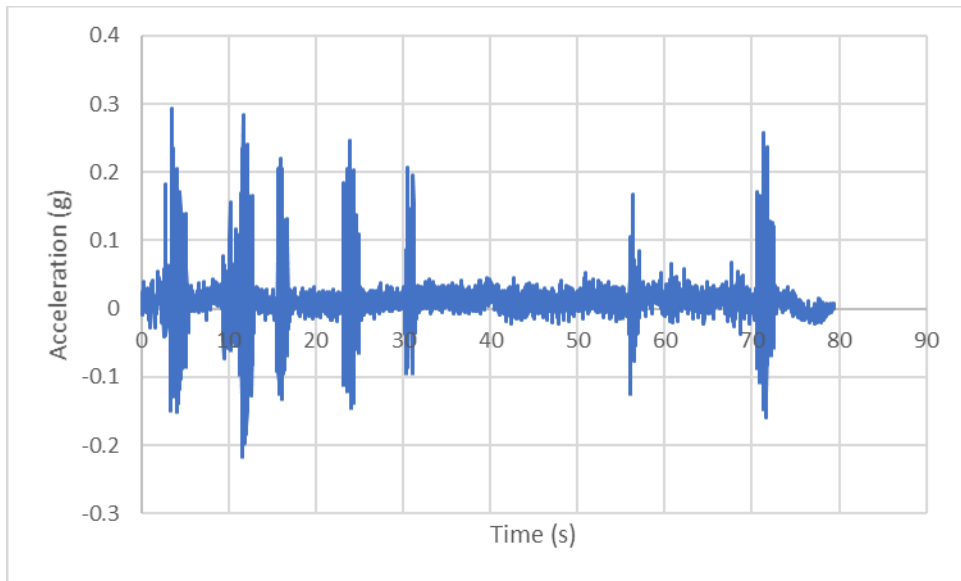
(b)

Figure C.7 Sound Profile at 40 mph (a: RW; b: WW)

Vibration Profiles Collected on Southbound Off-Ramp at Exit 208 on I-65

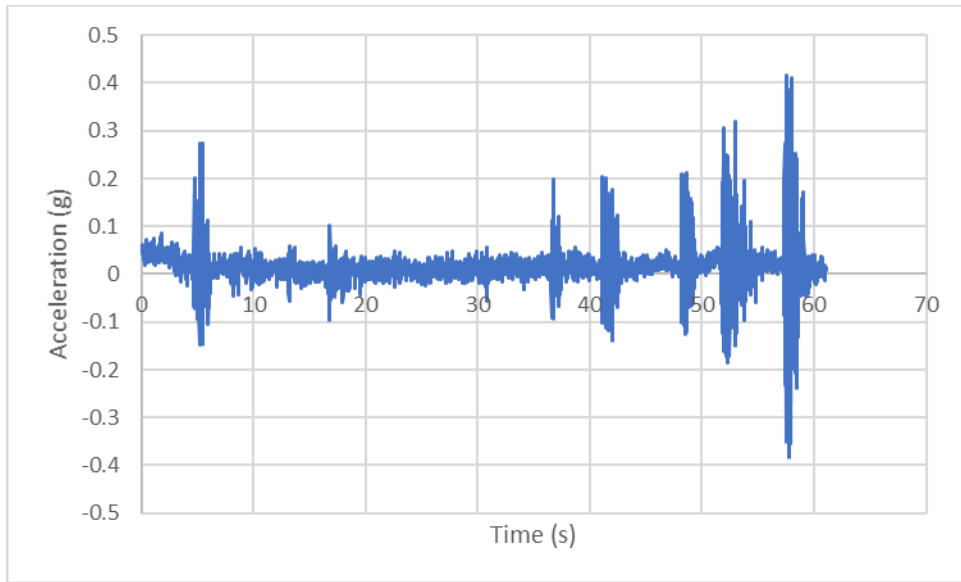


(a)

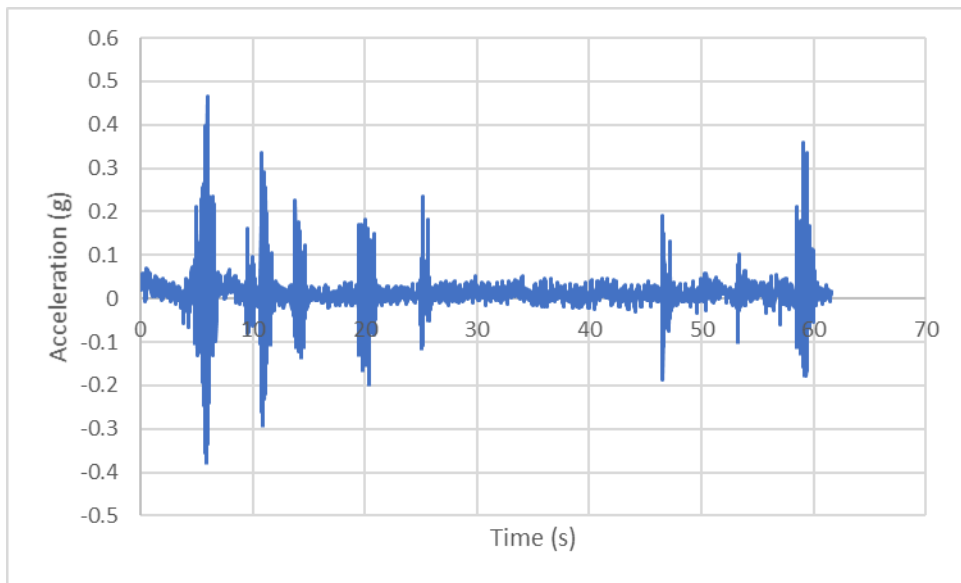


(b)

Figure C.8 Vibration Profile at 10 mph (a: RW; b: WW)

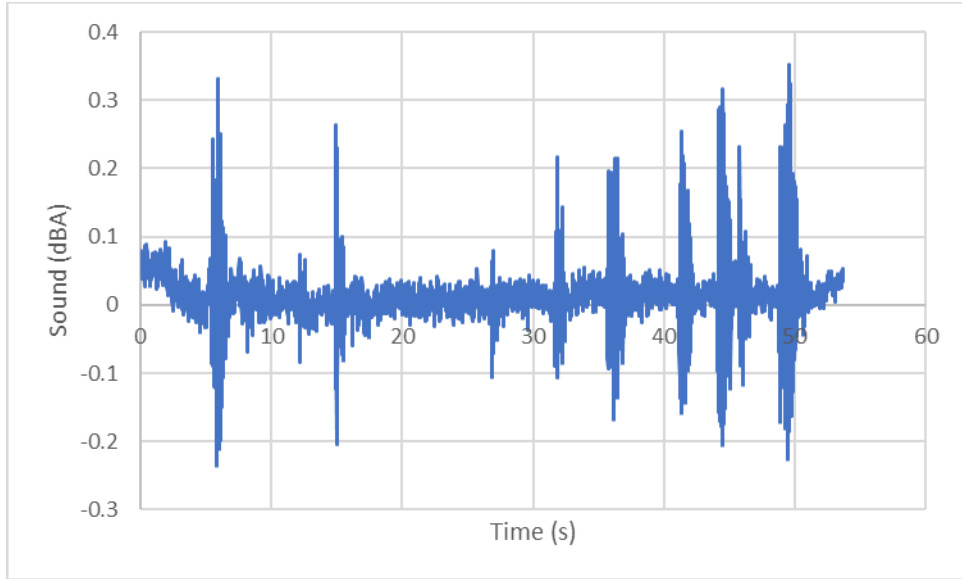


(a)

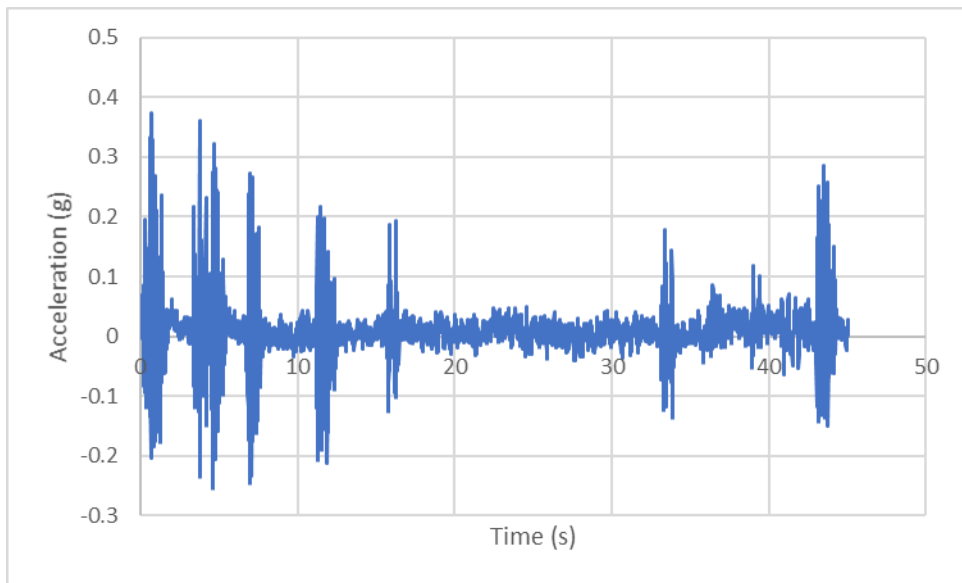


(b)

Figure C.9 Vibration Profile at 15 mph (a: RW; b: WW)

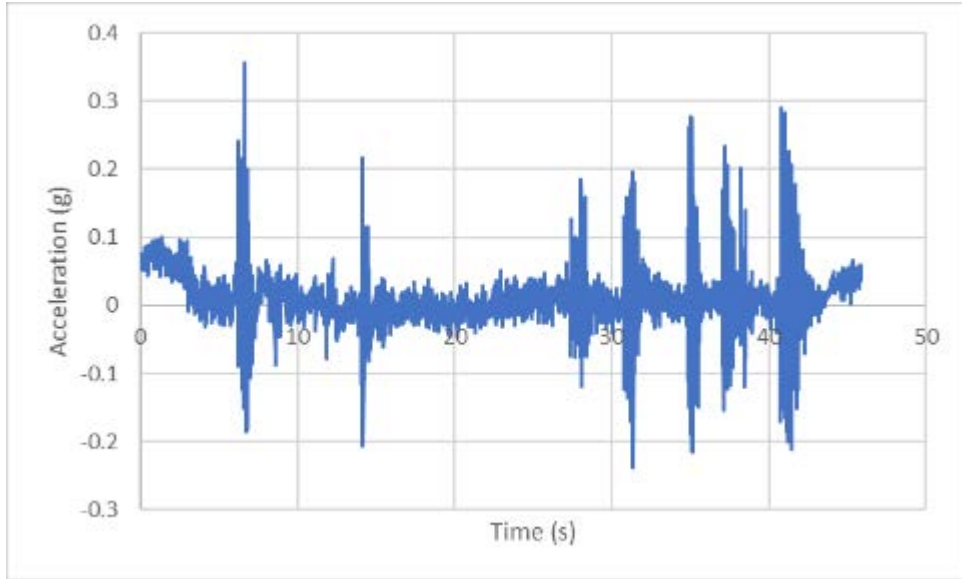


(a)

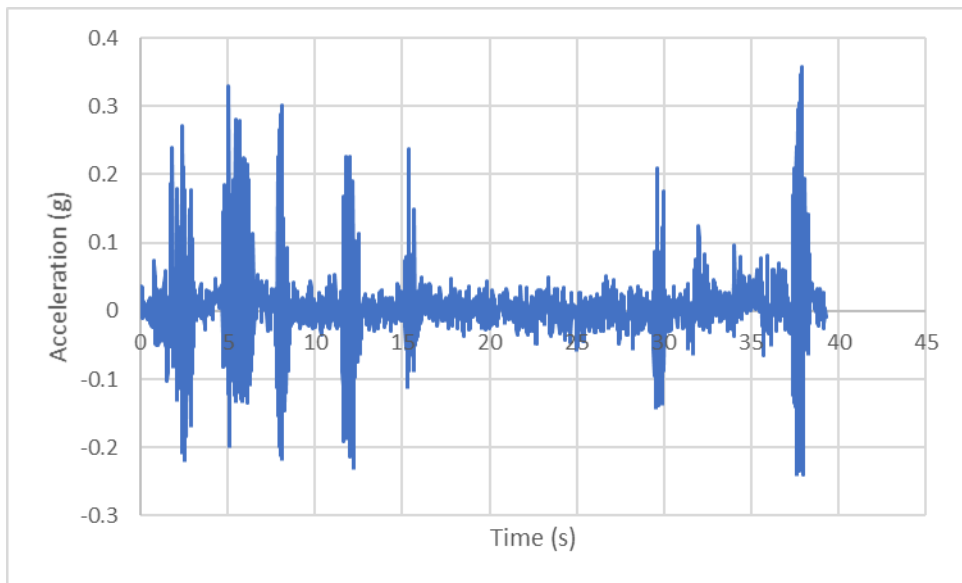


(b)

Figure C.10 Vibration Profile at 20 mph (a: RW; b: WW)

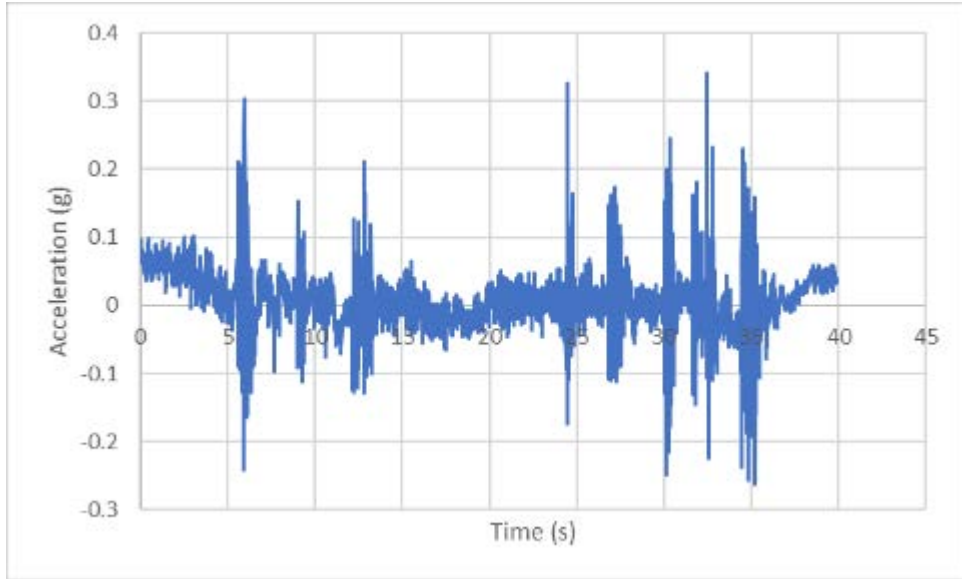


(a)

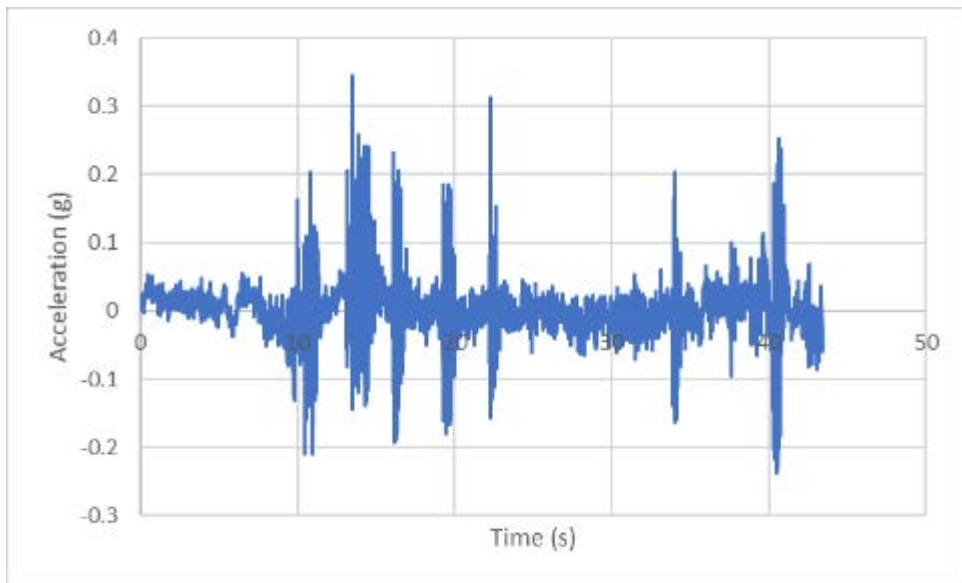


(b)

Figure C.11 Vibration Profile at 25 mph (a: RW; b: WW)

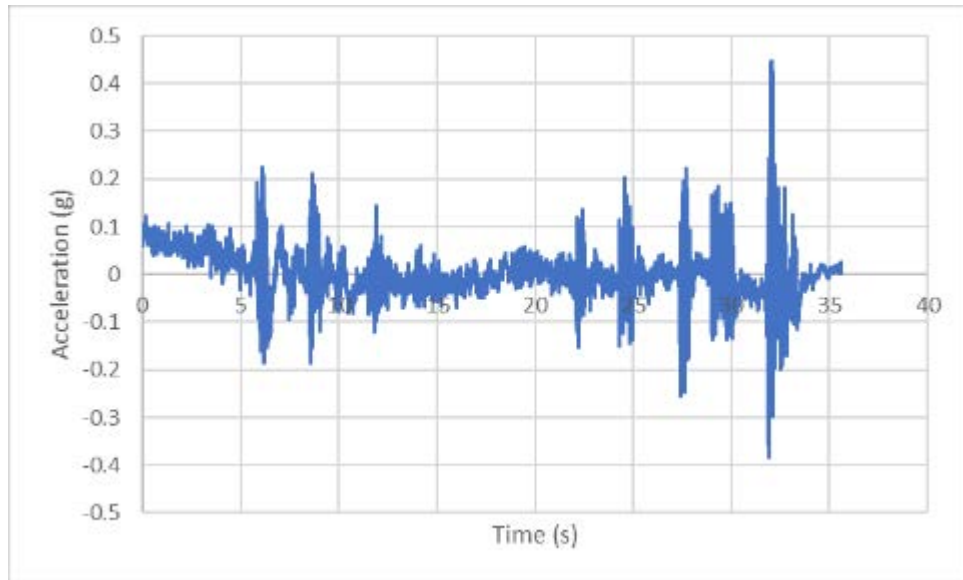


(a)

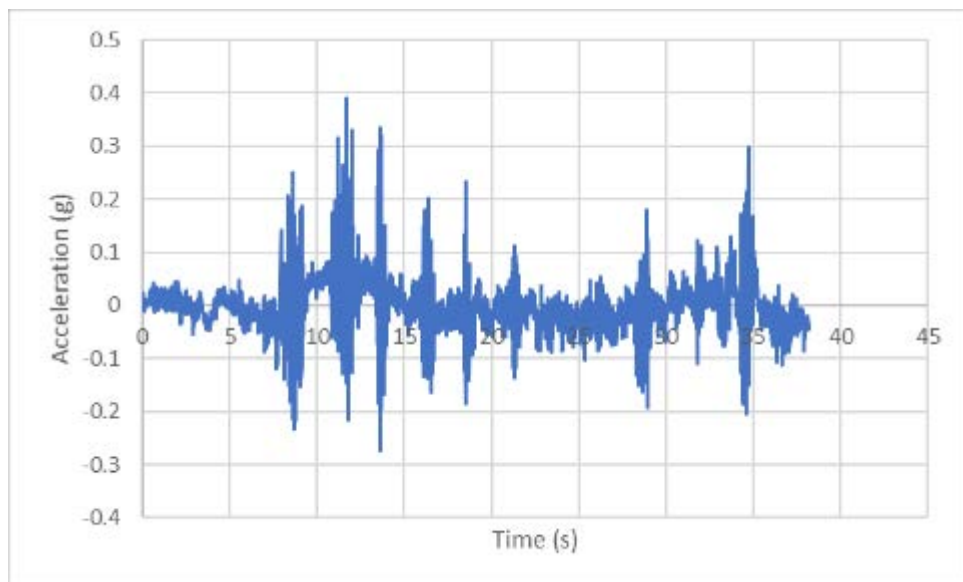


(b)

Figure C.12 Vibration Profile at 30 mph (a: RW; b: WW)

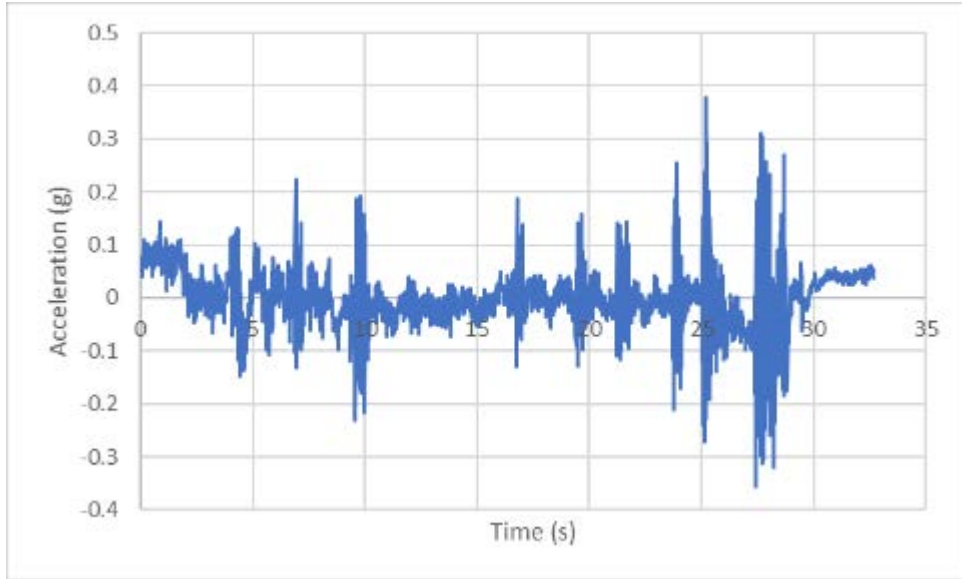


(a)

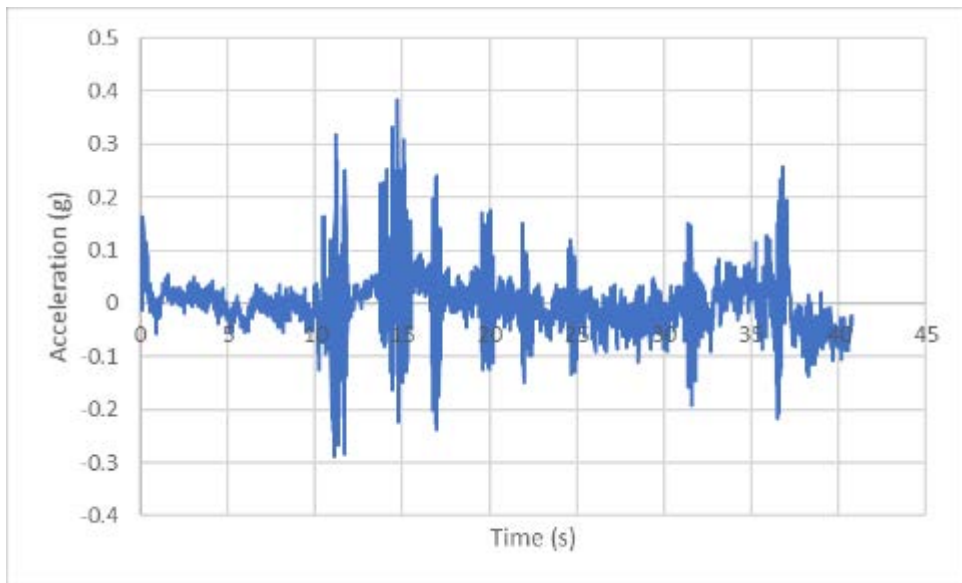


(b)

Figure C.13 Vibration Profile at 35 mph (a: RW; b: WW)



(a)



(b)

Figure C.14 Vibration Profile at 40 mph (a: RW; b: WW)

Appendix D: MATLAB Code

```
close all
clear all

%Get filename and path
[fname,pathname] = uigetfile('.csv','Select CSV File to Load, Plot, Compute RMS & FFT');
disp([pathname fname])

%Load CSV
tic %start timer
data = csvread([pathname fname]);
fprintf('%4.2f seconds - Time to Load Data\n',toc)

%Determine variables and Display size
[N,m] = size(data);
t = data(:,1); %time in seconds
x = data(:,2); %array of data for RMS and FFT
Fs = 1/(t(2)-t(1));
fprintf('%12.0f data points\n',N)

%Plot Data
tic %start timer
figure(1)
plot(t,x)
xlabel('Time (s)');
ylabel('Accel (g)');
title(fname);
grid on;
fprintf('%4.2f seconds - Time to Plot Data\n',toc)

%Determine RMS and Plot
tic %start timer
w = floor(Fs); %width of the window for computing RMS
steps = floor(N/w); %Number of steps for RMS
t_RMS = zeros(steps,1); %Create array for RMS time values
x_RMS = zeros(steps,1); %Create array for RMS values
for i=1:steps
    range = ((i-1)*w+1):(i*w);
    t_RMS(i) = mean(t(range));
    x_RMS(i) = sqrt(mean(x(range).^2));
end
figure(2)
plot(t_RMS,x_RMS)
xlabel('Time (s)');
ylabel('RMS Accel (g)');
```

```

title(['RMS - ' fname]);
grid on;
fprintf('%4.2f seconds - Time to Compute RMS and Plot\n',toc)

%Determine FFT and Plot
tic
freq = 0:Fs/length(x):Fs/2; %frequency array for FFT
xdft = fft(x); %Compute FFT
xdft = 1/length(x).*xdft; %Normalize
xdft(2:end-1) = 2*xdft(2:end-1);
figure(3)
plot(freq,abs(xdft(1:floor(N/2)+1)))
xlabel('Frequency (Hz)');
ylabel('Accel (g)');
% ylim([0,0.1]);
title(['FFT - ' fname]);
grid on;
fprintf('%4.2f seconds - Time to Compute FFT and Plot\n',toc)

hold on

%Get filename and path
[fname,pathname] = uigetfile('.csv','Select CSV File to Load, Plot, Compute RMS & FFT');
disp([pathname fname])

%Load CSV
tic %start timer
data = csvread([pathname fname]);
fprintf('%4.2f seconds - Time to Load Data\n',toc)

%Determine variables and Display size
[N,m] = size(data);
t = data(:,1); %time in seconds
x = data(:,2); %array of data for RMS and FFT
Fs = 1/(t(2)-t(1));
fprintf('%12.0f data points\n',N)

%Determine FFT and Plot
tic
freq = 0:Fs/length(x):Fs/2; %frequency array for FFT
xdft = fft(x); %Compute FFT
xdft = 1/length(x).*xdft; %Normalize
xdft(2:end-1) = 2*xdft(2:end-1);
figure(3)
plot(freq,abs(xdft(1:floor(N/2)+1)))
xlabel('Frequency (Hz)');

```

```
ylabel('Accel (g)');  
legend('right way','wrong way');  
% ylim([0,0.1]);  
title(['FFT - Pattern E.1']);  
grid on;  
fprintf('%4.2f seconds - Time to Compute FFT and Plot\n',toc)  
  
hold off
```